

**POLITECNICO DI MILANO**

Industrial Engineering Faculty

Master of Science in Mechanical Engineering



**Development of an automatic system  
for experimental modal analysis of large structures**

Supervisor: Prof. Alfredo Cigada

By:

Julio Enrique HERNÁNDEZ VALBUENA  
Matr. 755144

Academic year 2011 - 2012.

## Abstract

Experimental modal analysis (EMA) is the area of structural dynamics who deals with the methodologies and techniques necessary to evaluate the behaviour of structures using experimental approaches, where the measurements of excitation (input) and response (output) signals from an excited structure are used to estimate the modal parameters. The importance of the excitation in the EMA methodologies for large structures, explains the need of a controller in order to control an exciter with an stable behaviour in the range of frequencies between 0 to 10 Hz where the harmonic component of this kind of structures are expected to be found. The present work shows the model, design and implementation of a controlled system that satisfy the characteristic required by the EMA methodologies of large structures. The object of study is a servo-hydraulic actuator and a proportional, integral and derivative (PID) controller with input signal amplitude compensator is used as controller.

**Tag words:** Experimental modal analysis, servo-hydraulic system, controller, amplitude compensator.

## Sommario

L'analisi modale sperimentale (EMA) è il settore che nell'ambito della dinamica strutturale si occupa delle metodologie e delle tecniche necessarie per valutare il comportamento di strutture. Si adottano approcci sperimentali in cui le misure dei segnali di forzamento (input) e risposta (output) provenienti da una struttura eccitata si utilizzano per stimare i parametri modali. L'importanza del forzamento nelle metodologie EMA per grandi strutture, spiega la necessità di un controllore in grado di comandare un sistema di forzamento avente un comportamento stabile nell'intervallo di frequenze tra 0 a 10 Hz, intervallo in cui si trovano solitamente le frequenze proprie di tali strutture. Il presente lavoro è incentrato sulla modellazione, progettazione e implementazione di un controllore che soddisfi le caratteristiche d stabilità richieste dalle metodologie EMA. L'oggetto di studio è un attuatore servo-idraulico per cui è sviluppato un sistema di controllo basato nel algoritmo di controllo proporzionale, integrale e derivativo (PID) con un compensatore della ampiezza del segnale di ingresso.

**Parole chiave:** Analsi modale sperimentale, sistema servo-idraulico, controllore, compensatore della ampiezza.

## **Acknowledgements**

I would like to thank to Eng. Simona Moschini, Eng. Giogio Busca, Eng. Stefano Manzoni, Eng. Marcello Vanalli and Professor Alfredo Cigada for their dedication and support along the project.

To all my friends that had made this stay in Italy an incredible life experience, specially to Mauro, Toni, Camille, Angie, Edmundo, Leo and Fillipo.

Para mi amada familia, por toda su comprensión, apoyo y amor durante toda esta aventura.

Para Juanita y Caro, y el imaginario colectivo que siempre está y estará en mi corazón.

# Table of Contents

|  |    |
|--|----|
| List of figures.....   | 5  |
| List of tables.....  | 8  |
| Introduction.....  | 9  |
| Objectives.....  | 11 |
| Chapter 1 Servo-hydraulic system.....  | 13 |
| 1.1 Hydraulic actuator overview.....   | 13 |
| 1.1.1 Linear hydraulic actuator characteristics.....                               | 15 |
| 1.1.2 Linear hydraulic actuator dynamics.....                                      | 17 |
| 1.2 Hydraulic actuator overview.....   | 21 |
| 1.2.1 Servovalve characteristics.....  | 21 |
| 1.2.2 Servovalve dynamics.....   | 25 |
| 1.3 Servo-hydraulic system dynamic simulation.....                                 | 28 |
| 1.3.1 Linear approach - Linearisation.....   | 28 |
| 1.3.2 Linear approach - Space state representation.....                            | 29 |
| 1.3.3 Linear approach - System transfer function representation.....               | 31 |
| 1.3.4 Linear approach – Eigenvalues and transfer function evaluation....           | 32 |
| 1.3.5 Non linear approach – Space state representation.....                        | 34 |
| 1.3.6 Stability of the servo-hydraulic system.....                                 | 35 |
| Chapter 2 Control system.....  | 37 |
| 2.1 Automatic control methodologies – state of the art.....                        | 37 |
| 2.1.1 Feedback control.....  | 38 |
| 2.1.2 PID control algorithm.....   | 40 |
| 2.1.3 Pole placement method.....   | 42 |
| 2.1.4 Optimal control – Linear Quadratic Regulator.....                            | 44 |
| 2.1.5 Servo-hydraulic system: comparison between different control<br>methods..... | 45 |
| 2.2 Servo-hydraulic system controller design.....                                  | 45 |
| 2.3 Control system design – Numerical simulation.....                              | 46 |
| 2.3.1 General considerations.....  | 46 |
| 2.3.2 Simulation block diagrams.....   | 48 |
| 2.3.3 Controller tuning – Characteristics and tuning methodologies.....            | 49 |
| 2.3.4 Controller tuning – Simulation results.....                                  | 56 |
| 2.4 Control system design – implementation.....                                    | 71 |
| 2.4.1 Hardware requirements.....   | 71 |
| 2.4.2 Software configuration.....  | 75 |
| Chapter 3 Test rig.....  | 79 |
| 3.1.1 Controller electrical box.....   | 80 |
| 3.1.2 Linear hydraulic actuator.....   | 83 |

---

|  |     |
|--|-----|
| 3.1.3 LVDT sensor.....                       | 84  |
| 3.1.4 Double stage servovalve.....           | 85  |
| 3.1.5 Hydraulic circuit.....                 | 85  |
| Chapter 4 Experimental results.....          | 87  |
| 4.1 Non load case.....                       | 87  |
| Conclusions.....                             | 98  |
| Appendix A-I Simulation parameters.....      | 100 |
| Appendix A-II Simulation block diagrams..... | 101 |
| Appendix A-III Electrical schemes.....       | 105 |
| Appendix A-VI Controller user interface..... | 111 |
| Appendix A-V FPGA block diagrams.....        | 120 |
| Bibliography.....                            | 123 |

## List of figures

|   |    |
|---|----|
| Figure 1.1 Different hydraulic actuator types (A) rotational, (B) linear.....   | 14 |
| Figure 1.2 Linear hydraulic actuator's functional classification.....   | 16 |
| Figure 1.3 Schematic representation of double acting - double rod linear hydraulic actuator.....  | 16 |
| Figure 1.4 Mechanical and linear actuator schematics.....   | 19 |
| Figure 1.5 Schematic representation of (A) single stage servovalves and (B) double stage servovalves.....                                     | 21 |
| Figure 1.6 Functional servovalve classification.....  | 22 |
| Figure 1.7 Flow-pressure characteristic for different feedback technologies.....  | 23 |
| Figure 1.8 Schematic representation of a double stage flapper and spool servovalve with force feedback.....                                   | 24 |
| Figure 1.9 Double stage servovalve motion – equilibrium position.....   | 25 |
| Figure 1.10 frequency response function .....   | 26 |
| Figure 1.11 Block diagram of the servo-hydraulic system.....  | 31 |
| Figure 2.1 Feedback controlled process.....   | 39 |
| Figure 2.2 Step response for a simulated third order controlled system with proportional action.....  | 40 |
| Figure 2.3 Step response for a simulated third order controlled system with proportional and integral action.....                             | 41 |
| Figure 2.4 Step response for a simulated third order controlled system with proportional and derivative action.....                           | 41 |
| Figure 2.5 Servo-hydraulic feedback arrangements.....   | 46 |
| Figure 2.6 Controlled system schematic representation.....  | 47 |
| Figure 2.7 Open loop characteristic step responses.....   | 50 |
| Figure 2.8 Characteristic parameters for monotonic and oscillatory around steady state value step responses.....                              | 52 |
| Figure 2.9 Open loop frequency response function for controlled .....   | 55 |
| Figure 2.10 Open loop frequency response function for controlled .....  | 55 |
| Figure 2.11 Maximum amplitude vs signal frequency .....   | 57 |
| Figure 2.12 1.27 mm step response at different proportional gain values.....  | 59 |
| Figure 2.13 1.27 mm step response at different proportional gain values.....  | 60 |
| Figure 2.14 31.66 mm step response at different proportional gain values .....  | 60 |
| Figure 2.15 31.66 mm step response at different proportional gain values.....   | 61 |
| Figure 2.16 1.27 mm step response at different proportional gain values.....  | 61 |
| Figure 2.17 1.27 mm step response at different proportional gain values.....  | 62 |
| Figure 2.18 31.66 mm step response at different proportional gain values.....   | 62 |
| Figure 2.19 31.66 mm step response at different proportional gain values.....   | 63 |
| Figure 2.20 Speed profile comparison between linear and non linear models for characteristic proportional gain values – Load mass 450 kg..... | 64 |

---

|   |     |
|---|-----|
| Figure 2.21 Speed profile comparison between linear and non linear models for characteristic proportional gain values – Load mass 0 kg..... | 64  |
| Figure 2.22 Speed profiles for characteristic proportional gain values and limiting conditions – Load mass 450 kg.....                      | 65  |
| Figure 2.23 Speed profiles for characteristic proportional gain values and limiting conditions – Load mass 0 kg.....                        | 66  |
| Figure 2.24 Representative functional groups on servo-hydraulic controller device.....  | 74  |
| Figure 2.25 Servo-hydraulic controller software architecture.....   | 76  |
| Figure 3.1 Attached load structure for servo-hydraulic test rig.....  | 79  |
| Figure 3.2 Controller electrical box – Internal view.....   | 80  |
| Figure 3.3 Controller electrical box – External view.....   | 81  |
| Figure 3.4 Constructive configuration for a MTS 242.25 linear hydraulic actuator.....   | 83  |
| Figure 3.5 LVDT sensor – schematic representation.....  | 84  |
| Figure 3.6 Double stage servovalve.....   | 85  |
| Figure 3.7 Manifold electrovalve.....   | 86  |
| Figure 4.1 actual and simulated 5 mm step response for controlled servo-hydraulic system – non load case.....                               | 88  |
| Figure 4.2 actual and simulated 10 mm step response for controlled servo-hydraulic system – non load case.....                              | 88  |
| Figure 4.3 actual and simulated 20 mm step response for controlled servo-hydraulic system – non load case.....                              | 89  |
| Figure 4.4 actual and simulated 50 mm step response for controlled servo-hydraulic system – non load case.....                              | 89  |
| Figure 4.5 Proportional gain vs response speed for non load case.....   | 91  |
| Figure 4.6 Sinusoidal response non load case, 1 Hz – 90 mm.....   | 93  |
| Figure 4.7 Sinusoidal response non load case, 2 Hz – 90 mm.....   | 93  |
| Figure 4.8 Sinusoidal response non load case, 5 Hz – 50 mm.....   | 94  |
| Figure 4.9 Sinusoidal response non load case, 8 Hz – 20 mm.....   | 94  |
| Figure 4.10 Sinusoidal response non load case, 10 Hz – 20 mm.....   | 95  |
| Figure 4.11 Sinusoidal response non load case, 15 Hz – 10 mm.....   | 95  |
| Figure 4.12 Controlled servo-hydraulic system frequency response function estimation.....   | 96  |
| Figure 4.13 Servo-hydraulic system frequency response function estimation....   | 97  |
| Figure A-II.1 General structure for controlled servo-hydraulic system block diagram.....  | 101 |
| Figure A-I.2 Displacement transducer block diagram.....   | 102 |
| Figure A-I.3 Controller block diagram.....  | 102 |
| Figure A-II.4 Servo amplifier block diagram.....  | 102 |

---

|  |     |
|--|-----|
| Figure A-II.5 Actuator chambers block diagram.....   | 103 |
| Figure A-II.6 Load block diagram.....  | 103 |
| Figure A-II.7 Linear servovalve block diagram.....   | 103 |
| Figure A-II.8 Non linear servovalve block diagram.....   | 104 |
| Figure A-II.9 Numerical differentiation block diagram.....   | 104 |
| Figure A-VI.1 Visualization charts on controller user interface.....                                       | 111 |
| Figure A-VI.2 System controls on controller user interface.....  | 112 |
| Figure A-VI.3 Operational controls – configuration state user interface.....                               | 115 |
| Figure A-VI.4 Operational controls – control state user interface.....                                     | 117 |
| Figure A-V.1 FPGA block diagram – signal generation stage.....   | 120 |
| Figure A-V.2 FPGA block diagram - amplitude compensation and control stage<br>.....                        | 121 |
| Figure A-V.3 FPGA block diagram – output signalling and output user interface<br>communication stages..... | 122 |



# List of tables

|   |    |
|---|----|
| Table 1 Exciter type vs bandwidth and force amplitude characteristics [2].....  | 10 |
| Table 2-Excitation shape vs signal processing properties [2].....   | 10 |
| Table 2.1 Frequency-Normalized characteristic equations for ITAE Response [16].....   | 43 |
| Table 2.2 Ziegler Nichols frequency response method - PID parameters [15]...  | 51 |
| Table 2.3 Maximum speed for sinusoidal signals at test frequencies and amplitudes .....   | 56 |
| Table 2.4 Pole magnitude of servo-hydraulic transfer function.....  | 58 |
| Table 2.5 Limiting values of derivative time as function of pole magnitude.....   | 59 |
| Table 2.6 Error values on sinusoidal signals with proportional gains for 10% overshoot step responses – Load mass 450 Kg.....                             | 67 |
| Table 2.7 Error values on sinusoidal signals with proportional gains for critical speed step responses – Load mass 0 kg.....                              | 68 |
| Table 2.8 Error values on sinusoidal signals with proportional gain for minimum error – Load mass 450 kg.....   | 68 |
| Table 2.9 Error values on sinusoidal signals with proportional gains for critical speed step responses and amplitude compensator - Load mass 0 kg.....    | 70 |
| Table 2.10 Error values on sinusoidal signals with proportional gains for minimum error step responses and amplitude compensator – Load mass 450 kg ..... | 70 |
| Table 2.11 Inputs and output signal requirements for the servo-hydraulic system controller device.....  | 72 |
| Table 2.12 Power requirements for servo-hydraulic controller device.....  | 75 |
| Table 4.1 Time domain performance parameters for step input response at different amplitude values – non load case.....                                   | 90 |
| Table 4.2 Frequency and amplitude conditions for sinusoidal tests non load case .....   | 92 |

# Introduction

In order to study the dynamic response of complex structures submitted to loading conditions, there are different methodologies used to evaluate their behaviour. Analytical and numerical approaches were the first to be used but so often those are not able to obtain accurate and reliable models when high complex systems are studied, even if the structure has a global linear behaviour. This problematic has been overcome with experimental techniques, where the characterization in real conditions is obtained by the processing and analysis of measurements undertaken into the structure.

Experimental modal analysis (EMA) is the area of structural dynamics who deals with the methodologies and techniques necessary to evaluate the behaviour of structures using experimental approaches. The idea on EMS is submit the object of study to a know controlled excitation and measure the response of the system through adequate sensors; once bot set of data are recorded is possible to obtain the modal parameters that describe the structure behaviour using different modal identification methods whose application depends on either on estimates of frequency response functions (FRF) or impulse response functions (IRF), obtained through the inverse Fourier transform [1]. The identification method is selected according the domain of application (time or frequency), if the formulation is indirect or modal and direct, the number of modes analysed, and the number of inputs and the type of estimates [1]; finding methods in frequency domain like rational fraction polynomial (RFP), complex exponential frequency domain (CEFD), polyreference frequency domain (PRFD); and those in time domain like complex exponential (CE), least square complex exponential (LSCE), polyreference complex exponential (PRCE), Ibrahim time domain (ITD), eigen system realization algorithm (ERA) and autoregressive moving-average (ARMA) [1]. An additional type of modal identification method widely used on evaluation of large structures is called tuned-sinusoidal methods where a sinusoidal excitation is imposed into the structure at each natural frequency.

On EMA techniques, no matter which experimental approach is used, the excitation and it's correspondent excitation system is a core stone on modal analysis, therefore the obtained results through the chosen methodology reflect the characteristics and behaviour of the exciter system used. Intrinsically, such situation determines the exciter evaluation and selection in two different ways:

- Device characteristics: the physical characteristics of the devices used as exciter establish different ranges of application in terms of force amplitude and bandwidth. Table 1 summarizes the ranges of application for common exciter types used on modal analysis for large structures.

- Excitation signal shape: signal shape affects the estimation of the dynamic structural parameters in terms of the following signal properties [2]:
  - Analysis speed: amount of data necessary to obtain concrete results.
  - Leakage error: possibility to have leakage on the signal.
  - Linear approximation: possibility of have linear results by the implementation of this excitation shape.
  - Signal to noise (S/N) ratio: measure that compares the level of the signal to the level of background noise.
  - Spectrum control: capacity to limit the excitation to a suitable frequency range.

Table 1 Exciter type vs bandwidth and force amplitude characteristics [2]

| Attachment   | Exciter type            | Bandwidth          | Force amplitude |
|--------------|-------------------------|--------------------|-----------------|
| Attached     | Shaker                  | High (up to 5 kHz) | Low             |
|              | Hydraulic servoactuator | Low (limited)      | High            |
|              | Vibrodyne               | High               | Medium          |
| Non attached | Impact hammer           | High               | Medium          |
|              | Pendulum                | Low                | Medium          |
|              | Acoustic                | Medium             | Low             |

Table 2-Excitation shape vs signal processing properties [2]

|                 | Analysis speed | Leakage error                | Linear approximation | S/N ratio   | Spectrum control |
|-----------------|----------------|------------------------------|----------------------|-------------|------------------|
| Sinusoidal      | Very slow      | Yes                          | No                   | Good        | High             |
| Random          | Slow           | Yes                          | Yes                  | Fair        | High             |
| Pseudo random   | Fast           | No                           | No                   | Fair        | High             |
| Impact          | Fastest        | No (with exponential window) | No                   | Poor        | Limited          |
| Multiple impact | Slow           | Yes                          | Some                 | Poor - fair | Limited          |

Table 2 shows the limitations of different signal shapes according to the stated signal properties.

A complete evaluation of both group of characteristic has to be made in order to choose the best exciter and excitation signal. However there is a relationship between the allowable excitation shapes according to the exciter type. Thus, the exciter selection becomes a compromise between those characteristics.

## **Objectives**

The aim of the present work is to develop a control system for a servo-hydraulic system composed by a linear hydraulic actuator and a double stage servovalve, in order to be used as an attached hydraulic servoactuator exciter. Such system are typically used as exciter for EMA on large structures like bridges, arenas and stadiums, among others [1].

The overall controlled system (which includes the controller and the servo-hydraulic system), must be able to operate in the frequency range between 0 to 10 Hz, and exert forces up to 9.8 kN (limited by the characteristics of the available actuator). The controller must execute a position control of the hydraulic actuator in order to generate step signals at different amplitude levels, and sinusoidal wave form signals with frequencies inside the expected frequency range.

The present work is structured as follows:

Chapter 1 explains the servo-hydraulic system composed by the linear hydraulic actuator and a double stage servovalve, showing the operational characteristics of such devices, and presenting a detailed mathematical model about the system, defining a start point for the design of the controller.

Chapter 2 shows the controller design process, stating from the selection of the most suitable control methodology, passing through the simulation stage in order to verify the behaviour of the controlled system under the selected control methodology, and finishing with a final real time controller implementation.

Chapter 3 offers a detailed explanation of each component of the controlled system placed in a test rig, including the physical controller, the hydraulic actuator, the double stage servovalve, the linear variable differential transformer (LVDT) used as a position transducer in the system, among others.

Chapter 4 shows the experimental results carried on the experimental test rig, using different load and input signal conditions.

---

At the end, the conclusions collect all the theoretical and experimental experiences related to the controller design and implementation, and future suggested works that can be developed in order to enhance the characteristics of the solution presented along this work.

# Chapter 1 Servo-hydraulic system

Experimental modal analysis (EMA) makes use of excitation (input) and response (output) measurements obtained from an excited structure in order to estimate the modal parameters that describes the structure behaviour, conducted through frequency response function (FRF) or impulse response function (IRF) estimations. To obtain either the FRF or IRF estimations, is requested a controlled artificial excitation able to deliver to the structure enough energy to excite the flexible modes contained at an specific range of frequencies. Different technologies have been used along years to construct the devices which carry out the excitation work, where electrical and hydraulic branches are the most typical ones.

Servo-hydraulic exciters are a combination of both technologies, where the power system is conceived through hydraulic elements, while the command process is carried by a sort of electrical and electronic components coupling the hydraulic state variable to be commanded. Servo-hydraulic systems offer an excellent compromise between the amount of work in terms of stroke force or transmission torque, stability and controllability, allowing the imposition of considerable amounts of work into the structure to be evaluated neglecting the barrier imposed by the stiffness of the structure, in a frequency range where the most of modal analysis for large structures are developed.

Those systems are basically composed by two different elements, a hydraulic actuator which is considered as the power element of the system, and a servovalve which commands the actuator.

## 1.1 Hydraulic actuator overview

An hydraulic actuator is an hydraulic power device, which converts hydraulic into mechanical energy (work), with a physical behaviour shown either in force – linear displacement or torque – angular displacement relationship. The hydraulic power is obtained by means of a pressurized fluid flowing through the actuator at a variable flow rate allowing different force/torque and displacement values. In order to obtain the required flow characteristics, servovalves are included into the hydraulic circuit before the actuator, allowing the control of position and/or force/torque into the power devices. The hydraulic actuator - servovalve is one the most used configurations into controlled hydraulic power systems, and is widely know up to the point to understand both of them as a single device. However is important to differentiate one device from the other, as their working principles, functionality and technological characteristics are not the same. Hydraulic actuators are classified according to their displacement characteristics,

defining linear and rotational actuators. In both cases, the work principle and consequent physical laws which describe the dynamics of the devices, are similar and equivalent. The difference lays in the degree of freedom useful for mechanical proposes therefore, their application field. Figure 1.1 shows some rotational and linear hydraulic actuators. Their characteristics are not so different in accordance to their similar work principles except for the length – width ratio. Linear actuators are slender than rotational ones, for similar power levels. That obeys to a necessary hydraulic stiffness necessary into the motion direction in order to assure the stability of the device.



Figure 1.1 Different hydraulic actuator types (A) rotational, (B) linear [3], [4]

Lineal hydraulic actuators are used in a wide range of applications in the fields robotics, aeronautics, industrial machinery and testing devices where modal analysis methodologies have their application area; due to their characteristics in load application (mono directionality), and the useful load capability at a certain frequency range developing a precise lineal positioning when the actuator belongs to a system with an adequate control system. Rotational hydraulic actuators are also widely used in construction engineering, agricultural, industrial and transportation machinery but preferred by their high load capability with a low energy consumption. Even rotational actuator are well also know as hydraulic motors, and their constructive configurations includes an

internal gearbox in order to amplify/reduce torque and speed according to the application needs.

### 1.1.1 Linear hydraulic actuator characteristics

In general terms, a linear hydraulic actuator is a system where two separated synchronous hydraulic chambers are defined by the assembly of a circular piston and a hollow housing. These chambers are fulfilled by a pressurized incompressible fluid in order to exert a displacement along the axial piston dimension, and a force proportional to the differential pressure acting on the piston effective areas.

Linear hydraulic actuators can be classified according to their function. Figure 1.2 shows schematically this classification and describes the way how those elements are represented. Two mayor groups result:

- Single acting actuators: the fluid exerts a pressure only in one side of the cylinder during the displacement. A spring or an external load is used to return the piston to its original position. This kind of actuator is able to apply an effective hydraulic force just on the pushing direction.
- Double acting actuators: the fluid exerts a pressure in both chambers, so the force can be driven in both stroke directions. If the piston exits just on one housing's face is denominated double acting – single rod while if happens in both faces is know as double acting – double rod actuator.

Double acting rather than single acting actuators, are preferred on modal analysis methodologies due to their versatility in carry load in both stroke directions allowing the possibility to reproduce different type of controlled excitations as sine, square and sweep sine waves. Further explanations will take into account just double acting actuators.

Regardless the double acting actuator type, the components and functional principles are similar. Single rod case can be thought as a case of double rod actuator where one spool side is not included. As double rod type can be understood as the general case, descriptions and explanations covered from here and beyond will represent this kind of device.

Schematically, the Figure 1.3 represents the main components and characteristics of a double acting linear hydraulic actuator. As was described before the main components are the housing and the circular piston. This must be enough to define theoretically an actuator but in physical terms is not totally



true because is necessary to avoid metal-metal contact between the elements and avoid the leakages between chambers and environment. In order to correct these situation low friction gaskets are placed in the interaction points (tribological joints) between the piston and housing.

Regardless the manufacturer, those elements are almost standard for this kind of actuator's configuration. Further elements has been included along years to enhance the performance (as reducing friction losses, assuring no leakage which determines no flow and pressure losses within and through the chambers ) or the device capabilities (as position measuring, force measuring).

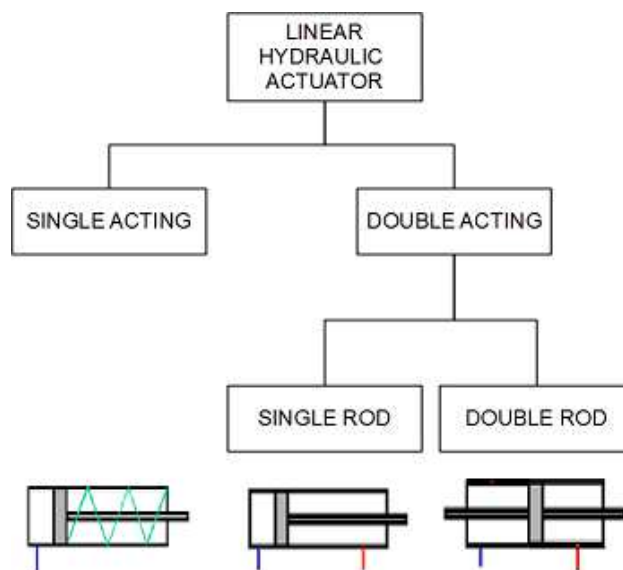


Figure 1.2 Linear hydraulic actuator's functional classification

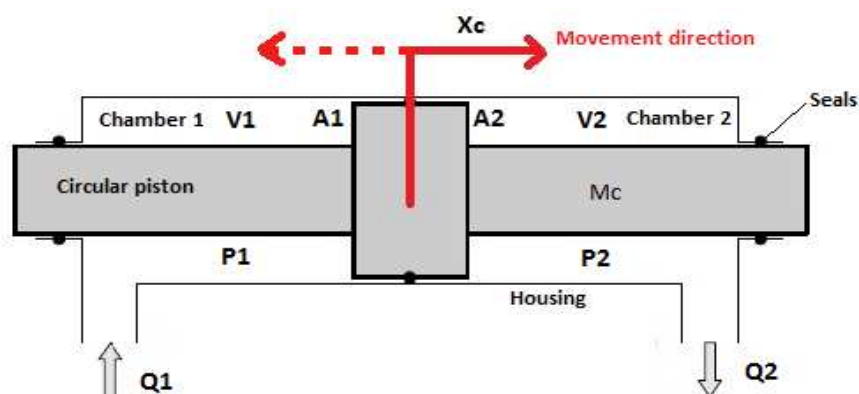


Figure 1.3 Schematic representation of double acting - double rod linear hydraulic actuator

### 1.1.2 Linear hydraulic actuator dynamics

There are two physical principles which describe the linear hydraulic actuator:

- Continuity at steady state temperature: Describes how the fluid behaves along the time on each actuator's chamber. No temperature variations on the fluid are taken into account as the temperature remains constant once the steady state temperature is reached.
- Newton's second law: Describes the dynamics between the actuator and load rigid bodies.

The continuity general equation at steady state temperature is as follows:

$$Q_{inp} - Q_{out} = \frac{dV}{dt} + \left(\frac{V}{\beta}\right)\left(\frac{dP}{dt}\right) \quad (1.1)$$

where:

$Q_{inp}$  : Flow entering into a chamber, in  $m^3/s$  .

$Q_{out}$  : Flow going out from a chamber, in  $m^3/s$  .

$\beta$  : Isothermal bulk modulus, in  $N/m^2$

Based on Figure 1.3, and applying eq.(1.1) on chamber 1, is obtained:

$$Q_1 - C_{il}(P_1 - P_2) = \dot{V}_1 + \left(\frac{V_1}{\beta}\right)(\dot{P}_1) \quad (1.2)$$

$$Q_1 - C_{il}(P_1 - P_2) - C_{el}P_1 = \dot{V}_1 + \left(\frac{V_1}{\beta}\right)(\dot{P}_1) \quad (1.3)$$

where:

$Q_1$  : Flow through linear hydraulic actuator chamber 1 port.

$C_{el}$  : External leakage coefficient.

$C_{il}$  : Internal leakage coefficient.

$V_1$  : Instantaneous linear hydraulic actuator chamber 1 volume.

$P_1$  : Linear hydraulic actuator pressure in chamber 1.

$P_2$  : Linear hydraulic actuator pressure in chamber 2.

where eq.(1.2) and eq.(1.3) are specified for a double acting - single rod and double acting - double rod respectively. From eq.(1.2) and eq.(1.3) is possible to obtain a single equation for chamber 1 which fits for any possible case on a double acting actuators, as is represented in eq.(1.4)

$$Q_1 - \hat{C} P_1 + C_{il} P_2 = \dot{V}_1 + \left(\frac{V_1}{\beta}\right)(\dot{P}_1) \quad (1.4)$$

where:

- $\hat{C}$  : Integrated leakage coefficient.
- $\hat{C} = C_{il} + C_{el}$  if is a double rod actuator
- $\hat{C} = C_{il}$  if is a single rod actuator

Applying eq.(1.1) on chamber 2, is obtained:

$$-Q_2 + C_{il}(P_1 - P_2) - C_{el} P_2 = \dot{V}_2 + \left(\frac{V_2}{\beta}\right)(\dot{P}_2) \quad (1.5)$$

where:

- $Q_2$  : Flow through linear hydraulic actuator chamber 2 port, in  $m^3/s$ .
- $V_2$  : Instantaneous linear hydraulic actuator chamber 2 volume, in  $m^3$ .

Eq.(1.5) models chamber 2 in every case.

Assuming a centred actuator position at time zero, the following geometrical relationship is constructed

$$V_1 = V_0 + A_1 X_c \quad (1.6)$$

$$V_2 = V_0 - A_2 X_c \quad (1.7)$$

where:

- $A_1$  : Linear hydraulic actuator active-force cross sectional area in chamber 1.
- $A_2$  : Linear hydraulic actuator active-force cross sectional area in chamber 2.
- $V_0$  : Linear hydraulic actuator chambers volume.
- $X_c$  : Linear hydraulic actuator position.

Combining eq.(1.6) and eq.(1.7) into eq.(1.5) and eq.(1.4) and neglecting the higher order terms, the final equations which describe the fluid dynamic behaviour of the actuator are:

$$Q_1 - \hat{C} P_1 + C_{il} P_2 = A_1 (\dot{X}_c) + \left(\frac{V_0}{\beta}\right)(\dot{P}_1) \quad (1.8)$$

$$-Q_2 + C_{il}(P_1 - P_2) - C_{el} P_2 = -A_2 (\dot{X}_c) + \left(\frac{V_0}{\beta}\right)(\dot{P}_2) \quad (1.9)$$

In order to model both chamber together, the chambers pressures and flows are joined respectively, obtaining two variables:

- Load pressure  $P_l$ : Defined as the axial differential pressure on actuator's rod as shown in eq.(1.10).
- Load flow  $Q_l$ : Defined as the mean flow passing through the actuator, as shown in eq.(1.11)

$$P_l = P_1 - P_2 \quad (1.10)$$

$$Q_l = \left( \frac{Q_1 + Q_2}{2} \right) \quad (1.11)$$

As the system is bounded by flow and pressure characteristics, the chamber pressures are related to supply pressure in the following way:

$$P_s = P_1 + P_2 \quad (1.12)$$

determining the characteristic equation

$$Q_l + P_s \dot{C}_2 - P_l \dot{C}_1 = A_{Hl} \dot{X}_c + \frac{V_0}{2\beta} \dot{P}_l \quad (1.13)$$

where:

$P_s$  : System supply pressure.

$$\dot{C}_1 = (C_{el} + \hat{C} + 3C_{il})/4$$

$$\dot{C}_2 = (C_{il} + C_{el} - \hat{C})/4$$

$$A_{Hl} = (A_1 + A_2)/2$$

The Newton's second law is applied to model on Figure 1.4

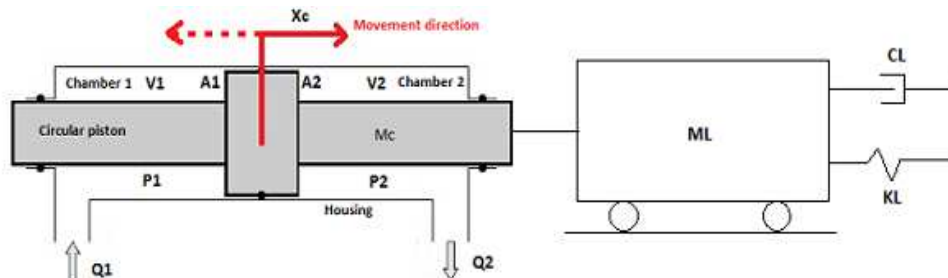


Figure 1.4 Mechanical and linear actuator schematics

leading the following equation, in terms of chamber pressures.

$$(M_l + M_c) \ddot{X}_c + C_l \dot{X}_c + K_l X_c = (P_1 A_1) - (P_2 A_2) - F_f \quad (1.14)$$

where:

- $M_c$  : Linear hydraulic actuator piston mass.
- $M_l$  : Attached load mass.
- $C_l$  : Attached load viscous damping coefficient.
- $K_l$  : Attached load stiffness coefficient.
- $F_f$  : Friction force.

Eq.(1.15) describes the model in terms of load and supply pressure as result of the combination of eq.(1.10) and eq.(1.12) into eq.(1.14). The expression which defines the friction force, is defined in a generic way, thus particular models can be included in order to calculate the friction force values. According to the approach the friction models can be static models as Striebeck or Tustin [5], or dynamic as Luge [6].

$$(M_l + M_c) \ddot{X}_c + C_l \dot{X}_c + K_l X_c = P_s \frac{(A_1 - A_2)}{2} + P_l \frac{(A_1 + A_2)}{2} - F_f \quad (1.15)$$

No friction effects are included in the current dynamic model assuming that the friction forces are neglectable compared to carry load forces. The assumption is correct due to the actuator technological characteristics where materials and sliding systems has been developed along years by manufacturers, reducing the friction coefficients and assuring really low friction forces. Including  $\overset{\circ}{M} = M_l + M_c$  and  $\overset{\circ}{A}_{H2} = (A_1 - A_2)/2$ , eq.(1.16) represents the model without the friction force.

$$\overset{\circ}{M} \ddot{X}_c + C_l \dot{X}_c + K_l X_c = P_s \overset{\circ}{A}_{H2} + P_l \overset{\circ}{A}_{H1} \quad (1.16)$$

Summarizing, the actuator dynamic model is represented by eq.(1.13) and eq.(1.16), representing both physical principles which govern the actuator actual behaviour, continuity at steady state temperature and Newton's second law respectively.

## 1.2 Hydraulic actuator overview

A servovalve is a device which allows volumetric flow variation along the time as function of an electrical command input. The variation of load flow also represents a variation of load pressure, which makes this kind of device a powerful system in order to control hydraulic flow-pressure power systems as hydraulic actuators and motors.

### 1.2.1 Servovalve characteristics

Servovalves are classified according to functional characteristics, highly related with constructive concerns. As matter of fact, in all the servovalve types the electrical input signal commands a permanent magnet torque motor; and the valve type which delivers the flow to the hydraulic power system is always a spool valve. In this order of ideas, is possible to recognize two groups according to the amount of stages the valve has:

- Single stage valves: have a singular valve which delivers the flow to the hydraulic power system and is directly attached to the permanent magnet torque motor. The way it works is the simplest one but has the drawback of a limited flow capacity leading to stability problems.
- Double stage servovalves: have a configuration where the permanent magnet torque motor is attached to the first stage valve which works as a flow multiplier; this is connected to the second stage valve which delivers the flow to the hydraulic power system. Finally, between both stages exists a feedback mechanism in order to establish a dynamic connection between them. The drawback observed in single stage valves is overcome with double stage servovalve.

Figure 1.5 shows schematically both single and double stage servovalves.

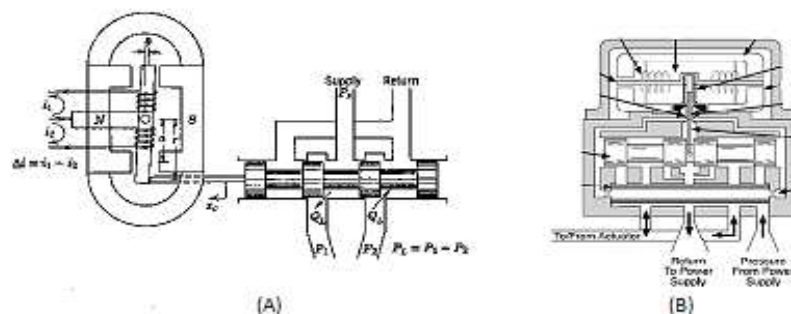


Figure 1.5 Schematic representation of (A) single stage servovalves and (B) double stage servovalves

Figure 1.6 represents the servovalve classification according to functional characteristics. The two stage servovalves present two classification groups, one related to first stage valve type and the according to mechanical feedback technology.

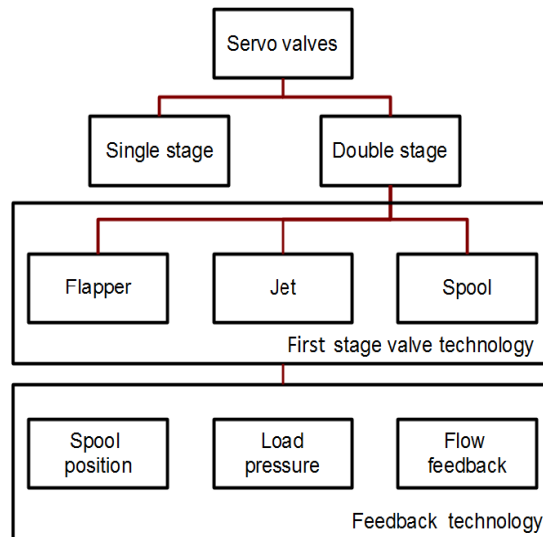


Figure 1.6 Functional servovalve classification

Despite the flexibility in the first stage configuration, flapper valves are the most extensively used in two stage servovalves. Some reasons which supports this choice are the relative low sensitivity to fluid contamination and no so tight constructive tolerances (which represents a lower production cost) compared to spool valves, and a predictable performance and faster response compared to jet valves. In the same idea, feedback technology plays an important role into the definition of servovalve characteristics and performance. The way how both stages are linked establishes different flow-pressure behaviours, so despite the almost non flexibility caused by the preferred flapper – spool configuration, the way how the feedback has been chosen allows to have different behaviours.

There are three feedback technological groups, defined by the measure used to verify the state of the servovalve, and exert a feedback represented as a recovering torque in the motor armature.

- Spool position feedback: is the most common feedback type, where the spool position of second stage valve is measured. Three basic types of measurement methodologies are used in order to obtain the spool position:

- Spring centred spool: uses a pair of springs placed at the spool ends centring the spool against the pressure differential of the pilot stage.
- Direct feedback: uses a configuration where the spool follows the first stage by means of a so called hydraulic follower in a one to one relationship.
- Force feedback: uses a spring to which is deflected by the spool displacement. The deflection in the spring generates a force which is the measurement which feedbacks the system.
- Load pressure feedback: some internal passages direct the load pressure into the first stage obtaining a resulting force balancing the armature torque.
- Flow feedback type uses a device to measure the flow and covert it into force to develop the same action.

Load pressure and flow feedback technologies establish particular flow-pressure relationships, different to those square root shaped developed by spool position feedback. Figure 1.7 shows different flow-pressure behaviours obtained through different feedback technologies. A squared root relationship lies between flow and pressure in position feedback (A). Applications where an almost constant pressure at a fixed rated current is requested are obtained through load pressure feedback (B), while almost constant flow at a fixed rated current are fitted with flow feedback (C). A combination of flow and pressure feedback methodologies defines the so called pressure-flow servovalves which have quite linear flow-pressure characteristics in between flow and pressure types [7].

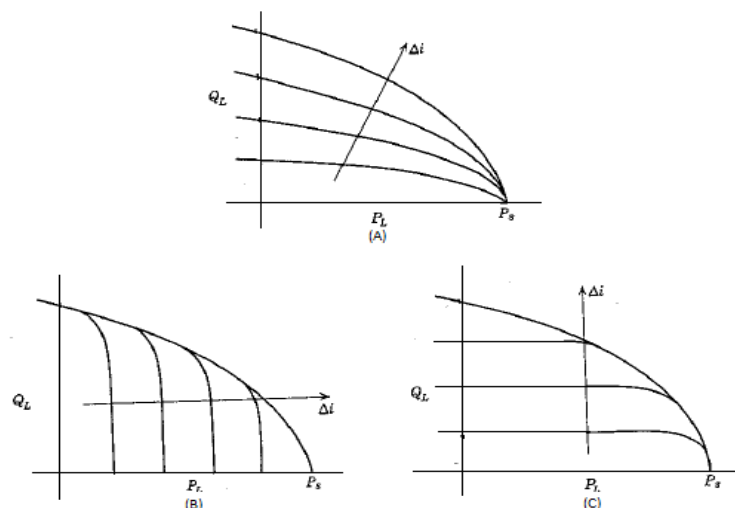


Figure 1.7 Flow-pressure characteristic for different feedback technologies [7]



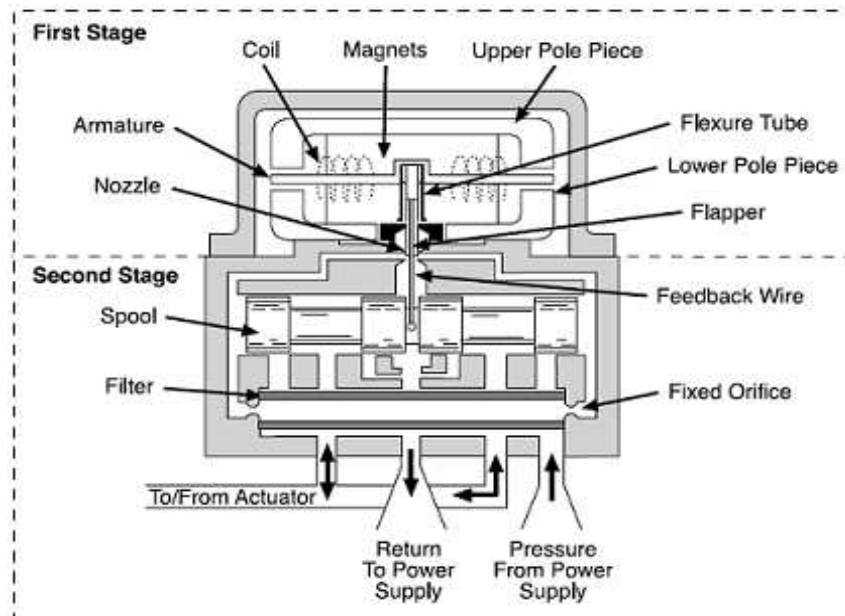


Figure 1.8 Schematic representation of a double stage flapper and spool servovalve with force feedback[8]

Summarizing, a two stage servovalve is composed by a permanent magnet torque motor, a first stage flapper valve, a second stage spool valve and a feedback element as shown in Figure 1.8. The torque motor consist of an armature mounted on a thin-walled sleeve pivot and suspended in the air gap of a magnetic field produced by a pair of permanent magnets. Once a current is applied into the armature coils a force is generated in the armature ends due to the presence of the magnetic field generated by the pair of permanent magnets. Those forces set a torque into the armature-flapper assembly allowing the angular displacement of this assembly about the fixture sleeve. This displacement of the flapper restricts the flow passing through one of the nozzles into the first stage valve changing the differential pressure between the two ends of the second stage valve and leading its motion inside the valve sleeve.

In the case of a spool position – force feedback system, the motion of the spool forces the deflection of the feedback wire which restores torque on the armature-flapper assembly. When the armature-flapper assembly is centred and the spool is stationary (with an offset respect to its centred position), the servovalve reaches its equilibrium state (when the feedback torque value equals the magnetic forces on the armature). The consequence and final servovalve scope is allow the oil to flow to and from the actuator, by the the opening of flow paths between the pressure and return ports, and the control ports. An schematic

representation of a servovalve at its steady state condition is shown in Figure 1.9.

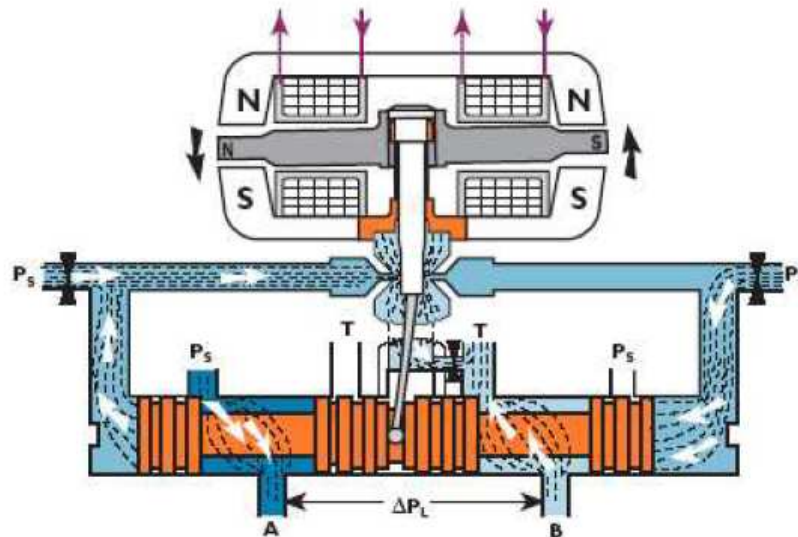


Figure 1.9 Double stage servovalve motion – equilibrium position [9]

Servovalves are widely used to command hydraulic power system due to the proportionality between the input (current) and output (load flow), and no pressure losses. These can be explained because the load flow delivered to the hydraulic power system is proportional to second stage spool position which is also to the electrical command input; and the internal servovalve arrangement have no pressure drops leading to have a constant load pressure for each spool position value.

### 1.2.2 Servovalve dynamics

There are two possible ways to model a servovalve. One uses the work principles for each component in the servovalve and determines its proper dynamic equations, while the other uses the data and equations given by the manufacturer which had been obtained form experimental procedures and reflects the actual device behaviour. The first approach is useful when valve design processes is taking place, while the second fits well when a valve selection is necessary in order to assemble it with an hydraulic actuator.

As referenced in [10], second order models can be used to represent the servovalve dynamics and reconstructed through the data present in frequency response plots given by manufactures as shown in Figure 1.10, without loss of

accuracy. As servovalve behaviour depends on the operation point, plots are obtained at a rated pressure drop through the valve ports, at maximum current applied in the coils and with no load attached, therefore the figure corresponds to the no-load flow  $Q_{NL}$  response to the rated input current  $\hat{I}$ .

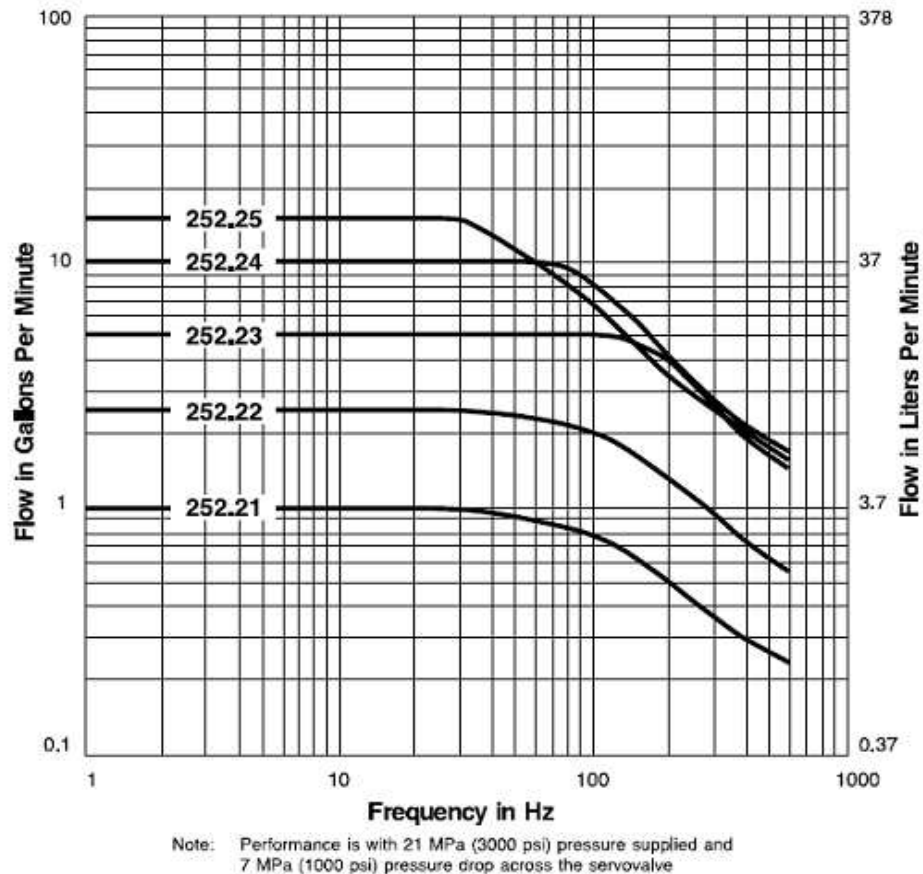


Figure 1.10  $Q_{NL}/(\hat{I})$  frequency response function for double stage servovalves [8]

Second order systems can be described through three parameters, natural frequency, damping ratio and gain, and can be obtained from the frequency response plots. Natural frequency is related to the frequency at -3dB intersection with the curve, while damping ratio is related to the peak amplitude ratio as show in eq.(1.17). The gain is obtained through eq.(1.18) and derives the representation of the servovalve in terms of command input current. Those parameters allow the construction of the dynamic model as represented in eq. (1.19).

$$M_V = \frac{1}{2 \delta_{SV} \sqrt{1 - \delta_{SV}^2}} \quad (1.17)$$

$$K_{SV} = \frac{Q_r}{I_{sat}} \quad (1.18)$$

$$\frac{Q_{NL}''}{\omega_{SV}^2} + 2 \frac{\delta_{SV}}{\omega_{SV}} Q_{NL}' + Q_{NL} = I K_{SV} \quad (1.19)$$

where

$Q_r$  : Servovalve rating flow.

$I$  : Servovalve input command current.

$I_{sat}$  : Permanent magnet torque motor saturation current.

$P_r$  : Servovalve rating pressure, corresponding to servovalve pressure drop.

$\delta_{SV}$  : Servovalve damping ratio

$\omega_{SV}$  : Servovalve natural frequency

$K_{SV}$  : Servovalve gain.

$M_V$  : Peak amplitude ratio

Once the servovalve is attached to a system, the flow is reduced compared to the no-load case due to the pressure across the load. Eq.(1.20) represents the relationship between load flow, no-load flow and load pressure.

$$Q_L = Q_{NL} \sqrt{\frac{P_s - P_l}{P_r}} \quad (1.20)$$

The load flow can oscillate between  $Q_{NL}$  and zero. Zero case is non desired condition with pressure saturation, associated to incorrect selection of the servovalve. In this case the load is higher than the available hydraulic power. To avoid this conditions, during selection process the maximum operative pressure load must be  $2P_s/3$  where maximum power is transferred.

### 1.3 Servo-hydraulic system dynamic simulation

Dynamic simulation step, allows the evaluation and characterization of the servo-hydraulic system, leading to obtain an idea about how the system behaves.

The most simple approach, models the system as a linear time invariant (LTI) system, exploiting the use of certain tools and representations such as System Transfer Function (STF) and the State Space Model (SSM) representation for LTI systems, while a more complex representation, involves a non linear model of the system. Both linear and non linear models are presented in order to compare both characterizations.

#### 1.3.1 Linear approach - Linearisation

Servo-hydraulic systems by definition are non linear on the different stages of the system. One clear example is the servovalve where the load flow is dependent on no-load flow, non linear function of the load pressure  $P_l$ , as observed in eq. (1.20). Other, which was described in eq. (1.14), is the friction force, not taken into account into the model. However there are other non linearities which are not included in the models described in chapters 1.1.2 and 1.2.2, as the non linearity of control flow to input current in the servo valve which becomes most sever in the null region due to variations in the second stage spool valve null cut [9].

Friction and control flow to input current non linearities are not included into the mathematical model of the servo-hydraulic system either by it's neglectable dimension or the particular operational point where the non linearity occurs. However, the feedback servovalve flow-pressure non linearity, defines completely the servovalve dynamics. Linearisation through Taylor's expansion is done, in order to obtain a linearised dynamic model for the device. Eq. (1.21) shows the Taylor expansion expression up the first order term for a multi variable dependent function.

$$f(\underline{X}) \approx f(\underline{A}) + Df(\underline{A})^T (\underline{X} - \underline{A}) + \dots \quad (1.21)$$

where

$f(\underline{X})$  : Multi variable dependent function.

$\underline{X}$  : State vector.

$\underline{A}$  : State evaluation points vector.

The linearisation is done up to the first order as further orders are neglectable. In the load flow case, the state vector and state evaluation points are:

$$\mathbf{X}=[P_s \ P_L \ Q_{NL}]^T \quad (1.22)$$

$$\mathbf{A}=[P_s(a)=P_{s0} \ P_L(a)=2P_{s0}/3 \ Q_{NL}(a)=Q_r]^T \quad (1.23)$$

$$Q_l(P_s, P_l, Q_{NL}) \approx Q_{NL} - \frac{3Q_r P_l}{2P_{s0}} \quad (1.24)$$

Eq. (1.24) represents the linearised model for the servovalve, where each variable does an independent action in the load flow.

### 1.3.2 Linear approach - Space state representation

Despite SSM representation is able to represents non linear and time invariant systems, the LTI model of the servo-hydraulic system is used, in order to obtain an idea of the system, and evaluate if a linear model is able to represent the system in a proper way. SSM representation of a dynamic system is shown in Eq. (1.25) and (1.26),

$$\dot{\mathbf{z}}(t)=[\mathbf{A}]\mathbf{z}(t)+[\mathbf{B}]\mathbf{u}(t) \quad (1.25)$$

$$\mathbf{y}(t)=[\mathbf{C}]\mathbf{z}(t)+[\mathbf{D}]\mathbf{u}(t) \quad (1.26)$$

where

$\mathbf{z}(t)$  : State vector, dimension [n x 1].

$\mathbf{y}(t)$  : State output vector, dimension [q x 1].

$\mathbf{u}(t)$  : Input vector, dimension [p x 1]

$[\mathbf{A}]$  : State matrix, dimension [n x n].

$[\mathbf{B}]$  : Input matrix, dimension [n x p].

$[\mathbf{C}]$  : Output matrix, dimension [q x n].

$[\mathbf{D}]$  : Feed-through or feed-forward matrix , dimension [q x p].

Recalling eq.(1.13), (1.16), (1.19), and (1.24) combining and organizing terms is possible to define the eq.(1.27) to (1.31), necessary to establish the SSM representation.

$$\ddot{X}_c = \frac{1}{M} [-C_l \dot{X}_c - K_l X_c + P_l \overset{\circ}{A}_{H1} + P_s \overset{\circ}{A}_{H2}] \quad (1.27)$$

$$\dot{X}_c = \dot{X}_c \quad (1.28)$$

$$\dot{P}_l = \frac{2\beta}{V_0} [-\overset{\circ}{A}_{H1} \dot{X}_c - P_l \overset{\circ}{C}_H + Q_{NL} + P_s \overset{\circ}{C}_2] \quad (1.29)$$

$$\ddot{Q}_{NL} = -2\delta_{SV} \omega_{SV} \dot{Q}_{NL} - \omega_{SV}^2 Q_{NL} + I K_{SV} \quad (1.30)$$

$$\dot{Q}_{NL} = \dot{Q}_{NL} \quad (1.31)$$

where

$$\dot{C}_H = \dot{C}_1 + \frac{3Q_r}{2P_s} \quad (1.32)$$

Being interested in piston position  $X_c$ , and no feed-forward is contemplated for the servo-hydraulic system, the matrices and vectors are

$$\underline{z}(t) = \begin{pmatrix} \dot{X}_c \\ X_c \\ P_l \\ \dot{Q}_{NL} \\ Q_{NL} \end{pmatrix} = \begin{pmatrix} X_1 \\ X_2 \\ X_3 \\ X_4 \\ X_5 \end{pmatrix} \quad \underline{u}(t) = \begin{pmatrix} P_s \\ I \\ Q_r \end{pmatrix} = \begin{pmatrix} u_1 \\ u_2 \\ u_3 \end{pmatrix}$$

$$[A] = \begin{bmatrix} -\frac{C_l}{\dot{M}} & -\frac{K_l}{\dot{M}} & \frac{\dot{A}_{H1}}{\dot{M}} & 0 & 0 \\ 1 & 0 & 0 & 0 & 0 \\ -\frac{2\dot{A}_{H1}\beta}{V_0} & 0 & -\frac{2\dot{C}_H\beta}{V_0} & 0 & \frac{2\beta}{V_0} \\ 0 & 0 & 0 & -2\delta_{SV}\omega_{SV} & -\omega_{SV}^2 \\ 0 & 0 & 0 & 1 & 0 \end{bmatrix}$$

$$[B] = \begin{bmatrix} \frac{\dot{A}_{H2}}{\dot{M}} & 0 \\ 0 & 0 \\ \frac{2\beta\dot{C}_2}{V_0} & 0 \\ 0 & \omega_{SV}^2 K_{SV} \\ 0 & 0 \end{bmatrix}$$

$$[C] = [0 \ 1 \ 0 \ 0 \ 0]$$

$$[D] = [0 \ 0 \ 0 \ 0 \ 0]$$

### 1.3.3 Linear approach - System transfer function representation

Applying the Laplace transform to eq. (1.25) and (1.26), and rearranging terms is obtained:

$$z(s) = (s[I] - [A])^{-1}[B]u(s) \quad (1.33)$$

$$y(s) = [C](s[I] - [A])^{-1}[B]u(s) + [D]u(s) \quad (1.34)$$

In Laplace domain, the transfer function concept is defined as:

$$y(s) = [G(s)]u(s) \quad (1.35)$$

so

$$[G(s)] = [C](s[I] - [A])^{-1}[B] + [D] \quad (1.36)$$

An easy visualization of STF representation is done through block diagram as shown in Figure 1.11. Block diagrams, are graphical representations which easily show the relationship between inputs and the outputs of the system.

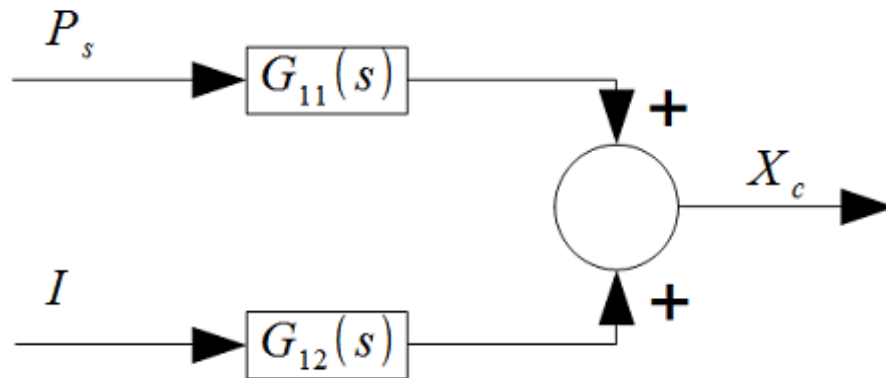


Figure 1.11 Block diagram of the servo-hydraulic system

In the case of the servo-hydraulic system, there are three transfer functions according to the amount of inputs and outputs the system.  $G_{11}(s)$  is the piston position to supply pressure transfer function  $X_c/P_s = X_2/u_1$ ,  $G_{12}(s)$  corresponds to cylinder position to armature current transfer function  $X_c/I = X_2/u_2$ , and  $G_{13}(s)$  is piston position to rated flow transfer function  $X_c/Q_r = X_2/u_3$ .

As transfer functions are rational functions, it is possible to interpret as:



$$G_{11}(s) = \frac{Num_{G_{11}(s)}}{Den_{G(s)}} ; G_{12}(s) = \frac{Num_{G_{12}(s)}}{Den_{G(s)}} ; G_{13}(s) = \frac{Num_{G_{13}(s)}}{Den_{G(s)}} \quad (1.37)$$

where:

$$\begin{aligned} (s[I] - [A]) = Den_{G(s)} &= (s^3 \tau_3 + s^2 \tau_2 + s \tau_1 + \tau_0) \left( \frac{s^2}{\omega_{SV}^2} + 2 \frac{\delta_{SV}}{\omega_{SV}} s + 1 \right) \quad (1.38) \\ \tau_3 &= \dot{M} V_0 ; \quad \tau_2 = C_l V_0 + 2 \dot{M} \dot{C}_H \beta ; \\ \tau_1 &= K_l V_0 + 2 C_l \dot{C}_H \beta + 2 A_{HI}^2 \beta \quad \tau_0 = 1 \quad (1.39) \end{aligned}$$

The transfer function denominator is composed by two polynomials, one determined by the actuator and the attached load, and other by the servovalve. Neglecting load stiffness and viscous damping coefficient, the characteristic equation of the system is represented as

$$Den_{G(s)} = s \left( \frac{s^2}{\omega_H^2} + 2 \frac{\delta_H}{\omega_H} s + 1 \right) \left( \frac{s^2}{\omega_{SV}^2} + 2 \frac{\delta_{SV}}{\omega_{SV}} s + 1 \right) \quad (1.40)$$

where

$$\begin{aligned} \omega_H &= \sqrt{\frac{2 A_{HI}^2 \beta}{\dot{M} V_0}} \text{ is the hydraulic actuator natural frequency.} \\ \delta_H &= \frac{\dot{C}_H}{A_{HI}} \sqrt{\frac{\dot{M} \beta}{2 V_0}} + \frac{C_l}{2 A_{HI}} \sqrt{\frac{V_0}{2 \beta \dot{M}}} \text{ is the hydraulic damping ratio.} \end{aligned}$$

therefore

$$G_{12}(s) = \frac{\frac{K_{SV} \omega_{SV}^2}{A_{HI}}}{s \left( \frac{s^2}{\omega_H^2} + 2 \frac{\delta_H}{\omega_H} s + 1 \right) \left( \frac{s^2}{\omega_{SV}^2} + 2 \frac{\delta_{SV}}{\omega_{SV}} s + 1 \right)} \quad (1.41)$$

### 1.3.4 Linear approach – Eigenvalues and transfer function evaluation

On control and dynamics, eigenvalues are the values corresponding to the damped natural frequencies, and allow the study of the stability characteristics of the system.

The eigenvalue calculation comes through the solution of the characteristic equation of the system, hence the eigenvalues are the zeros of this equation. In SSM approach the roots of the characteristic equation are the eigenvalues of the state matrix, while in STF they are the poles of the system transfer function.

Overlooking from the SSM point of view, the eq. (1.42) and (1.43) are the time domain solutions for eq. (1.25) and (1.26).

$$\mathbf{z}(t) = e^{[A]t} \mathbf{z}(0) + \int_0^t e^{[A](t-\tau)} [B] \mathbf{u}(\tau) d\tau \quad (1.42)$$

$$\mathbf{y}(t) = [C] e^{[A]t} \mathbf{z}(0) + [C] \int_0^t e^{[A](t-\tau)} [B] \mathbf{u}(\tau) d\tau + [D] \mathbf{u}(t) \quad (1.43)$$

The solution of  $\mathbf{z}(t)$  depends on  $e^{[A]t}$ . Thus, the characteristic equation of the system depends just on the state matrix  $[A]$ . Recalling the Calley-Hamilton theorem [11], the characteristic polynomial of a matrix A is:

$$\Delta(\lambda) = \det(\lambda[I] - [A]) \quad (1.44)$$

and its eigenvalues are calculated as:

$$\det(\lambda[I] - [A]) = 0 \quad (1.45)$$

On STF approach, the characteristic equation of the system correspond to the system transfer function denominator, as observed in eq. (1.40), and its eigenvalues, called poles of the system, calculated as:

$$\det(s[I] - [A]) = 0 \quad (1.46)$$

Both eq.(1.45) and (1.46) are equivalent, so the solution can be achieved through any of the previous ways, obtaining:

$$s_1 = 0 \quad (1.47)$$

$$s_{2,3} = -\delta_H \omega_H \pm \omega_H \sqrt{\delta_H^2 - 1} \quad (1.48)$$

$$s_{4,5} = -\delta_{SV} \omega_{SV} \pm \omega_{SV} \sqrt{\delta_{SV}^2 - 1} \quad (1.49)$$

In order to have an idea of the behaviour of the system, the transfer function  $G_{11}(s)$  must be evaluated in its characteristic parameters:

- Poles: The study of the poles in the servo-hydraulic systems is just a raw

evaluation about the behaviour of the system and its stability as the hydraulic part depends on the operation point. Particular evaluations must be done in the desired operation points in order to verify the poles. However, there are three groups of poles, two pair of complex conjugated poles, one associated to the servovalve and other to the hydraulic actuator. The other is the zero pole and its presence implies that actuator speed is proportional to servovalve current for slowly varying inputs [5]. This differentiation is important to visualize which element will limit the bandwidth of the controlled system. While the servovalve have almost constant poles, with small variation despite the operation point, the hydraulic actuator poles depends on the load characteristics determined by the load mass, and piston speed.

- **Natural frequencies:** The hydraulic natural frequency establish the overall speed of response of the servo-hydraulic system therefore if fast responses are desired, natural hydraulic frequencies must be larger [7]. For the same actuator, the natural hydraulic is reduced as the load mass is increased so, lower responses are expected as the mass is increased. In other hand, servovalve natural frequency is less conditioning for the servo-hydraulic system performance if the servovalve is not the primary dynamic element in the system achievable if the frequency of the 90 degree phase point is a factor of at least three higher than that of the actuator [10]. If
- **Damping ratios:** the hydraulic actuator damping ratio increases as the load mass increases. If the damping ratio increases to a value in excess of unity (overdamped behaviour) the poles become real negative with one increasing and the other decreasing from the value of  $\omega_H$  [7]. Also the system stability is most critical when damping ratios are lowest, hence the need to have overdamped systems is preferred at expenses of speed on the response.

### 1.3.5 Non linear approach – Space state representation

As expressed in chapter 1.3.2 , non linear and time variant systems can be represented through SSM, by the following equations:

$$\dot{\mathbf{z}}(t) = \mathbf{f}(t, \mathbf{z}(t), \mathbf{u}(t)) \quad (1.50)$$

$$\mathbf{y}(t) = \mathbf{g}(t, \mathbf{z}(t), \mathbf{u}(t)) \quad (1.51)$$

Recalling the state and input vectors defined for the linear SSM case, and the eq. (1.13), (1.16), (1.19) and (1.20), is obtained

$$\dot{X}_1 = \frac{1}{M} [-C_l X_1 - K_l X_2 + X_3 A_{HI}^\circ + u_1 A_{H2}^\circ] \quad (1.52)$$

$$\dot{X}_2 = X_1 \quad (1.53)$$

$$\dot{X}_3 = \frac{2\beta}{V_0} [-A_{HI}^\circ X_1 - X_3 C_H^\circ + X_5 \sqrt{\frac{u_1 - X_3}{u_1}} + u_1 C_2^\circ] \quad (1.54)$$

$$\dot{X}_4 = -2 \delta_{SV} \omega_{SV} X_4 - \omega_{SV}^2 X_5 + u_2 K_{SV} \omega_{SV}^2 \quad (1.55)$$

$$\dot{X}_5 = X_4 \quad (1.56)$$

### 1.3.6 Stability of the servo-hydraulic system

The stability evaluation problem is not just an evaluation to decide if the the system is stable or unstable. Beyond this, it is necessary to define how stable a system is. In order to be able of handle both situations there are two concepts to take into account, absolute and relative stability.

On the field of SISO and LTI systems, absolute stability is the property of the system to obtain bounded outputs or responses for every input to the system which is bounded too. The actual idea of absolute stability, has overcome thanks to the superposition principle, studying independently the two recognized cases, BIBO and asymptotic stabilities, in order to obtain and establish a general criteria and evaluation methods able to determine the stability of the system. Those studies also, have determined that the requirements to satisfy the stability criteria on each stability case are the same in both of the cases, so if a system is BIBO or simply stable implies that is asymptotically stable too [12].

The stability criteria is directly related to the poles or the roots of the characteristic equation of the system. In order to satisfy the stability property, no poles or roots can be located in the right half plane of the s-plane or on the  $j\omega$  axis; it means that a pole, with the structure of a complex number  $s_k = \sigma_k + \omega_k i$ , must have its real part  $\sigma_k$  higher than zero. For practical reasons, three cases has been identified to classify the stability [12]:

- Stable: All poles or roots of the characteristic equation lie in the left plane of s-plane. So  $\sigma_k > 0$  for all  $k=1, 2, 3, \dots, n$ .
- Marginal stable or marginal unstable: No pole lies in the right plane of s-plane and no multiple order poles lie in the  $j\omega$  axis, So  $\sigma_k > 0$  for all  $k=1, 2, 3, \dots, n$  and  $\sigma_k = 0$  for any  $k$  for simple poles.
- Unstable: At least one pole lies in the right plane of s-plane or there are multiple order poles in the  $j\omega$  axis. So  $\sigma_k < 0$  for any  $k=1, 2, 3, \dots, n$ .

As described before, the system is marginal unstable as a zero pole exists, despite the other poles which always have real negative part, as all parameters are always positive. As load mass is increased, the lower hydraulic real pole is moving towards zero, reducing therefore the range of frequencies where the system shows a stable behaviour. The same behaviour is observed with  $\overset{\circ}{C}_H$  which varies according to maintenance conditions of the actuator seals.  $\overset{\circ}{M}$  is limited to the maximum carry load force value, characteristic for each actuator, while  $\overset{\circ}{C}$  depends on constructive and operative conditions, increasing its value according to the damage present in the tribological joint formed by the internal and external seals and the bore of the actuator.

The precedent case, neglects the load stiffness and load damping coefficient, assuming the structure as a rigid body. Just one real configuration represent this case, when no load is attached to the hydraulic actuator, which is the no-load test configuration. The inclusion of structural viscous damping coefficient increases the damping ratio of the system, and moves the hydraulic actuator poles around the hydraulic natural frequency, thus the lower real negative pole is reduced too. Including structural stiffness into consideration, the zero pole disappears bringing neither three real negative poles or a negative pole and a pair of complex conjugated poles with real negative part which represents a low frequency lag.

The lack of information about those parameters is due to the difficulties to estimate them. A trustful estimation of those values require either experimental techniques or finite element simulations with the structure to be evaluated, which is not the propose of this project. For simulation and controller design process, this assumptions are valid.

## **Chapter 2 Control system**

The importance of the excitation in the EMA methodologies explains the need of a control system in order to obtain a reliable, repeatable and customized excitation. In addition, there is a strong relationship between the excitation characteristics and the FRF or IRF estimations, in terms of analysis speed, leakage error, signal to noise (S/N) ratio and spectrum control. Thanks to that, the control system plays an important and active role inside the exciter functional behaviour and special care in the control system design must be taken.

In order to accomplish a desired operation in repeatable conditions on a physical system, the behaviour of the systems must be directed or regulated by any kind of device which establishes a control action through a control methodology.

In the present work, the aim of the control system is allow the servo-hydraulic system to reproduce an specific excitement profile in a certain frequency and amplitude range, along the time. The present chapter shows the controller design process, starting with an overview of different control methodologies, passing through the selection and simulation of the proper control method, in order to obtain an implemented real time controller able to carry a control action in the servo-hydraulic system required for modal analysis.

### **2.1 Automatic control methodologies – state of the art**

Along the history automatic control solutions and methodologies had been formulated, studied, matured and developed, being traced to the ancient water clock in Alexandria, Egypt, or the ancient compass vehicle on the Han Dynasty in China. The first automatic control device is recognized to James Watt who developed the fly ball governor in 1788. On late 19<sup>th</sup> century, theoretical research on control system was initiated by Maxwell in 1868, Roth in 1874 and Hurwit in 1895. On early 20<sup>th</sup> the first control strategies were proposed by Minorsky in 1922 where the PID controller was first formulated. Development on practical algorithms for PID controller adjustment were formulated on 1945 by Ziegler and Nichols being used on present times on industrial applications. Linear feedback control and its study in the frequency domain was established with the work of Nyquist in 1932, Bode in 1945 and Nichols in 1947, and in 1948 Evans proposed the root locus analysis an important achievement on control theory. On mid 20<sup>th</sup> century, further studies opens a new field on control theory called “modern control” thanks to the works developed by Pontryagin in 1956, Bellman in 1957, and Kalman in 1959 with the state space representation. On the 80's decade further control theories were developed, giving origin to robust control and the first traces of optimal control through the investigations

carried by Zames in 1981 and Doyle in 1989 [13]. Nowadays, the research focused on control theories and applications, is in continuous development, facing all the control methodologies created along the time (classic, modern, robust and optimal control), towards better and suitable implementations, and systems with high complexity due to their non linear behaviour.

There are two different control methodologies according to the continuity of the control action applied on the physic system [14]:

- Discrete control: On this type of control, the command action does not control how the controlled system variable behaves. The control action can be achieved through timing where the individual control actions take place through fixed time schedule; or through events where a control action can start just when the precedent activity have finished. Such control structure is also know as logic or sequential control, because in order to develop a complete task a sequential development of control actions executes the task on the physical system.
- Continuous control: the command action controls the system along the time, using transducers in order to have a measure about the status of the variable. Such control methodology is also know as feedback control.

### **2.1.1 Feedback control**

The feedback control is based on the feedback principle where actual or precedent information about a phenomenon influences the same phenomenon in present or future. Feedback is a process which is present in nature and can be observed everywhere. Thermal body regulation is clear example of a feedback process, in order to keep a constant temperature inside the body, different cells and organs in the body, take a measure of the internal temperature and according to the actual state and the ideal state, activates other organs in order to cool down or heat up the body. Industrial applications uses the same feedback principle in order develop controllers able to achieve specific tasks on displacement, speed, acceleration, flow among other variables.

A feedback controlled process is shown in Figure 2.1. The controlled variable  $y$  is measured along time in order to be referenced with the set-point variable  $y_{sp}$  which determines the expected behaviour of the control variable.

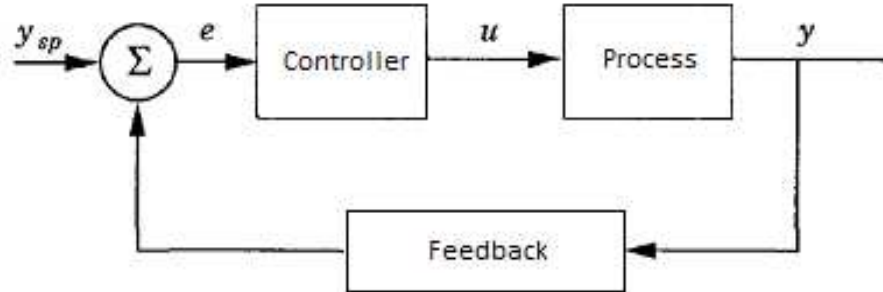


Figure 2.1 Feedback controlled process

Different controlled systems can be obtained according to the type of feedback present in the systems. Two possible cases can occur:

- Positive feedback: if a change occurs in a variable the response is to change that variable even more in the same direction that results in a unstable condition. Is commonly used in applications where the variable is required to go far from a stable condition, or such unstability is a property required. Chemical industry uses the positive feedback in order to increase the rate of reactions for specific processes. On motion mechanical control, no controller with positive control loop is used.
- Negative feedback: the controlled variable moves in opposite direction to the set-point process variable therefore the controlled variable increases when it is smaller than the set-point variable, and decreases when it is larger than the set-point value [15]. This type of feedback is particularly useful as the controlled variable comes close the set-point variable despite the variation of the process. Negative feedback is widely used to control mechanical systems.

The use of feedback control became necessary as the servo-hydraulic system presents a marginal unstable condition originated by the presence of a zero pole in the system transfer function, as explained in Chapter 1. To achieve the desired stable frequency range where the modal analysis will take place, an adequate control algorithm or methodology who takes advantage of the benefits of negative feedback, must be selected.



### 2.1.2 PID control algorithm

Since its formulation in 1922 by Minorsky, and its development on 1945 by Ziegler and Nichols, the PID control algorithm has become the most common control algorithm due to the easy and natural analytical understanding of the independent proportional, integral and derivative actions, and the possibility to be operated with few rules of thumb. On industrial applications, PID controllers is the most common algorithm included on control applications, either as stand alone controller or as a part of a hierarchical distributed process control system [15]. PID comes from the initials P – proportional, I – integral and D – derivative, and reflects the possible actions the controller execute to the controller input signal. On a negative feedback controlled system, this input signal is defined as:

$$e(t) = y_{sp}(t) - y(t) \quad (2.1)$$

which is called error calculated as the difference between the set-point value and the actual value of the controlled variable.

The three actions available in the PID controller act on the error input signal as follows:

- P – Proportional action: In this case, the control action is proportional to the control error for small errors. The error tends to become smaller as the proportional gain associated to the proportional control is increased, while the response become more oscillatory as shown in Figure 2.2. If the control error is zero, the control action does have zero value too.

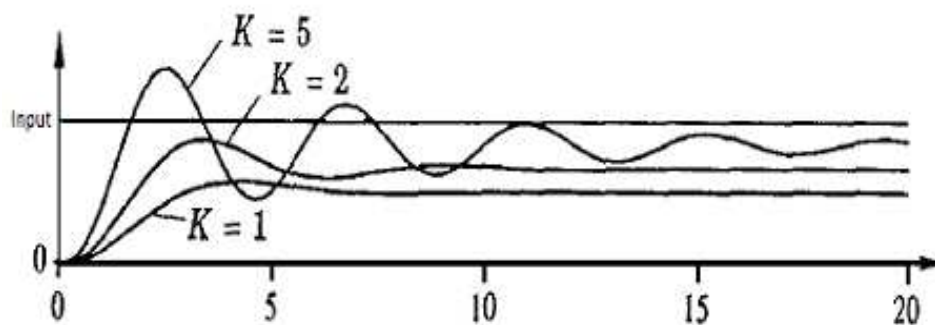


Figure 2.2 Step response for a simulated third order controlled system with proportional action [15]

- I – Integral action: On a proportional control, the error at steady-state condition will always occur. A zero steady-state error value can be achieved using a control which is proportional with the time integral of the error. In such case, a small positive error will always lead to an increasing control signal, and a negative error will give a decreasing control signal no matter how small the error is [15]. The lower the value of the integral time, the faster the steady state condition is achieved with zero control error, but the transient response become more oscillatory as depicted in Figure 2.3.

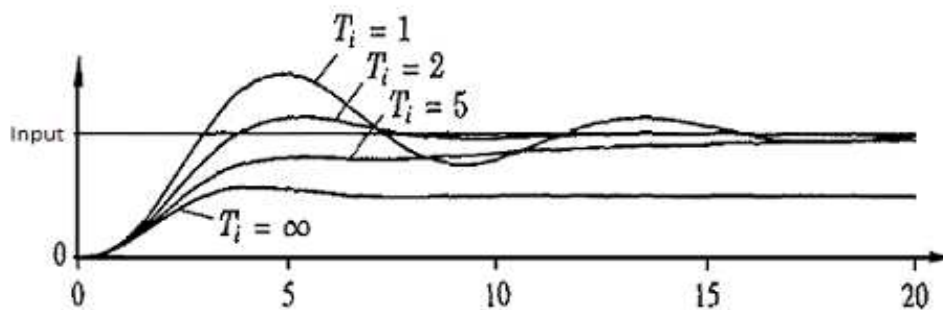


Figure 2.3 Step response for a simulated third order controlled system with proportional and integral action [15]

- D – Derivative action: Due to the process dynamics, a change in the control variable can be observed in the process output after some time have passed, therefore the control system will be late in correct the error. The derivative action predicts the process output through the derivative of the control error, improving the closed-loop stability of the system [15]. Figure 2.4 shows how the response of a controlled system with proportional and derivative control action varies according the derivative time varies.

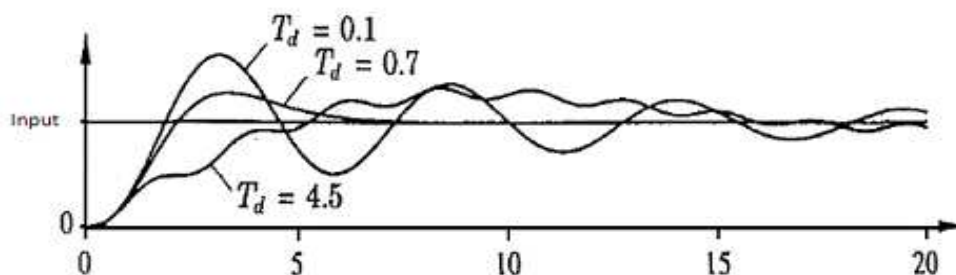


Figure 2.4 Step response for a simulated third order controlled system with proportional and derivative action [15]

The proportional, integral and derivative actions in a PID controller, can be written through the following expression:

$$u(t) = K_p \left( e(t) + \frac{1}{T_i} \int_0^t e(\tau) d\tau + T_d \frac{de(t)}{dt} \right) \quad (2.2)$$

where

$u(t)$  : command action signal.

$e(t)$  : controller error signal.

$K_p$  : controller proportional gain.

$T_i$  : controller integral time.

$T_d$  : controller derivative time.

In order to implement a PID controller, a model of the controlled system is required in order to verify which actions are the most effective to apply and satisfy stability and set-point following requirements, however an accurate model of the system is not required, as the controlled system characteristics can be modified easily varying the parameters  $K_p$ ,  $T_i$  and  $T_d$ . Such condition makes the PID a flexible tool to control several processes.

### 2.1.3 Pole placement method

Pole placement method is a control theory used on systems where a desired performance is required. The idea behind this method is set the a desired pole location and move the pole location of the system to that desired pole location in order to obtain the desired system response. This method is restricted to LTI, SISO, controllable systems where all the states are accessible.

In order to apply this method, an accurate LTI model of the system is required. With such model is possible to obtain the transfer function and therefore the poles of the system. Being defined the system transfer function, the desired transfer function must be defined too in order to make a comparison between the coefficients of same order of both characteristic polynomial equations. What is expected is to have equal coefficients on each order, therefore some gains are obtained to satisfy such condition. In order to select the pole locations, two main methods are commonly used [16]:

- Select pole locations such that a dominant complex pole pair exists.

- Select pole locations that have been determined to give a prototype time domain response. The ITAE response is a widely used criteria in order to define pole locations as function of the order of the system and the expected bandwidth of the system. Table 2.1 shows the frequency-normalized characteristic equations for ITAE responses for systems up to 5<sup>th</sup> order.

Table 2.1 Frequency-Normalized characteristic equations for ITAE Response [16]

| Order | Characteristic equation  |
|-------|--|
| 1     | $s + \omega$   |
| 2     | $s^2 + 1.41 \omega s + \omega^2$   |
| 3     | $s^3 + 1.75 \omega s^2 + 2.15 \omega^2 s + \omega^3$                                   |
| 4     | $s^4 + 2.1 \omega s^3 + 3.4 \omega^2 s^2 + 2.7 \omega^3 s + \omega^4$                  |
| 5     | $s^5 + 2.8 \omega s^4 + 5 \omega^2 s^3 + 5.5 \omega^3 s^2 + 3.4 \omega^4 s + \omega^5$ |

In order to implement a controller through pole placement method, the systems must be represented in space state representation, as described in eq. (1.33) and (1.34). If the Laplace transform of the control action for pole placement method is

$$\underline{u}(s) = -[K]z(s) \quad (2.3)$$

then, the poles of the controlled system can be calculated as

$$\det [s[I] - ([A] - [B][K])] = 0 \quad (2.4)$$

where the unknowns are the gain values inside the matrix  $[K]$ . Gain coefficients can be obtained through the Ackerman formula as follows:

$$[K] = [0 \ 0 \ \dots \ 1][Q]^{-1}[\hat{P}(A)] \quad (2.5)$$

where

$[K]$  : controller gain matrix.

$[Q]$  : controllability matrix.

$[\hat{P}(A)]$  : desired polynomial matrix as function of state matrix  $[A]$ .

Once the gain matrix  $[K]$  is obtained, a pole placement based controller is developed in order to obtain a controlled system with a response, similar to that the one shown by the desired system.

### 2.1.4 Optimal control – Linear Quadratic Regulator

Optimal control methodologies involves the development of a control law for a given system such that a defined optimality criterion is achieved. The linear quadratic regulator (LQR) is an regulator based on optimal control theory where the optimal control action is obtained minimizing the quadratic criterion shown in eq. (2.6) [14].

$$J = \frac{1}{2} \int_0^{t_f} \left( \underline{z}^T [\hat{Q}] \underline{z} + \underline{u}^T [R] \underline{u} \right) dt \quad (2.6)$$

where

$J$  : Objective function.

$[\hat{Q}]$  : State weighting matrix. Weights the squared state variable error.

$[R]$  : Control action weighting matrix. Weights the squared control error

The control action for a LQR controller is defined as:

$$\underline{u}(t) = -[K] \underline{z} \quad (2.7)$$

$$[K] = [R]^{-1} [B]^T [G] \quad (2.8)$$

Recalling the space state representation of a LTI system described in eq. (1.25) and (1.26), eq. (2.6), (2.7) and (2.8), the solution of the system, and therefore the optimal controller parameters can be obtained if the value of the matrix  $[G]$  is obtained. Such values can be calculated through the solution of the differential Riccati equation (DRE), represented on the eq.(2.9).

$$\frac{d[G]}{dt} = -[G][A] + [G][B][R]^{-1}[B]^T[G] - [\hat{Q}] - [A]^T[G] \quad (2.9)$$

Optimal control is restricted to systems which are controllable.

The application of an optimal control methodology become necessary when [17]:

- A compromise between the dynamic response and the control action is required.

- The system restrictions do not allow a controller design through dominant poles.
- When zeros are present in the system transfer function.
- When adaptive gains are required in order to satisfy different operational points with best dynamic response characteristics.

### **2.1.5 Servo-hydraulic system: comparison between different control methods**

Pole placement is not a suitable method to implement in the controller for the servo-hydraulic system, as an accurate model of the system is required, and the model presented on Chapter 1 do not include phenomenon such friction, and approximates the servovalve behaviour through the use of manufacturer charts. In addition, pole placement method is restricted to LTI systems and the non linearities will not be taken into account. This drawback can be overcome through the linearisation done during the modelling stage however, differences between linear and non linear models can be observed according to the operative points where the servo-hydraulic system is working. Furthermore, the measurement of the state variables become complicated. Position, speed and acceleration values are easy to obtain, but load pressure and load flow are not.

Between the presented control methodologies, PID is the simplest but also the less accurate in terms of performance. However if a well PID tuning is developed, the controller characteristics can be enhanced to the most. Its flexibility allows the implementation even if the model of the system lacks of accuracy, and the performance can easily be modified according to the characteristic operational conditions. Optimal control it is also a good solution for the specific application but PID controller is selected rather than optimal due to its simplicity during the implementation, while the response characteristics between both type of controllers are not expected to change drastically.

## **2.2 Servo-hydraulic system controller design**

The design of the controller for the servo-hydraulic system is process where the dynamic model of the servo-hydraulic system presented in Chapter 1, and the control method selected on the chapter 2.1.5 are taken into account. This process involves two stages:

- Numerical simulation stage: the aim is simulate the entire system including both, control system and servo-hydraulic system; and verify the theoretical behaviour of the controlled system at different input

- motion profiles (step, sine wave).
- Real time controller implementation: the aim is develop a real time controller able to control a servo-hydraulic system at different input motion profiles (step, sine wave).

## 2.3 Control system design – Numerical simulation

The objective of this stage, is simulate the behaviour of the controlled servo-hydraulic system based on their dynamic models shown in the current and previous chapters. The simulations will be done using both linear and non linear models of the servo-hydraulic system, in order to verify if the the linear one a sufficient approximation to the system.

### 2.3.1 General considerations

In feedback controlled hydraulic systems with linear actuators, the manufacturers had conceived and recommend two possible arrangements, position or force control, as shown in Figure 2.5.

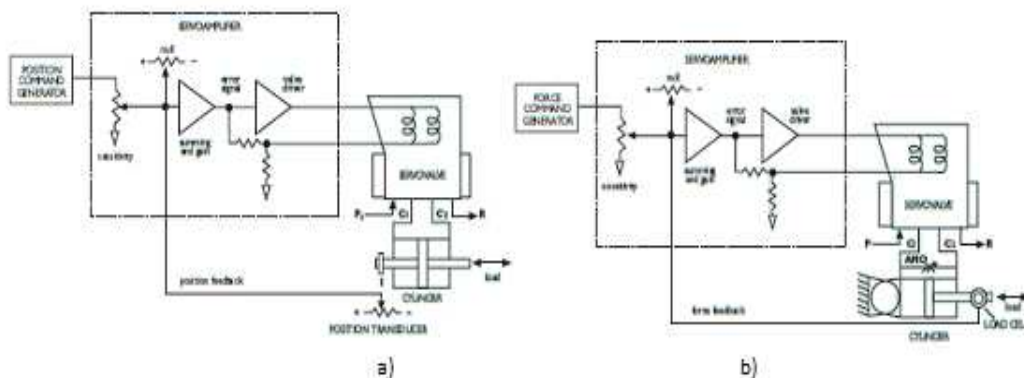


Figure 2.5 Servo-hydraulic feedback arrangements [9]

The type a) measures the piston position while the type b) measures the axial force generated by the actuator. This project is conceived through a position control system, as the EMA evaluation is expected to do in terms of displacements instead of forces.

Schematically the controlled system is composed by the elements observed in Figure 2.6. Those components represent the behaviour of the physical devices needed in the controlled servo-hydraulic system.

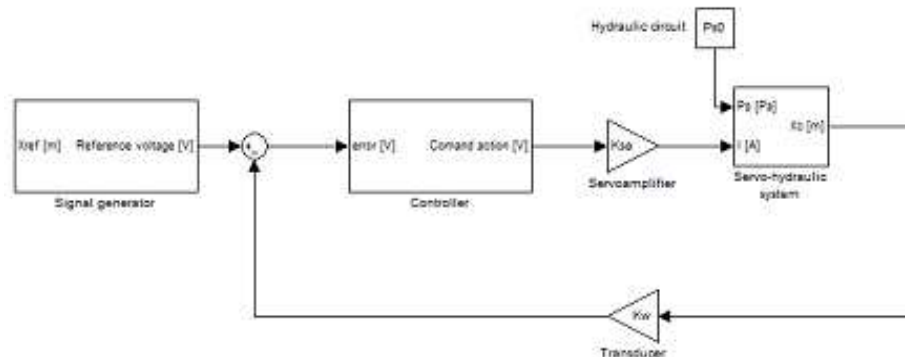


Figure 2.6 Controlled system schematic representation

The controlled system is composed by:

- Signal generator: Component conceived to generate sine and constant signals. The amplitude of the signals is generated in meters, but the output must be in voltage.
- Hydraulic circuit: External hydraulic system necessary to supply the servo-hydraulic system with the oil at constant supply pressure.
- Controller: Voltage-voltage PID controller. The dynamic model corresponds to the model explained in Chapter 2.
- Servo amplifier: Electrical/electronic device which converts a voltage signal in a current signal. As the PID controller has a voltage output and the servovalve a current input, the servo amplifier is required to operate the servo-hydraulic system. Conceived as a linear element.
- Transducer: Element which measures the position of the actuator's spool and gives an output signal in voltage. Conceived as a linear element.
- Servo-hydraulic system: Represents the assembly composed by the servovalve and the linear hydraulic actuator. The dynamic model correspond to the model explained in Chapter 2.

The transducer and servo amplifier models are conceived as linear devices and defined by

$$K_w = \frac{Trans_{Out_{max}} - Trans_{Out_{min}}}{Stroke_{max} - Stroke_{min}} \quad (2.10)$$

$$K_{sa} = \frac{SA_{Out_{max}} - SA_{Out_{min}}}{SA_{Imp_{max}} - SA_{Imp_{min}}} \quad (2.11)$$

where



- $K_w$  : Transducer sensitivity.  
 $K_{sa}$  : Servo amplifier amplification.  
 $Trans_{Out_{max}}$  : Transducer maximum output value.  
 $Trans_{Out_{min}}$  : Transducer minimum output value.  
 $Stroke_{max}$  : Actuator maximum stroke or displacement.  
 $Stroke_{min}$  : Actuator minimum stroke or displacement.  
 $SA_{Out_{max}}$  : Servo amplifier maximum output value.  
 $SA_{Out_{min}}$  : Servo amplifier minimum output value.  
 $SA_{Imp_{max}}$  : Servo amplifier maximum input value.  
 $SA_{Imp_{min}}$  : Servo amplifier minimum input value.

In addition, numerical differentiation is used to solve the differential equations present in the system dynamics. Two point backwards numerical differential method is chosen as  $h < 0$ , and forward information is no available during the simulation. Backwards numerical differentiation has been defined in [18], as

$$\dot{f}(x) \approx \frac{f(x) - f(x-h)}{h} \quad (2.12)$$

where

$h$  : Simulation step.

### 2.3.2 Simulation block diagrams

Two different block diagrams have been developed using National Instruments – Labview® software, corresponding to the servo-hydraulic models defined for linear and non linear cases. Each simulation model has been constructed to be solved in the time domain, and is composed by blocks which represent the dynamics of the different devices present in the controlled servo-hydraulic system. Displacement transducer, servo amplifier, controller, actuator chambers and load dynamics are equally represented in both, linear and non linear, cases. The difference between them lies in the servovalve block diagram, as result of the linearisation done into the flow gain equation of the servovalve. Further information about structure and implementation of the block diagrams is summarized in Appendix A-II Simulation block diagrams.

The model presented in the Chapter 1 do not include operational limitations of the servo-hydraulic system. Eq. (2.13) to (2.15) model such conditions, and are included in the block diagrams as saturation ports. Including those limits values do not modify the behaviour of the model except when the system is

submitted to operative points where those limit values are predominant; and represents a more realistic behaviour of the physical device.

$$Stroke_{max} \geq X_c \geq Stroke_{min} \quad (2.13)$$

$$P_s \geq P_l \geq -P_s \quad (2.14)$$

$$I_{sat} \geq I \geq -I_{sat} \quad (2.15)$$

### 2.3.3 Controller tuning – Characteristics and tuning methodologies

There are some characteristics to take into account in controller system design and tuning. Those are stability in the desired range of frequencies, attenuation to load disturbances, sensitivity to noise measurement and set point following [15]. It is also customary to take into account that the servo-hydraulic system behaviour depends on the operation conditions as described in Chapter 1. Hence, the considerations for a controller used in a servo-hydraulic system for EMA proposes are:

- **Stability:** The system must present absolute stability in the range of frequencies from 0 to 10 Hz, where the modal analysis for large structures takes place.
- **Attenuation to load disturbances:** Load disturbances are disturbances that drive the process variables away from their desired values often at low frequencies and prototyped as step inputs [15]. Applying a step input, what is expected is a non oscillatory error and a zero steady state error in the closed loop transfer function.
- **Sensitivity to noise measurement:** Measurement of noise is typically at high frequencies fed into the system through the feedback line [15]. This phenomena is controlled placing low-pass filters in the feedback line with a cut off frequency of 100 Hz. Therefore sensitivity to noise measurement is not a relevant factor to take into account.
- **Set-point following:** Two types of signals are considered to be imposed by the controlled system, step and sine wave signals, due to the characteristics of EMA methodology. The EMA experimental set-up establishes the placement of sensors in the structure in order to measure its response to the imposed excitation, which is measured in the actuator. Therefore the signal imposed by the signal generator and the measured signal in the actuator must satisfy amplitude, frequency and offset, but phase delay is allowed.
- **Operational:** Once the actuator is attached to the load, the transient response must be over-damped or at least critically damped to avoid

possible damages in the structure. The operative conditions, frequency and amplitude of the sine wave signal, are determined and limited by the maximum allowable acceleration in the structure.

Ziegler Nichols PID controller tuning method is a wide used tuning methodology, developed in 1942 with satisfactory results in industrial applications along the years. It had been widely used due to its simplicity during the implementation. This tuning method is based on oscillatory responses of the system with a quarter amplitude decay ratio [15].

There are two possible ways to apply the method, the step response and the frequency response methods:

- Step response method: Is based on a registration of the open-loop step response of the system, which is characterized by two parameters determined from a unit step response of the process [15]. It is suitable for systems with an step response which changes monotonically to a new steady state value (Figure 2.7 A) or oscillates around its final steady state value (Figure 2.7 B). Systems with an unstable step response (Figure 2.7 C) can not be tuned through this method.

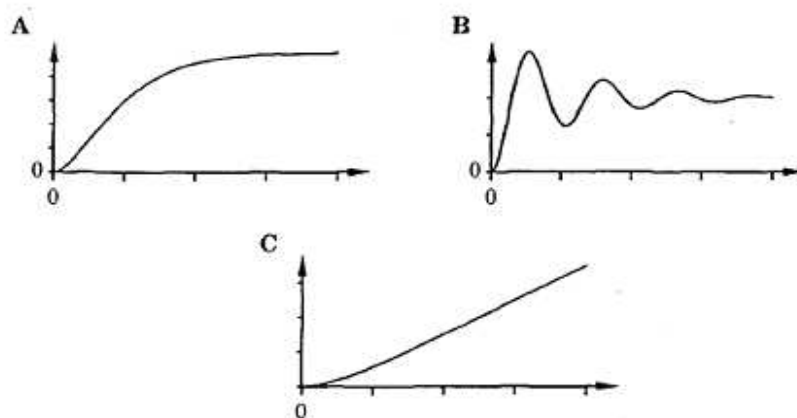


Figure 2.7 Open loop characteristic step responses [15]

- Frequency response method: Is based on a characterization through two parameters, the ultimate gain  $K_u$  and the ultimate period  $T_u$ , of the closed loop system dynamics [15] so its application is suitable for stable and unstable open loop systems. The characteristic values are obtained setting the controller without integral and derivative action ( $T_i = \infty$

and  $T_d=0$ ), and increasing the proportional action ( $K_p$ ) until a sustained oscillatory response is achieved, so the system is carried up to the stability limit.  $K_u$  corresponds to  $K_p$  value, while  $T_u$  is the period of the oscillation.  $K_p$ ,  $T_i$  and  $T_d$  values are function of  $K_u$  and  $T_u$ , and are summarized in the Table 2.2 for P, PI and PID controllers.

Table 2.2 Ziegler Nichols frequency response method - PID parameters [15]

| Controller | Kp        | Ti        | Td          |
|------------|-----------|-----------|-------------|
| <b>P</b>   | 0.5 $K_u$ |           |             |
| <b>PI</b>  | 0.4 $K_u$ | 0.8 $T_u$ |             |
| <b>PID</b> | 0.6 $K_u$ | 0.5 $T_u$ | 0.125 $T_u$ |

As the Ziegler Nichols tuning method is based on oscillatory responses at a certain decay ratio, and do not fit properly according to the established controller characteristics. Further PID tuning methods have similar assumptions including modified Ziegler Nichols methods, or are not suitable to apply in the servo-hydraulic system as Chien, Hrones and Reswick (CHR) method because requires and stable open loop transfer function [15]. A new tuning method has to be performed in order to satisfy the requirements.

Monotonic and oscillatory around steady state value step responses are characterized by the parameters shown in Figure 2.8. These parameters are defined by [15] as follows:

- Rising time  $t_r$ : is either defined as the inverse of the largest slope of the step response or the time it takes the step to pass from 10% to 90% of its steady state value.
- Settling time  $t_s$ : is the time it takes before the step response remains within p% of its steady state value. The value  $p = 2\%$  is commonly used.
- Decay ratio  $d$ : is the ratio between two consecutive maxima of the error for a step change in set point or load.
- Overshoot  $O$ : is the ratio between the difference between the first peak and the steady state value and the steady state value of the step response. In industrial control applications it is common to specify an overshoot of 8%-10%.
- Steady-state error  $e_{ss}$ : is the value of control error  $e$  in steady state condition.

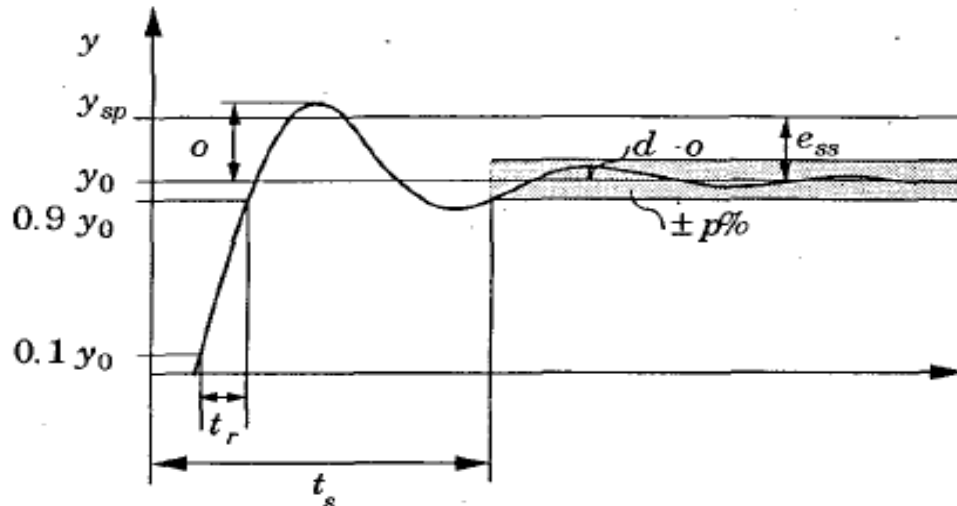


Figure 2.8 Characteristic parameters for monotonic and oscillatory around steady state value step responses [15]

Due to the relationship between the load flow - load pressure, and load pressure - piston displacement, and the intrinsic speed feedback into the hydraulic actuator, stable and suitable responses of the system are expected to be limited by the maximum load flow the servovalve can achieve. As servovalve flow gain depends on the term  $\sqrt{(P_s - P_l)/P_s}$ , in the neighbourhood of  $P_l = 2P_s/3$  where the maximum load condition occurs, there is a gain reduction of  $\sqrt{1/3}$  or 57.7%. As described in [7], if the servo-hydraulic system tends or behaves as a conditional stable system, gain reductions could cause stability problems.

According to the definition of rising time, the maximum achievable speed in the step response  $S_r$  is calculated as

$$S_r = \frac{0.8 \text{ Amplitude}}{t_r} \quad (2.16)$$

which corresponds to speed of response of the servo-hydraulic system. Taking into account that operative conditions requires sinusoidal input signals, the maximum linear acceleration and speed are defined as

$$acc = \omega_{signal}^2 \text{ Amplitude} \quad (2.17)$$

$$Sp = \omega_{signal} \text{ Amplitude} \quad (2.18)$$

where

$acc$  : Maximum acceleration for sinusoidal signal.

$S_p$  : Maximum speed for sinusoidal signal.

$\omega_{signal}$  : Signal frequency.

$Amplitude$  : Signal amplitude, measured as half peak to peak value.

Under maximum load conditions, the maximum sinusoidal signal speed corresponds to the critical speed under such load and signal conditions. Both values are related to the maximum speed response by

$$S_r < \sqrt{3} S_p = S_{pc} \quad (2.19)$$

If proportional gain is increased, rising time  $t_r$ , steady state error  $e_{ss}$  is reduced, while the overshoot  $O$  maximum response speed  $S_r$  are increased. Hence, the range of proportional gain are limited by the condition established by eq.(2.19). In addition, as non oscillatory responses are expected, different values of proportional gains have to be found respect to those proposed by standard PID tuning methods. However,  $K_p$  range is still wide and must be narrowed. Lower limit is imposed by the gains of critically damped responses which have the best  $S_r$  with no overshooting.

A simple P controller can be enough to satisfy the considerations established in the beginning of this chapter, if at the selected  $K_p$  the response signal satisfies the set-following characteristics, and  $K_p$  is lower than the proportional gain associated to the critical speed ( $K_{spc}$ ). Values beyond this gain can still be imposed but involves the inclusion of further modes no desired into the response. No integral action is expected to be included in the controller as the servo-hydraulic system have an integral behaviour with the pole in the origin. Including another pole in the origin can cause total instability for multiple order poles in the  $j\omega$  axis on the open loop transfer function. Instead, derivative action is preferred on servo-hydraulic systems, and can be included into the controller.

$$OL_{cs}(s) = \frac{K_w K_{sa} K_{sv} \omega_H^2 K_p (1 + T_d)}{A_{HI} s (s^2 + 2\delta_H \omega_H s + \omega_H^2) (s^2 + 2\delta_{sv} \omega_{sv} s + \omega_{sv}^2)} \quad (2.20)$$

where

$OL_{cs}(s)$  : open loop transfer function for the controlled servo-hydraulic system

Eq. (2.20) shows the open loop transfer function for the controlled system with proportional and derivative action. According to the value of the derivative time, the zero included by the PD action in the open loop transfer function has a different position and therefore a different behaviour is expected. Three possible cases can occur:

- Case 1: The inverse of the derivative time is lower than the magnitude of the lower hydraulic pole of the system (  $1/T_d < \omega_{phl}$  ).
- Case 2: The inverse of the derivative time lies between the magnitude of the lower hydraulic pole and the magnitude of the the complex conjugated servovalve poles (  $\omega_{phl} < 1/T_d < \omega_{sv1,2}$  ).
- Case 3: The inverse of the derivative time is beyond the magnitude of the complex conjugated servovalve poles (  $1/T_d > \omega_{sv1,2}$  ).

Special care must be taken when derivative time is imposed as the damping initially increases with increasing derivative time, but decreases again when derivative time becomes too large [15]. The selection of the derivative time depends on the place where the zero of the open loop transfer function generates an stable behaviour, dependent on the relationships between  $T_d$ ,  $\omega_{phl}$  and  $\omega_{sv1,2}$ . When  $1/T_d$  is placed before  $\omega_{phl}$ , the relation  $T_d > 1/\omega_{phl}$  must be satisfied. Alike, if the zero in the open loop frequency response function is placed between  $\omega_{phl}$  and  $\omega_{sv1,2}$ , then  $T_d > 1/\omega_{sv1,2}$ . The last possible case when  $1/T_d$  is higher than  $\omega_{sv1,2}$  determines  $T_d < 1/\omega_{sv1,2}$ . Through the evaluation of the precedent cases, is possible to observe that no possible value determined inside the  $T_d < 1/\omega_{sv1,2}$  condition is useful for the servo-hydraulic controlled system because there is no change in the frequency transfer function in the frequency range between 0 to 10 Hz, as the the zero generated by the PD controller is placed at a frequency higher than the one associated with the servovalve poles, which is at least 4 or 5 times higher than the expected bandwidth value of the system, as defined in chapter 1. On the contrary, cases 1 and 2 define useful time derivative ranges, stabilizing the system on certain range of frequencies as shown in Figures 2.9 and 2.10.

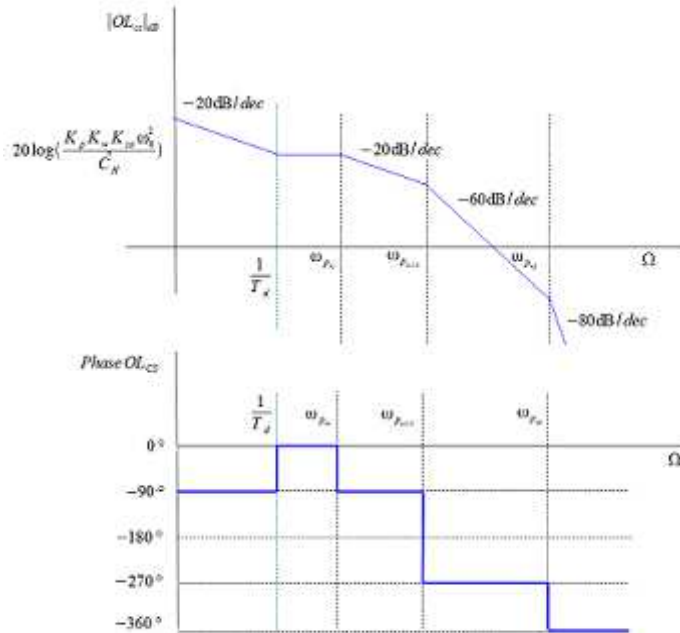


Figure 2.9 Open loop frequency response function for controlled servo-hydraulic systems with PD action - Case 1

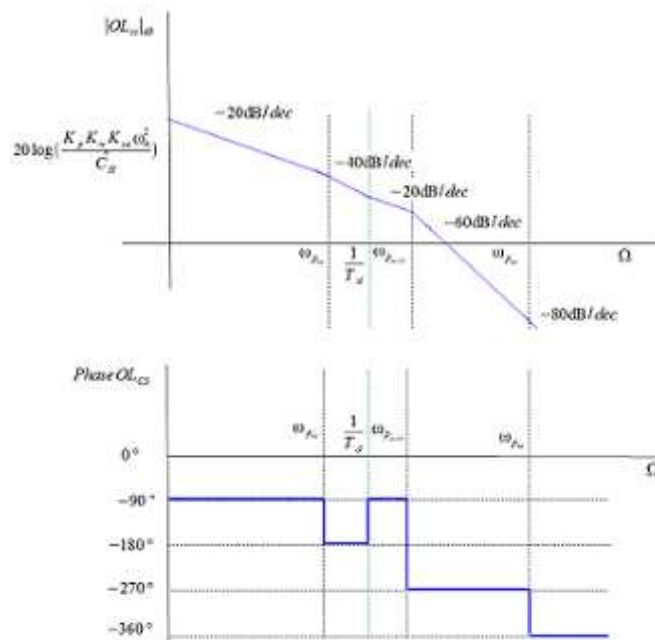


Figure 2.10 Open loop frequency response function for controlled servo-hydraulic system with PD action- Case 2



Both cases offer a solution range according to the present load conditions in the servo-hydraulic system. In any case a fine derivative time tuning to the particular load condition must be developed, taking into account the derivative time ranges defined before. Derivative action must be included if the single proportional action do not assure a proper behaviour in term of stability, attenuation to load disturbances, sensitivity to noise measurement and set-point following characteristics.

### 2.3.4 Controller tuning – Simulation results

Simulations are carried out in two different situations. The first corresponds to the bench test condition where no load mass is attached to the servo-hydraulic system. The second is a condition with load mass, evoking the objective structures where the controlled servo-hydraulic system will be used. The operative conditions for each simulation depend on the operative frequencies and amplitudes that are expected to apply in the actual structure. As mentioned in Chapter 2.3.3, those values are limited by the maximum allowable acceleration of the mass. Figure 2.11 shows the maximum allowable amplitude at a determined frequency for different maximum acceleration values for an actuator with 103 mm of maximum stroke. For both simulation cases, the maximum acceleration is  $5 \text{ m/s}^2$ , and signals frequencies each 0.5 Hz in the range of 2 to 10 Hz. The specific amplitudes and frequencies to the simulation are summarized in Table 2.3.

Table 2.3 Maximum speed for sinusoidal signals at test frequencies and amplitudes

| Frequency [Hz] | Amplitude [mm] | Sp [mm/s] |
|----------------|----------------|-----------|
| 2.0            | 31.66          | 397.89    |
| 2.5            | 20.26          | 318.31    |
| 3.0            | 14.07          | 265.26    |
| 3.5            | 10.34          | 227.36    |
| 4.0            | 7.92           | 198.94    |
| 4.5            | 6.25           | 176.84    |
| 5.0            | 5.07           | 159.15    |
| 5.5            | 4.19           | 144.69    |
| 6.0            | 3.52           | 132.63    |
| 6.5            | 3.00           | 122.43    |
| 7.0            | 2.58           | 113.68    |
| 7.5            | 2.25           | 106.10    |
| 8.0            | 1.98           | 99.47     |
| 8.5            | 1.75           | 93.62     |
| 9.0            | 1.56           | 88.42     |
| 9.5            | 1.40           | 83.77     |
| 10.0           | 1.27           | 79.58     |

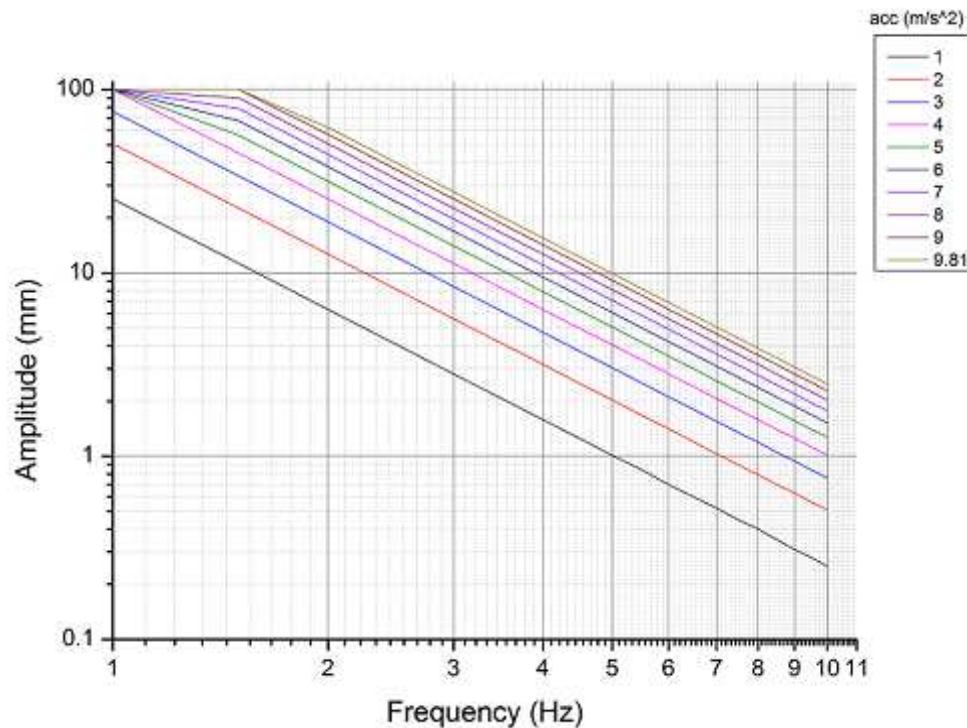


Figure 2.11 Maximum amplitude vs signal frequency at different acceleration values

The parameters imposed into the simulation software are shown in Appendix A-I Simulation parameters. For each load mass, amplitude and frequency case, the simulation is done according to the following procedure:

- 1) For the linear case, calculate the pole magnitude of servo-hydraulic system transfer function.
- 2) Calculate the maximum linear speed  $S_p$ , for a sinusoidal signals at the applied frequency and amplitude as described in eq.(2.18).
- 3) With no integral and derivative action, apply a step input signal with the desired amplitude in the controlled system. Vary the gain to obtain ultimate gain ( $K_u$ ), critical gain at  $\sqrt{3}S_p$  ( $K_{spc}$ ), gain at  $S_p$  value ( $K_{sp}$ ), gain with a response with 10% of overshoot ( $K_{OS}$ ) if is not higher than  $K_{spc}$ , and gain for critically damped response ( $K_{CD}$ ).
- 4) For each gain value calculate the performance parameters speed response  $S_R$  and overshoot  $O$ .
- 5) Using just proportional action, apply a sinusoidal input signal at the

- corresponding combination of amplitude and frequency using the characteristic proportional gain values obtained in previous steps.
- 6) Modify the gain up to obtain a value (  $K_{sine}$  ) with better set point following characteristics, but lower than  $K_{spc}$  .
  - 7) Evaluate the harmonics in the input and response signal in terms of frequencies and amplitudes, under a threshold of 2% of signal amplitude. For identified harmonics, and static condition, calculate the error.
  - 8) Calculate the limiting values of  $T_d$  as function of pole magnitudes.
  - 9) With the proportional  $K_{sine}$  or  $K_{spc}$  , include derivative action according to the limiting values of derivative time, apply a step input signal to the controlled system. Calculate speed response  $S_R$  and overshoot  $O$  .
  - 10) If derivative action is feasible, apply sinusoidal input signal at the corresponding combination of amplitude and frequency.
  - 11) Apply step 7 using the PD controller signals.

Table 2.3 shows the maximum speed for sinusoidal signals at different frequency – amplitude simulation conditions, while Table 2.4 shows the pole magnitude of the servo-hydraulic system at different load conditions, not including the zero pole which is common for any condition. Through the magnitudes of  $\omega_{ph}$  and  $\omega_{sv1,2}$  are established the limit values for derivative time time as summarized in Table 2.5.

Table 2.4 Pole magnitude of servo-hydraulic transfer function

|  | Load mass [kg] |        |        |        |        |
|--|----------------|--------|--------|--------|--------|
|  | 0              | 50     | 100    | 200    | 450    |
| Hydraulic actuator natural frequency $\omega_h$ [Hz] | 244.50         | 95.49  | 70.26  | 50.74  | 34.24  |
| Hydraulic actuator damping ratio $\bar{D}_h$         | 3.03           | 7.76   | 10.55  | 14.61  | 21.65  |
| $\omega_{sv1}$ [Hz]                                  | 70.00          | 70.00  | 70.00  | 70.00  | 70.00  |
| $\omega_{sv2}$ [Hz]                                  | 70.00          | 70.00  | 70.00  | 70.00  | 70.00  |
| $\omega_{h1}$ [Hz]                                   | 92.07          | 12.51  | 6.72   | 3.49   | 1.58   |
| $\omega_{h2}$ [Hz]                                   | 649.29         | 728.84 | 734.64 | 737.87 | 739.77 |

Table 2.5 Limiting values of derivative time as function of pole magnitude

|                              | Load mass [kg] |         |         |         |         |
|------------------------------|----------------|---------|---------|---------|---------|
|                              | 0              | 50      | 100     | 200     | 450     |
| Td<br>- $\omega_{sv1,2}$ [s] | 0.00227        | 0.00227 | 0.00227 | 0.00227 | 0.00227 |
| Td<br>- $\omega_{h1}$ [s]    | 0.00173        | 0.01272 | 0.02369 | 0.04562 | 0.10044 |

For each load mass case, have been chosen the extreme amplitude cases to show their corresponding step responses at different proportional gains, disaggregated in linear and non linear simulation cases. Figures 2.12 to 2.15 shows the  $M_L=450\text{ kg}$  case while Figures 2.16 to 2.19 the non load case.

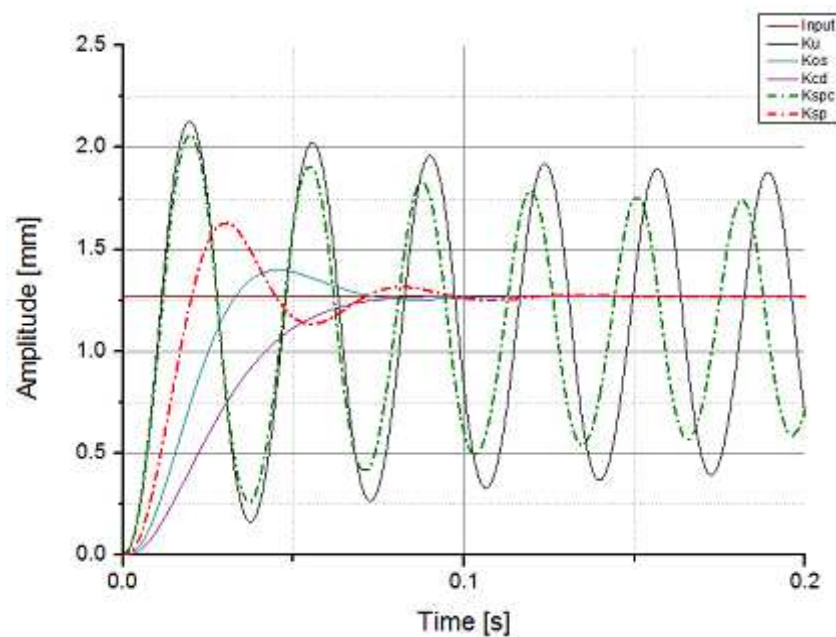


Figure 2.12 1.27 mm step response at different proportional gain values  
Load mass 450 kg - Non linear model

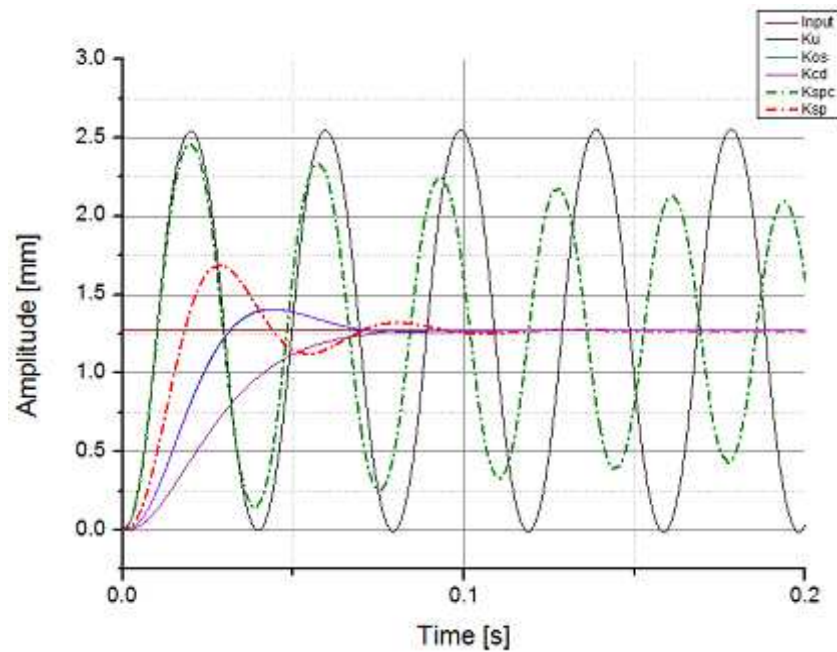


Figure 2.13 1.27 mm step response at different proportional gain values  
Load mass 450 kg - Linear model

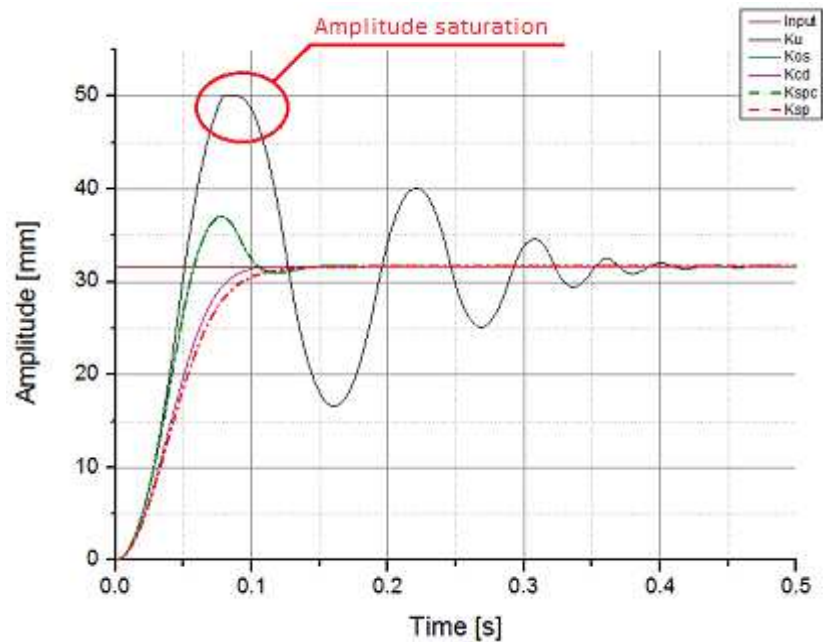


Figure 2.14 31.66 mm step response at different proportional gain values  
Load mass 450 kg - Non linear model

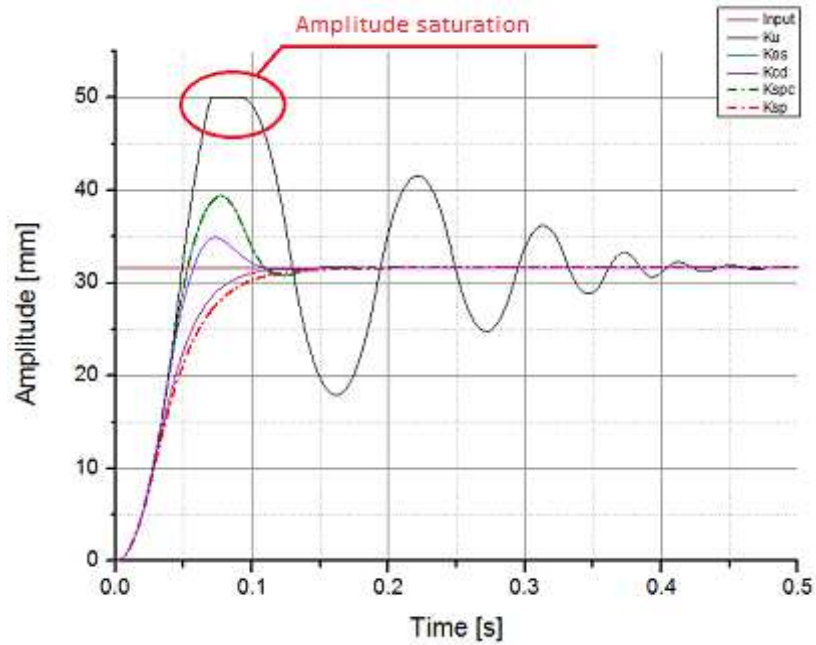


Figure 2.15 31.66 mm step response at different proportional gain values  
Load mass 450 kg - Linear model

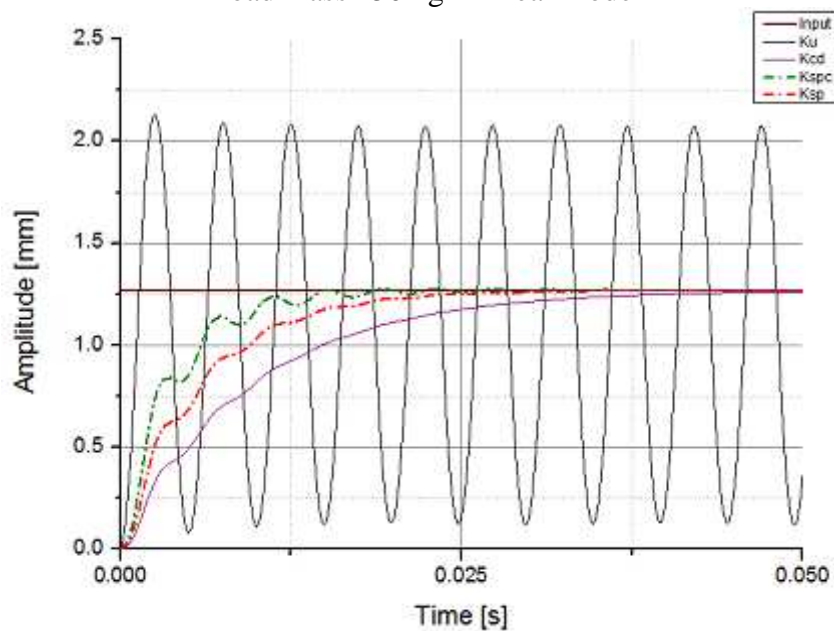


Figure 2.16 1.27 mm step response at different proportional gain values  
Load mass 0 kg - Non linear model

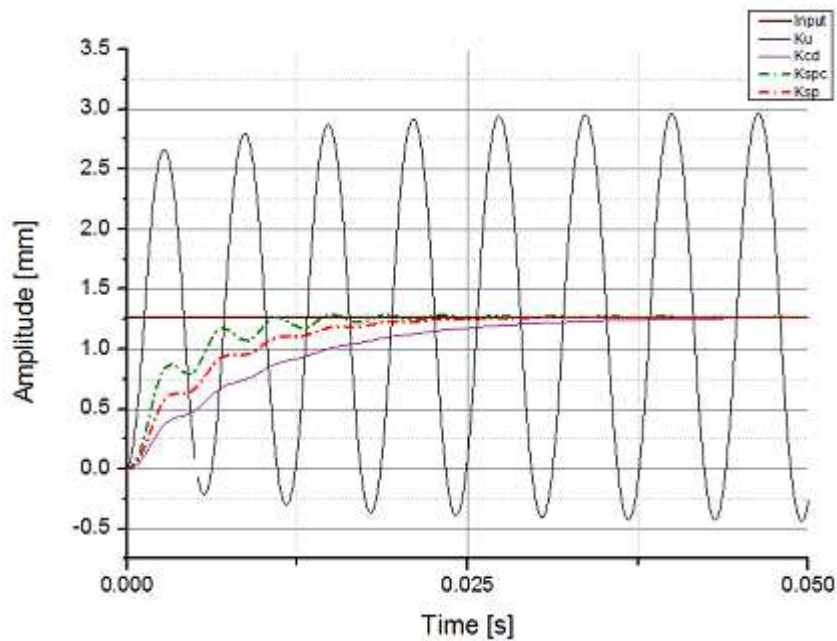


Figure 2.17 1.27 mm step response at different proportional gain values  
Load mass 0 kg - Linear model

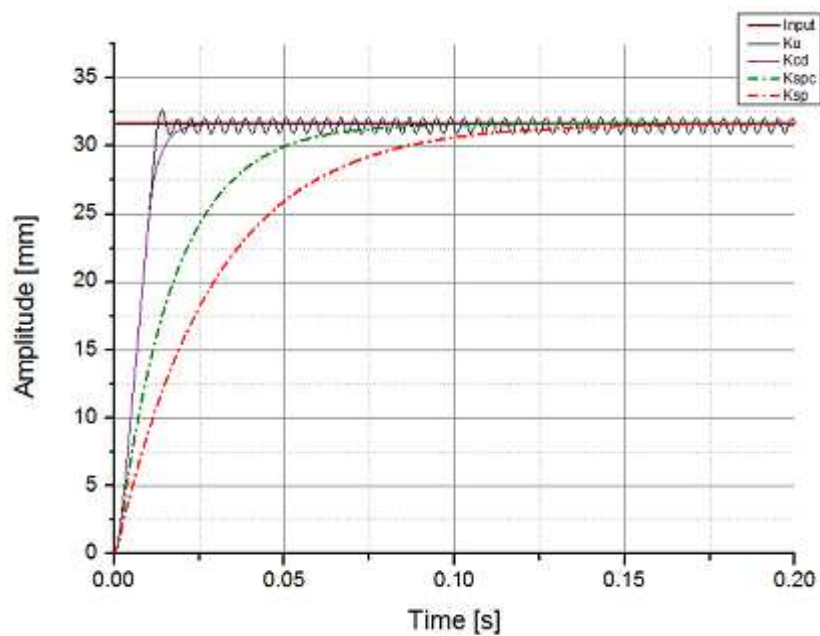


Figure 2.18 31.66 mm step response at different proportional gain values  
Load mass 0 kg - Non linear model

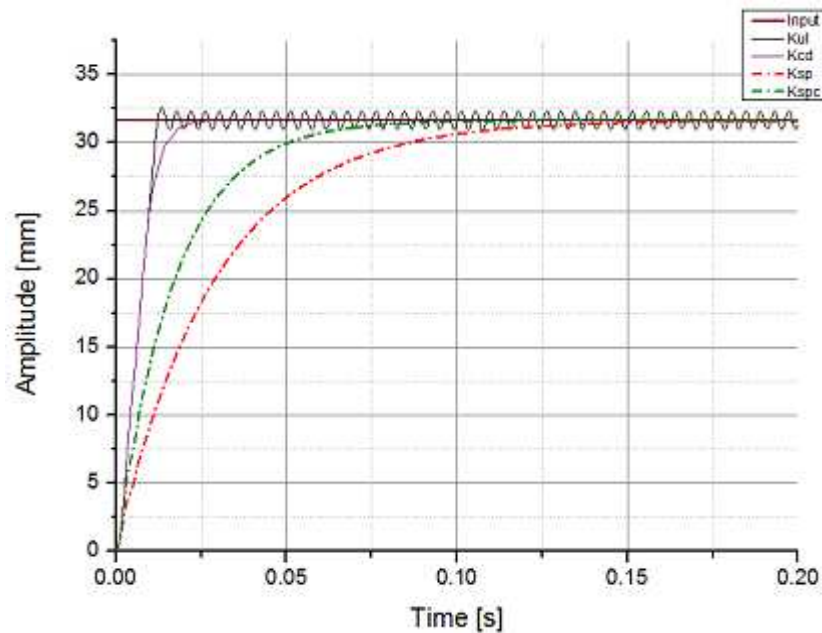


Figure 2.19 31.66 mm step response at different proportional gain values  
Load mass 0 kg - Linear model

Speed profiles as function of amplitude, for  $K_u$ ,  $K_{CD}$  and  $K_{OS}$  in both model cases are shown in Figures 2.20 and 2.21 for different load mass conditions. An evaluation of those results shows the differences between the linear and non linear models. For every case, the speed values are higher in linear simulations which is explained as a clear result of linearisation, where a single and particular operative point in the no-load flow function was selected. Such differences oscillates between 0.1% to 25% according to operation conditions, less critical on overdamped responses where behaviour of both models are comparable.

The use of linear model is a conservative method to establish the range of proportional gains of the controller, but as discussed in Chapter 1, operative conditions changes the behaviour of the frequency response function of the system, therefore the non linear model is more accurate. Linear case is useful as starting point to evaluate the system through LTI approach and define which type of controller fits better among the PID possible combinations, however performance and corrections on the controller are established and developed through non linear model results.



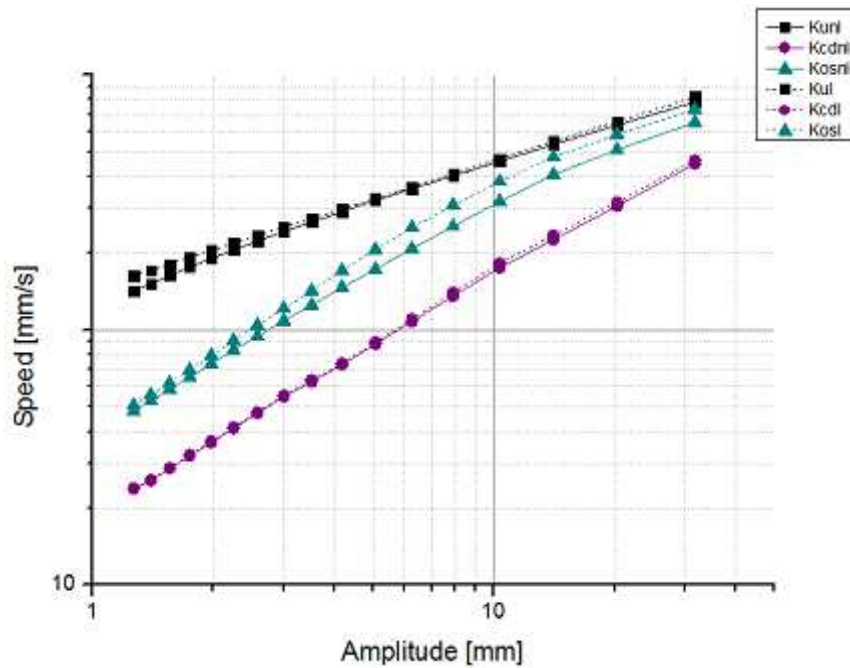


Figure 2.20 Speed profile comparison between linear and non linear models for characteristic proportional gain values – Load mass 450 kg

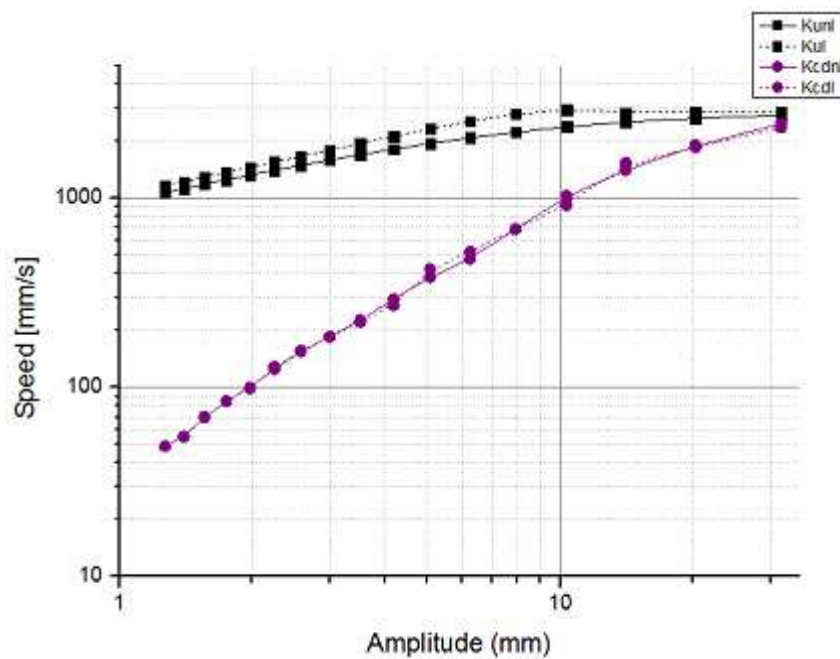


Figure 2.21 Speed profile comparison between linear and non linear models for characteristic proportional gain values – Load mass 0 kg

As defined in eq. (2.19), suitable speed responses must not surpass the critical speed. Values below this limit have associated  $K_p$  values that can be used in the controller. On the case with attached load, the condition is satisfied by the conditions where responses are critically damped, or have a 10% overshoot as shown in Figure 2.22. The gain according to Ziegler Nichols tuning methodology is suitable just for the cases with amplitudes between 1.27mm to 1.98 mm. On the other case, ultimate gains generate speed responses far greater than the critical speed leaving Ziegler Nichols criteria out, for this load condition. 10% overshoot responses were obtained only with oscillating responses, leaving out this criteria too. The last case, critically damped responses, is not a good estimator under this load condition, as oscillations should appear during rising period, making difficult the estimation of the performance parameters. Because of this limitation, on Figure 2.23 some speed values associated to critically damped responses are higher than the critical speed.

If step responses at  $K_{spc}$  are over-damped or critically damped, this value become the suggested proportional gain value to use in sine wave input signals, despite the drawbacks in amplitude difference. On the contrary, if the response is under-damped, there are better proportional gain values rather than  $K_{spc}$ . Better results can be found on values below of it but higher than  $K_{CD}$ .

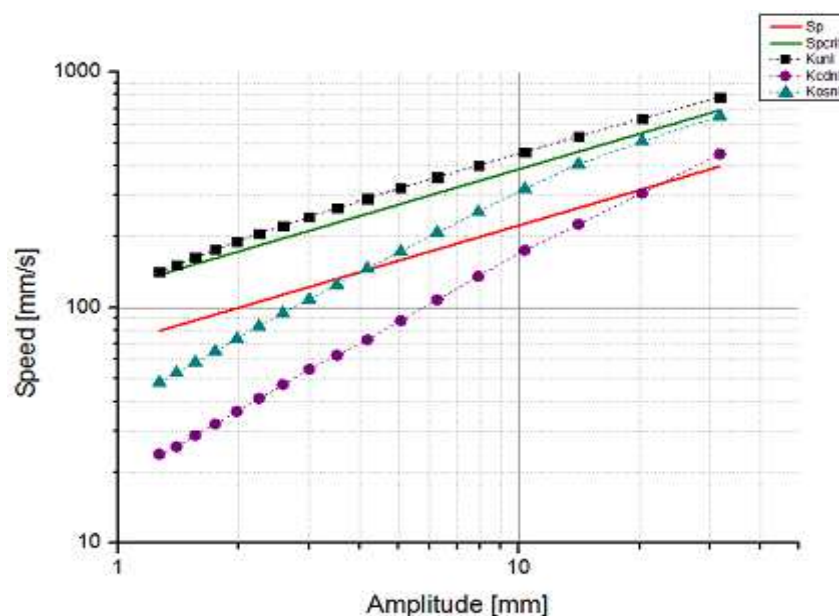


Figure 2.22 Speed profiles for characteristic proportional gain values and limiting conditions – Load mass 450 kg

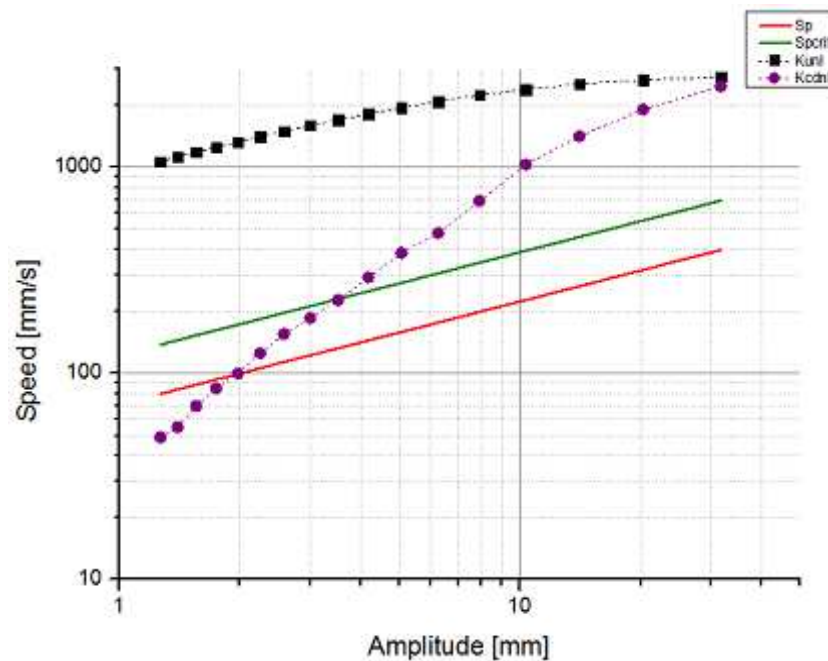


Figure 2.23 Speed profiles for characteristic proportional gain values and limiting conditions – Load mass 0 kg

Using proportional action, sinusoidal input signals are applied into the model, using  $K_{OS}$  and  $K_{spc}$  gain values, on load mass cases 450 kg and 0 kg, respectively. Harmonic analysis through the application of discrete Fourier transform, allow the evaluation of the accuracy of the controller, allowing the evaluation of the amplitudes, harmonic by harmonic, between the input and response signals. Pure sinusoidal signals can be decomposed in a static value and one harmonic component, at zero and signal frequency, and amplitude values according to offset and signal amplitude respectively. This case applies in the case of the signal generator. If the controller is set with the adequate proportional gain in order to avoid oscillatory responses, the harmonic components of the signal will be at zero and signal frequency too, with amplitude values determined by the controlled system characteristics, and other possible harmonics with low amplitude values. If other condition occurs, other  $K_p$  values can be obtained.

Defining error at main harmonic component, and static errors as

$$error_{MH} = \frac{H_{Inp}(\omega_{signal}) - H_{Res}(\omega_{signal})}{H_{Inp}(\omega_{signal})} \quad (2.21)$$

$$error_s = \frac{H_{Inp}(0) - H_{Res}(0)}{H_{Inp}(\omega_{signal})} \quad (2.22)$$

where

$error_{MH}$  :Error at main harmonic component.

$error_s$  : Static error.

$H_{Res}(\omega_{signal})$  :Response signal amplitude value at main harmonic component.

$H_{Res}(0)$  :Response signal amplitude value at zero frequency.

$H_{Inp}(\omega_{signal})$  :Input signal amplitude value at main harmonic component.

$H_{Inp}(0)$  :Input signal amplitude value at zero frequency.

is possible to have a measure of the accuracy of the controller. Tables 2.6 and 2.7 show the error values for the imposed proportional gains at different input signal conditions. Error values can be either positive or negative, according to the main harmonic amplitude on the response signal. The values can oscillate in a wide range of values according to  $K_p$ , however error magnitudes above 1% are not allowed. To reduce them, point by point evaluation of further proportional gains values must be developed, if the gain value associated to the critical speed is not been reached. If this is not the case, no possible combination of P, I or D actions can have a faster response with the specifications proposed in chapter 2.3.3 .

Table 2.6 Error values on sinusoidal signals with proportional gains for 10% overshoot step responses – Load mass 450 Kg

| Frequency [Hz] | Amplitude [mm] | Kp   | Error at main harmonic [%] | Static error [%] |
|----------------|----------------|------|----------------------------|------------------|
| 2.0            | 31.66          | 1.04 | -0.275%                    | 0.205%           |
| 2.5            | 20.26          | 1.23 | -0.850%                    | 0.196%           |
| 3.0            | 14.07          | 1.34 | -1.415%                    | 0.224%           |
| 3.5            | 10.34          | 1.3  | -1.841%                    | 0.372%           |
| 4.0            | 7.92           | 1.26 | -2.277%                    | 0.584%           |
| 4.5            | 6.25           | 1.24 | -2.772%                    | 0.814%           |
| 5.0            | 5.07           | 1.22 | -3.225%                    | 1.054%           |
| 5.5            | 4.19           | 1.22 | -3.774%                    | 1.247%           |
| 6.0            | 3.52           | 1.21 | -4.159%                    | 1.403%           |
| 6.5            | 3.00           | 1.21 | -4.576%                    | 1.488%           |
| 7.0            | 2.58           | 1.21 | -4.914%                    | 1.489%           |
| 7.5            | 2.25           | 1.21 | -5.164%                    | 1.405%           |
| 8.0            | 1.98           | 1.2  | -5.084%                    | 1.128%           |
| 8.5            | 1.75           | 1.19 | -4.713%                    | 0.915%           |
| 9.0            | 1.56           | 1.19 | -4.496%                    | 0.587%           |
| 9.5            | 1.40           | 1.19 | -4.092%                    | 0.216%           |
| 10.0           | 1.27           | 1.19 | -3.465%                    | 0.186%           |

Table 2.7 Error values on sinusoidal signals with proportional gains for critical speed step responses – Load mass 0 kg

| Frequency [Hz] | Amplitude [mm] | Kp    | Main harmonic error [%] | Static error % |
|----------------|----------------|-------|-------------------------|----------------|
| 2.0            | 31.66          | 1.046 | 2.202%                  | 0.007%         |
| 2.5            | 20.26          | 1.303 | 2.208%                  | 0.007%         |
| 3.0            | 14.07          | 1.558 | 2.214%                  | 0.007%         |
| 3.5            | 10.34          | 1.81  | 2.223%                  | 0.007%         |
| 4.0            | 7.92           | 2.055 | 2.812%                  | 0.011%         |
| 4.5            | 6.25           | 2.307 | 2.242%                  | 0.007%         |
| 5.0            | 5.07           | 2.54  | 2.273%                  | 0.007%         |
| 5.5            | 4.19           | 2.78  | 2.286%                  | 0.007%         |
| 6.0            | 3.52           | 3.08  | 2.207%                  | 0.007%         |
| 6.5            | 3.00           | 3.28  | 2.274%                  | 0.007%         |
| 7.0            | 2.58           | 3.39  | 2.456%                  | 0.008%         |
| 7.5            | 2.25           | 3.57  | 2.531%                  | 0.008%         |
| 8.0            | 1.98           | 3.96  | 2.331%                  | 0.007%         |
| 8.5            | 1.75           | 4.7   | 1.858%                  | 0.006%         |
| 9.0            | 1.56           | 4.7   | 2.075%                  | 0.007%         |
| 9.5            | 1.40           | 4.67  | 2.333%                  | 0.007%         |

Table 2.8 Error values on sinusoidal signals with proportional gain for minimum error – Load mass 450 kg

| Frequency [Hz] | Amplitude [mm] | Kp    | Error at main harmonic [%] | Static error [%] |
|----------------|----------------|-------|----------------------------|------------------|
| 2.0            | 31.66          | 0.932 | 0.00143%                   | 0.27668%         |
| 2.5            | 20.26          | 0.933 | 0.00005%                   | 0.43055%         |
| 3.0            | 14.07          | 0.933 | 0.00653%                   | 0.61900%         |
| 3.5            | 10.34          | 0.936 | 0.00605%                   | 0.82280%         |
| 4.0            | 7.92           | 0.942 | 0.00039%                   | 1.01778%         |
| 4.5            | 6.25           | 0.949 | 0.01840%                   | 1.18171%         |
| 5.0            | 5.07           | 0.96  | 0.01156%                   | 1.30104%         |
| 5.5            | 4.19           | 0.972 | 0.01848%                   | 1.36468%         |
| 6.0            | 3.52           | 0.986 | 0.00850%                   | 1.36941%         |
| 6.5            | 3.00           | 1     | 0.02301%                   | 1.31266%         |
| 7.0            | 2.58           | 1.015 | 0.03000%                   | 1.19172%         |
| 7.5            | 2.25           | 1.031 | 0.02574%                   | 1.01902%         |
| 8.0            | 1.98           | 1.048 | 0.00580%                   | 0.79721%         |
| 8.5            | 1.75           | 1.065 | 0.01187%                   | 0.53004%         |
| 9.0            | 1.56           | 1.083 | 0.01235%                   | 0.23374%         |
| 9.5            | 1.40           | 1.102 | 0.01087%                   | 0.08404%         |

The conditions of case  $M_L=450\text{kg}$ , had been improved finding proportional gains that reduce the error, as is seen in Table 2.8. Reductions up to 0.2% in the error at main harmonic component has been achieved setting the controller with an adequate proportional gain. On the contrary, the cases where

proportional gains had been limited by  $K_{spc}$ , can not be controlled satisfactory under the current controller arrangement.

In order to solve this problem a signal amplitude compensator is included into the system. The compensator is an element which compares the amplitudes at the fundamental harmonic between the input and response signals in order to obtain a compensation ratio as shown in eq.(2.23).

$$R_c = \frac{H_{Inp}(\omega_{signal})}{H_{Res}(\omega_{signal})} \quad (2.23)$$

where

$R_c$  : Compensation ratio

When compensation is applied, the signal amplitude corresponds to the multiplication between the imposed signal amplitude and the compensation ratio. Therefore the signal generator generates a signal with a different amplitude to the one defined by the test conditions, but the servo-hydraulic system will reproduce a motion profile with the required amplitude and frequency.

Applying the compensation, the critical speed is modified as the amplitude is changed. Therefore values out of the range between 0.9 and 1.1 are not allowed. It is important to obtain the best gains for the controller according to the procedure defined in this chapter, and then apply the compensation to reduce the error values.

Correction through amplitude compensator had been applied in both load conditions, reducing the error at main harmonic around 0.0005% respected to the original input signal, as shown in Tables 2.9 and 2.10.

On each simulation case, the systems behaves stable, the steady-state error in step responses is zero and set point following in amplitude and frequency occurs using the amplitude compensator. Its main objective do a final reduction on the error at main harmonic component, leaving the control action to the PID controller. The conditions to rely on compensator action are the same to those to be confident on PID controller through speed limitation.

Table 2.9 Error values on sinusoidal signals with proportional gains for critical speed step responses and amplitude compensator - Load mass 0 kg

| Frequency [Hz] | Amplitude [mm] | Kp    | Error at main harmonic [%] | Static error % |
|----------------|----------------|-------|----------------------------|----------------|
| 2.0            | 31.66          | 1.046 | -0.0003%                   | 0.0071%        |
| 2.5            | 20.26          | 1.303 | 0.0005%                    | 0.0072%        |
| 3.0            | 14.07          | 1.558 | -0.0001%                   | 0.0072%        |
| 3.5            | 10.34          | 1.81  | 0.0003%                    | 0.0072%        |
| 4.0            | 7.92           | 2.055 | -0.0001%                   | 0.0112%        |
| 4.5            | 6.25           | 2.307 | 0.0003%                    | 0.0073%        |
| 5.0            | 5.07           | 2.54  | -0.0001%                   | 0.0074%        |
| 5.5            | 4.19           | 2.78  | 0.0003%                    | 0.0075%        |
| 6.0            | 3.52           | 3.08  | 0.0001%                    | 0.0073%        |
| 6.5            | 3.00           | 3.28  | -0.0004%                   | 0.0075%        |
| 7.0            | 2.58           | 3.39  | 0.0003%                    | 0.0080%        |
| 7.5            | 2.25           | 3.57  | 0.0001%                    | 0.0082%        |
| 8.0            | 1.98           | 3.96  | 0.0001%                    | 0.0077%        |
| 8.5            | 1.75           | 4.7   | 0.0000%                    | 0.0063%        |
| 9.0            | 1.56           | 4.7   | 0.0003%                    | 0.0069%        |
| 9.5            | 1.40           | 4.67  | 0.0000%                    | 0.0077%        |
| 10.0           | 1.27           | 4.64  | 0.0002%                    | 0.0085%        |

Table 2.10 Error values on sinusoidal signals with proportional gains for minimum error step responses and amplitude compensator – Load mass 450 kg

| Frequency [Hz] | Amplitude [mm] | Kp    | Main harmonic error [%] | Static error % |
|----------------|----------------|-------|-------------------------|----------------|
| 2.0            | 31.66          | 0.932 | 0.00043%                | 0.27669%       |
| 2.5            | 20.26          | 0.933 | 0.00005%                | 0.43055%       |
| 3.0            | 14.07          | 0.933 | -0.00046%               | 0.61904%       |
| 3.5            | 10.34          | 0.936 | 0.00005%                | 0.82285%       |
| 4.0            | 7.92           | 0.942 | 0.00039%                | 1.01778%       |
| 4.5            | 6.25           | 0.949 | 0.00040%                | 1.18193%       |
| 5.0            | 5.07           | 0.96  | -0.00044%               | 1.30119%       |
| 5.5            | 4.19           | 0.972 | 0.00050%                | 1.36492%       |
| 6.0            | 3.52           | 0.986 | -0.00048%               | 1.36953%       |
| 6.5            | 3.00           | 1     | 0.00009%                | 1.31295%       |
| 7.0            | 2.58           | 1.015 | 0.00013%                | 1.19207%       |
| 7.5            | 2.25           | 1.031 | -0.00012%               | 1.01928%       |
| 8.0            | 1.98           | 1.048 | -0.00016%               | 0.79726%       |
| 8.5            | 1.75           | 1.065 | -0.00065%               | 0.53011%       |
| 9.0            | 1.56           | 1.083 | 0.00044%                | 0.23377%       |
| 9.5            | 1.40           | 1.102 | 0.23377%                | 0.08405%       |
| 10.0           | 1.27           | 1.119 | 0.00122%                | 0.42916%       |

## 2.4 Control system design – implementation

In order to control the servo-hydraulic system through the established control methodology, a solution which integrates in a singular device hardware and software elements, is required. The device must satisfy some functional and operative requirements as follows:

- Functional - the device must works and executes the following actions:
  - Acquire data from the position transducer placed at the hydraulic actuator.
  - Generate sinusoidal and step signals.
  - Calculate the control action according to the imposed input signal the gathered data coming from the position transducer.
  - Develop harmonic decomposition and calculate the amplitude compensation factor
  - Send a control signal to control the servovalve on the servo-hydraulic system.
- Operative - the device must be able to:
  - Be portable, to carry to field conditions.
  - Establish communication to other computational devices. Be controlled by a user interface which include basic controls of some important functional parameters.
  - Transfer data either generated or gathered to other devices.
  - Control the servo-hydraulic system with a high level of security, including enough over-limit and emergency controls.

The implementation of the controller involves the development of both hardware and software structures, in order to integrate the controller requirements, and available technologies able to execute the controlling tasks.

### 2.4.1 Hardware requirements

Controller device must interact with the servo-hydraulic system commanding the double stage servovalve, and acquiring data from the position transducer which measures the piston position. It must also command the manifold electrovalve on the hydraulic circuit allowing the oil flow to the servovalve, and establish a bidirectional communication with an user interface in order to receive operational parameters or send operational information. Signals and information coming from the systems defines the device inputs, while the signals going from the device to execute a command actions are the device



outputs. Internally, the controller takes the inputs, executes processing and control tasks and generates the outputs

The hardware required to carry the input and output interfaces is determined by the signal characteristic required by the devices on the external systems which interact with the controller, as summarized in Table 2.11.

Table 2.11 Inputs and output signal requirements for the servo-hydraulic system controller device

| From/to                                      | Inputs                         | Output                                |
|--|--------------------------------|---------------------------------------|
| Hydraulic circuit – Manifold valve control   |                                | 24VDC signal                          |
| Servo-hydraulic system – Position transducer | LVDT analogical voltage signal |                                       |
| Servo-hydraulic system – servovalve command  |                                | $\pm 50$ mA analogical current signal |
| User interface device                        | Digital information packages   |                                       |

In other hand, the processing and control tasks requires a hardware able to be programmable according to the control characteristics defined in this chapter, and be able to establish communication between the hardware devices for input and output handling. On industrial control applications, three groups of technologies has been used along the years to develop the processing and control task, recognizing application-specific integrated circuits (ASICs), processor for signal and processing, and field-programmable gate array (FPGA) technologies . Along the years, FPGA had gained place on industrial applications due to their benefits in performance, flexibility, cost, reliability and long term maintenance [19]. FPGA are reprogrammable silicon chips with prebuilt logic blocks and programmable routing resources configurable to implement customized hardware functionality without modifications on the hardware mainframe. In addition, through reprogrammable silicon chips, truly parallel processing takes place, so different processing operations can be handle at same time and do not compete for the same processing resources. Due to flexibility and parallel processing characteristics, the servo-hydraulic controller device is conceived with the use of a FPGA technology to develop the processing and control tasks, granting a reliable operation from the hardware point of view and the possibility to be programmed in order to satisfy the functional and operational characteristics of the controller.

The controller device can be decompose in functional groups, which have a particular function in the controller as seen in Figure 2.24. Blue-lighted blocks represent the inputs of the system, white the processing and control task and red ones the outputs. The green group corresponds to the necessary hardware to keep in function the other groups. Each functional group requires specific devices to assure the signal characteristics and its interactions with other groups either in the information or power loop. The composition of each group is as follows:

- Processing and control: A National Instruments ® C-RIO 9004 processor is selected as FPGA device. Is integrated to a National Instruments ® C-RIO 9111 chassis in order to allow an easy communication structure with the LVDT transducer signal acquisition, servovalve signalling and manifold electrovalve signalling groups. Inputs and outputs handled by this group are either analog or digital voltage signals.
- LVDT transducer signal acquisition: the analogical signal coming from the LVDT transducer requires a signal conditioner in order to demodulate, amplify to an specific voltage range and correct the original signal, minimizing the signal quadrature and maximizing the noise rejection. The LDM 1000 signal conditioner from Measurementspecialists ® takes the LVDT transducer signal and gives an analog output in the range of  $\pm 5$ Volts. Such signal is acquired through a National Instruments ® C-RIO 9205 module in order to complete the LVDT transducer signal acquisition group. C-RIO 9205 is compatible with C-RIO 9111 chassis allowing an easy communication process with the processing and control block.
- Servovalve signalling: The motor on the servovalve requires an analog current input in the range of  $\pm 50$  mA, while the processing and control block gives an analog voltage signal output. In order to assure the servovalve requirements a voltage-current servo amplifier is required. The signal coming from the processor is taken by a National Instruments ® C-RIO 9263 module gives a  $\pm 10$  V analog signal and treated by a servo amplifier AEXI ® Tipo AX 178 giving the current analog signal in the required range. Voltage analog output module and servo amplifier, are the component of the servovalve signalling group.
- Manifold electrovalve signalling: In order to command the manifold valve a  $\pm 24$  VDC at 1 A current is required. No C-RIO modules can handle such levels of current, so the signalling requires a different electronic mechanism in order to satisfy the conditions. a National

Instruments ® 9472 voltage digital output module commands a Finder ® 94.74 relay with a 24 VDC bobine 55.34, in order to allow the 24VDC feeding from the power electronics group to the manifold electrovalve.

- User communication interface input and output: the digital information packages are transferred through a ethernet network, using the RJ-45 ethernet port available in the C-RIO 9004 module. Any user device with ethernet protocols can share and transfer data with the processing and control group. In order to avoid network constructions and configurations [20], an ethernet crossover cable is also included in the user communication interface blocks.
- Power electronics: The different devices assembled on the functional groups requires power in order to be functional. A Phoenix Contacts ® Quint PS 100 240 AC24DC5 power supply is used in order to satisfy the power requirements of the devices shown in Table 2.12.

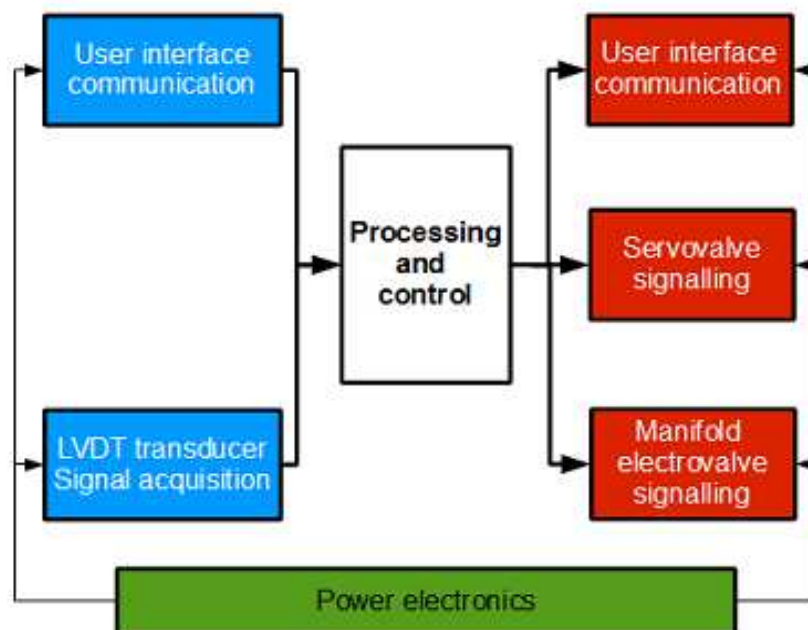


Figure 2.24 Representative functional groups on servo-hydraulic controller device

Table 2.12 Power requirements for servo-hydraulic controller device

| Device                | Required voltage supply [VDC] | Required current [mA] | Power supply [mW]        |
|-----------------------|-------------------------------|-----------------------|--------------------------|
| CRIO 9111             |                               |                       | 2600                     |
| CRIO 9004             | 24                            |                       | 17000                    |
| CRIO 9205             |                               |                       | Included into C-RIO 9111 |
| CRIO 9263             |                               |                       | Included into C-RIO 9111 |
| NI 9172               |                               |                       | Included into C-RIO 9111 |
| AXI-178               | 24                            | 150                   | 3600                     |
| LDM-1000              | 24                            | 65                    | 1560                     |
| Manifold electrovalve | 24                            | 1000                  | 24000                    |

Further information about wiring and connections of the devices, can be found in Appendix A-III Electrical schemes.

#### 2.4.2 Software configuration

One of the FPGA outstanding characteristics is the flexibility to be configured to implement customized hardware functionality. Each FPGA manufacturer uses particular software in order to create the required routines that satisfy the application. As the processing and control group in the servo-hydraulic controller hardware is based on a National Instruments ® devices, Labview ® software is the platform which supports the FPGA programming of the controller.

Figure 2.25 shows the controller architecture in terms of hardware groups determined in chapter 2.4.1 . Two different software structures are developed to execute the processing and control tasks and user interface communication processes, the first directed on FPGA programming and the other on Real time programming.

Labview ® FPGA module allow the programming of the routing resources on the C-RIO module 9004, in order to create the PID controller, the amplitude compensator and establish communication between the C-RIO modules 9205, 9263 and 9171 and the C-RIO 9004 through the communication gates placed in the C-RIO 9111. Alike, Real time module allows a fast data transferring and real deterministic processes and is used to generate the user interface and the necessary communication tasks with the FPGA.

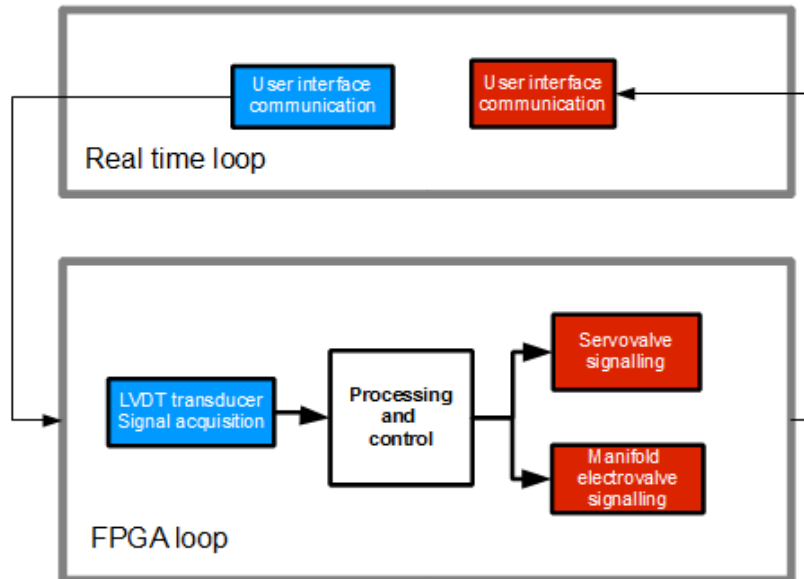


Figure 2.25 Servo-hydraulic controller software architecture

The controller user interface is composed by three groups, organized according to similar operational and functional characteristics.:

- Visualization charts: allow the user to visualize in real time the measured variables involved in the control process.
- System controls: allow the visualization of system performance parameters and the configuration of the visualization charts group.
- Operational controls allow the imposition of the operational parameters for the controller operation. Is divided in two tabs, according the state of the controller, configuration and control. Configuration state allows the configuration of the common parameters that are used on every test and must not be modified unless hardware, cylinder or overall test conditions are changed. Control state allow the user to modify the actual service parameters while the controller is executing a command action in the servovalve.

A detailed explanation of each component in the controller user interface can be found in Appendix A-VI Controller user interface.

The user interface software had been designed in order to develop two different types of analysis, free and modal analysis. Particular procedures must be developed in order to satisfy security and operative conditions.

In both cases, before starting the test, all the security conditions on the hydraulic circuit and the servo-hydraulic system must be verified and assured. Once those conditions are satisfied, become necessary to verify the oil supply pressure, measured in the manifold electrovalve. A constant pressure value must be present along the test, in the range of 200 MPa to 310 MPa. If the servo-hydraulic system works with a lower pressure, the hydraulic actuator can be damaged. Higher values are also not allowed by the constructive characteristics of both, servovalve and hydraulic actuator.

Every time the controller is started is run the configuration mode. Verify that system parameters like maximum stroke, and the operative voltage ranges for C-RIO modules and LVDT are imposed. The controller brings the default values according to the hardware characteristics described in chapter 2.4.1, and the physical characteristics of the linear hydraulic actuator. Being confirmed those parameters, is possible to decide between free and modal analysis.

Free analysis allow the user to modify along the time the signal type and the signal characteristic values, like amplitude, offset or frequency, according to the signal type. To run under this analysis type, select the signal type and then change to control mode. When control mode is started, the system recovers the default PID controller parameters to avoid gain values that can drive the servo-hydraulic system to unstable conditions. Impose the signal parameters, and modify the PID values in order to obtain a piston displacement with the required conditions. If amplitude compensation is required, turn on the amplitude compensator without changing the PID gain values.

Otherwise, modal analysis imposes sinusoidal signals according to a configuration file where the amplitudes and the frequencies are tabulated. Therefore the user can not modify during the control action neither the signal type nor the signal parameters. Compared to free analysis, the user must undergo almost the same steps in order to carry an analysis, except that instead of impose the signal type and the signal parameters manually, must load the \*.txt file which contains the signal characteristics. The other steps remain the same.

As mentioned before, user interface communication is developed on Labview Real time module, while FPGA requires another programming structure. Such FPGA programming just executes the processing and control tasks, and receives and send data to other processes. No user interface is significant for this proposes.

The FPGA programming for the controller device, is divided according to the

functional processes defined in the software architecture. Data acquisition takes the signals obtained by the analogical input modules, saturates the signal according to the servo amplifier limitations, and filters the LVDT transducer signal in order to reduce the noise sensitivity of the system. Processing and control tasks, is divided in three actions, the signal generation where the step or sine wave signal is created according to the user needs, and the PID control action using the acquired and generated signals and the amplitude compensation where another signal generator with a compensated amplitude takes the place of the main signal generator. Output signalling process, is also divided in three tasks, one where takes the signal generated by the PID controller and sends a command action to the hardware associated with the double stage servovalve, another which commands the manifold electrovalve taking the a signal coming from the user interface, and a final task which send information to the user interface device. Input communication tasks are inherently associated to another processes which requires the data coming from the user communication interface. A detailed explanation of the FPGA block diagrams used in the controller are shown in Appendix A-V FPGA block diagrams.

## Chapter 3 Test rig

In order to evaluate the controller performance, a test rig which integrates the controller, servo-hydraulic system, and hydraulic circuit, is required

Each subsystem have particular components as follows:

- Controller: is composed by the controller electrical box and all the required cables which connect the electrical box with the different devices in the other systems, like the crossover ethernet cable, a 17 pin – 4 pin cable to control the servovalve, a 17 pin – 6 pin to acquire the signal coming from the LVDT, and a cable with a solenoid connector as terminal to control the manifold electrovalve.
- Servo-hydraulic system: is composed by the linear hydraulic actuator and a double stage servovalve, according to the functional descriptions given in Chapter 1. The LVDT sensor is also included in this system, due to the actual constructive characteristics of the actuator which includes a LVDT.
- Hydraulic circuit: is the system which provides to the servo-hydraulic the oil at certain constant pressure. There is no interest in define how the hydraulic system works, or the type of hydraulic circuit is. For test rig proposes the circuit is a black box and a solenoid 3/2 proportional valve is the only element required to integrate with the other subsystems.
- Attached load: the attached load is connected to the servo-hydraulic system through the actuator's piston rod. In order to simulate the conditions of an actual structure, the attached load and the servo-hydraulic system are assembled in an arrangement like the one presented on Figure 3.1.

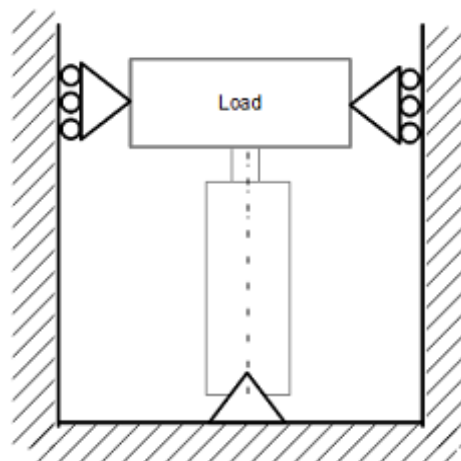


Figure 3.1 Attached load structure for servo-hydraulic test rig



### 3.1.1 Controller electrical box

The controller electrical box contains all the devices, as shown in Figure 3.2, required to have a functional controller according to the characteristics determined in Chapter 2, in order to develop data gathering, processing and control, data signalling and user interface communication tasks.

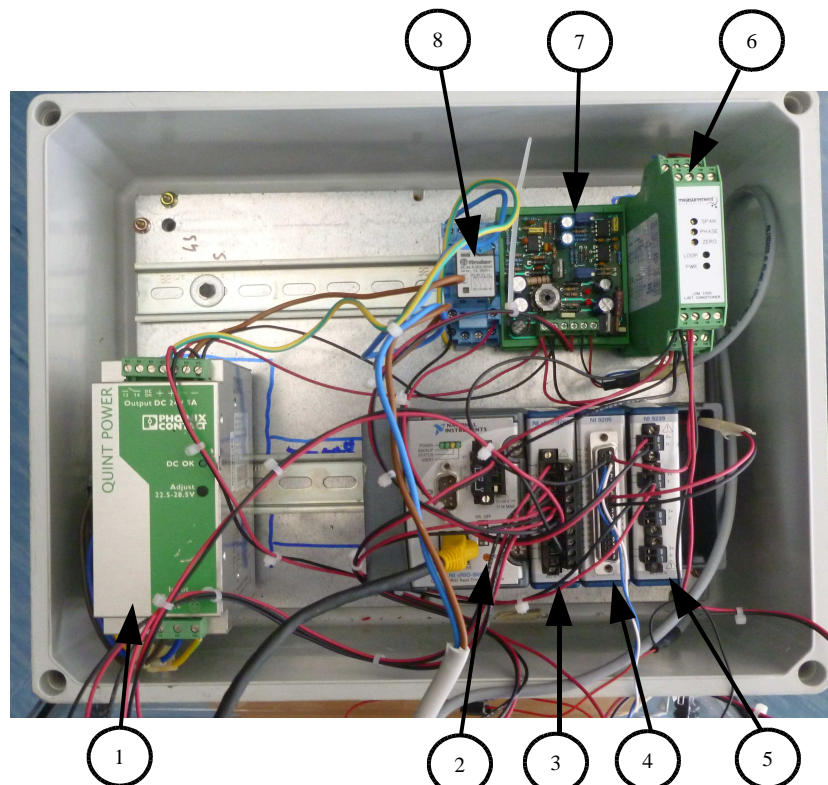


Figure 3.2 Controller electrical box – Internal view

Internally, the controller electrical box is composed by:

- Power supply Phoenix contacts Quint PS 100 240AC24DC5 (1).
- C-RIO 9004 FPGA controller (2).
- C-RIO 9263 voltage analog output module (3).
- C-RIO 9263 voltage analog input module (4).
- NI 9172 voltage digital output module (5)
- LDM 100 LVDT conditioner (6).
- AEXI AX 178 voltage-current servo amplifier (7)
- Finder 94.74 and 55.34 electromechanical relay and coil (8).

The final user must interact with a electrical front panel as the one shown in Figure 3.3. The components of the front panel are:

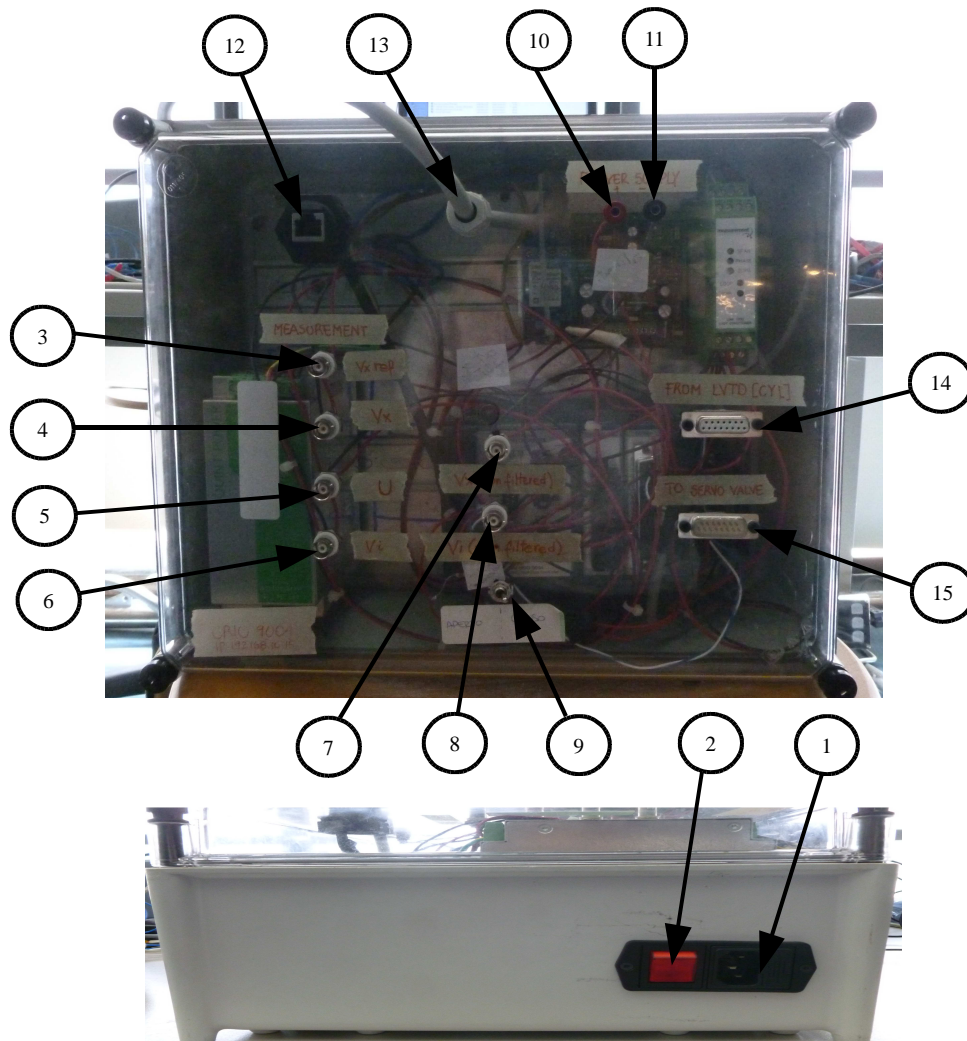


Figure 3.3 Controller electrical box – External view

- External power supply connector (1): allow to connect the controller to an external power supply source of 240 VAC at 50 Hz.
- ON – OFF selector (2): the selector is used to handle the power supply over the main circuit. If is turned towards ON position, the selector lights itself.
- Reference Voltage (3): is a BNC connector carrying the reference voltage

signal generated by the signal generator inside the controller.

- Actual position Voltage (4): is a BNC connector carrying the actual position signal relative to the LVDT transducer placed in the hydraulic linear actuator.
- Controller command signal (5): is a BNC connector carrying the voltage signal generated by the PID controller.
- Spare BNC connector (6): spare BNC connector for future controller modifications.
- Actual position Voltage (7): is a BNC connector carrying the actual position signal before the filtering on the FPGA relative to the LVDT transducer placed in the hydraulic linear actuator.
- Servovalve command voltage signal (8): is a BNC connector carrying the voltage signal measured on the shunt resistance placed on the circuit going to the servovalve. Is a voltage value related to the servovalve current command signal.
- Servovalve command voltage signal selector (9): when the selector is turn towards “close”, the servovalve command voltage signal can be measured. If no measuring is taking place, turn the selector towards “open” position and short-circuit this loop using the BNC connector developed for this proposes.
- DC power supply input – output connectors (10) and (11): if there is an internal 24VDC power supply inside the electrical box both connectors work as output terminals for external applications which require such voltage values. If no internal 24VDC power supply exists, the electrical box can be powered externally through the connectors. If last option occurs, elements (1) and (2) do not work.
- Ethernet port (12): RJ-45 ethernet port for user interface communication proposes.
- Manifold electrovalve output port (13): port dedicated to carry the signal to the manifold electrovalve. Have a proper solenoid connector at the end of a 5 metres cable, necessary to command the electrovalve.
- Servovalve output connector (14): 17 pin connector required to send the command signal generated by the controller, to the servovalve. A 17 pin - 4 pin proper cable is required to connect this interface with the servovalve connector.
- LVDT input connector (15): 17 pin connector required to get the signal coming from the LVDT transducer placed on the hydraulic actuator. A 17 pin – 6 pin proper cable is required to connect this interface with the LVDT connector.

### 3.1.2 Linear hydraulic actuator

A MTS-242.25 has been chosen as hydraulic power element on the servo-hydraulic system, recommended and widely used in applications like fatigue test, structural resonance searching and modal analysis [21]. Such actuator have a constructive configuration depicted on Figure 3.4.

A servovalve can be attached to the actuator through the porting arrangement (2), where high-pressure hydraulic fluid is supplied through the pressure port. As the servovalve does the flow control action, sends the fluid to one or another side of the actuator in order to extend or retract the piston rod. The fluid on the other side of the piston returns as pass through the return port (8).

This series of actuators includes a coaxial and internal LVDT assembly to provide an accurate displacement indication of the actuator piston rod.

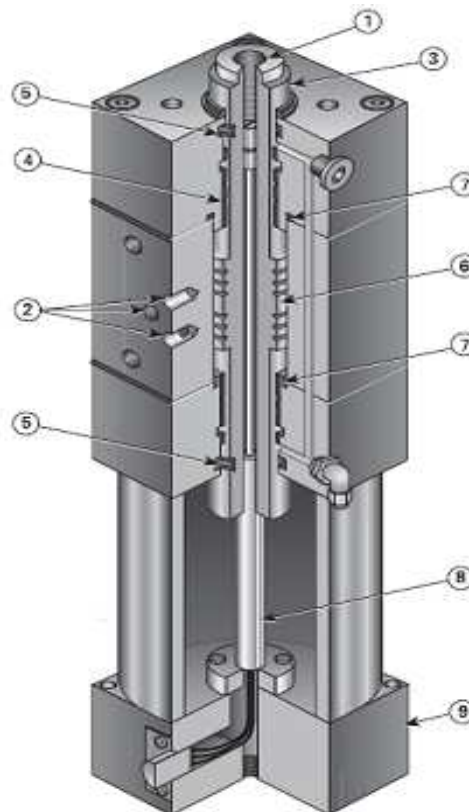


Figure 3.4 Constructive configuration for a MTS 242.25 linear hydraulic actuator [21]

### 3.1.3 LVDT sensor

Linear Variable Differential Transformers (LVDT) is a type of sensor used to measure position and displacement using the principle of electromagnetic induction, where a magnetic flux coupled between two coils may be altered by the movement of an object and subsequently converted into voltage [22].

A LVDT is a transformer composed by a primary coil, a secondary coil group and a mechanically actuated core. The primary coil is driven by a sinusoidal excitation signal with a stabilized amplitude in order to eliminate the error related to harmonics in the transformer [22]. The secondary coil group is composed by two coils connected in the opposed phase, and the core is inserted coaxially into the cylindrical opening avoiding any physical contact with any coil. When the core is positioned on the magnetic centre of the transformer, the output signals in each secondary coil are cancelled and no output voltage occurs. If the core moves away the central position, the induced magnetic flux ratio between the coils in the secondary changes and an output voltage signal appears. As the core moves, the reluctance of the flux path changes, hence the degree of flux coupling depends on the axial position of the core [22], and consequently the voltage may be used as a measure of a displacement. Figure 3.5 shows a schematic representation of a LVDT sensor, representing its actual constructive characteristics and an electrical representation of the transformer.

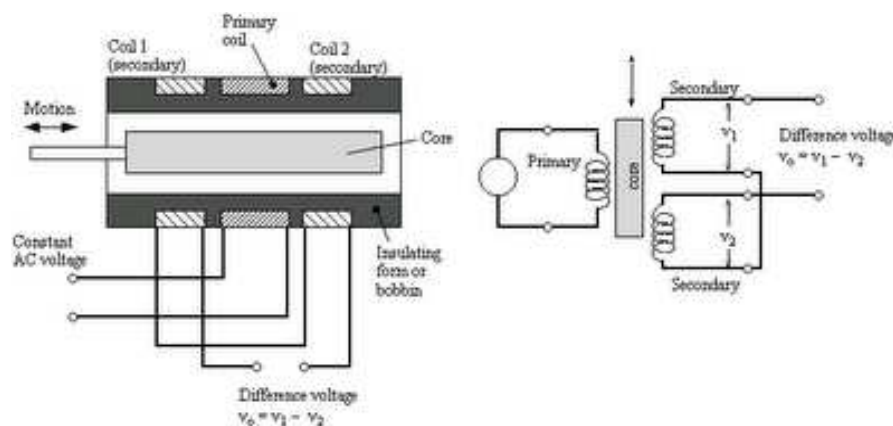


Figure 3.5 LVDT sensor – schematic representation [23]

Characteristics like no friction resistance and therefore small resistive forces, negligible mechanical and magnetic hysteresis, low output impedance, low susceptibility to noise and interferences, the possibility to have infinitesimal resolution and a compact and solid constructive configuration [22], make the

LVDT sensor a reliable and wide used sensor type in position and displacement measurement applications.

### 3.1.4 Double stage servovalve

A MTS-252.25 servovalve as the one shown in Figure 3.6, is attached to the linear hydraulic actuator, defining the overall servo-hydraulic system for modal analysis proposes.

The double stage servovalve is a device composed by a torque motor and two stages of hydraulic power regulation. The flapper-nozzle first stage valve is controlled by the torque motor positioning flapper, which controls the flow coming from a pair of nozzles in an inversely proportional manner [8]. The change in the flow passing by the nozzles due to the flapper action, creates a differential pressure used to position the second stage spool valve which controls the direction and rate of hydraulic fluid flowing to the actuator [8]. Further functional characteristics of double stage servovalves is described in Chapter 1.



Figure 3.6 Double stage servovalve [8]

### 3.1.5 Hydraulic circuit

An external hydraulic circuit is to the controlled servo-hydraulic system, is required to provide the servovalve and actuator with the fluid required to operate the system. As the hydraulic circuit do not belong to the servo-hydraulic system structure, some characteristics are required in order to have adequate operative conditions; a constant oil supply pressure must be granted in the range of 20 to 31 MPa, which are the suggested and maximum pressure operative values for a MTS-252.25 servovalve. Values beyond the maximum value can not be handled

by the servo-hydraulic system, and values lower than the suggested value, reduces the hydraulic power of the system.

A second characteristic required on the hydraulic circuit, is a directional electrovalve in order to stop the flow from the circuit to the servo-hydraulic system according to the operative conditions. The user can allow the pass of oil, according to the procedures defined in Chapter 2, activating or deactivating the manifold electrovalve. Also if an insecure condition is present in the servo-hydraulic system, the user can use the emergency stop and blocks the oil flow passing to the electrovalve and the servo-hydraulic systems does not work.

The electrovalve is a 3/2 solenoid proportional hydraulic valve, with pressure regulator to set the constant pressure value required by the servo-hydraulic system. The solenoid is activated by a solenoid connector, included in the controller electrical box. Figure 3.7 shows a typical solenoid proportional hydraulic valve as the one used in the hydraulic circuit in this project.



Figure 3.7 Manifold electrovalve [24]

## Chapter 4 Experimental results

Experimental tests are required in order to evaluate the performance of the controller at different operational conditions, and verify that the responses of the controlled servo-hydraulic system, satisfies the characteristics defined in chapter 2.3.3, in terms of stability, attenuation to load disturbances, sensitivity to noise measurement, set-point following and operational characteristics.

An additional goal on the experimental stage, is compare the actual and simulated behaviour of the servo-hydraulic system in order to verify the accuracy of the models (linear and non linear), and therefore PID tuning methodology based on simulations.

### 4.1 Non load case

The non load case is the simplest test condition where non attached load is present in the test rig. This case has the most secure conditions to verify the operation of the system at different operational points, even those where high acceleration values are present and can not be afforded under load conditions due to the associated values of the dynamic load.

Different tests had been conducted on the servo-hydraulic system. The first round of them, submits the servo-hydraulic system to a step input signal at different amplitude levels and only proportional action on the controller, in order to obtain the time domain performance parameters as response speed, overshooting, response time, steady-state error and signal to noise ratio on the steady-state response. In all the cases, the proportional gain remain the same in order to evaluate the behaviour of the responses only in terms of the input amplitude.

The response of the system for step input amplitudes of 5, 10, 20 and 50 millimetres, are shown in Figures 4.1 to 4.4. In all the cases the proportional gain imposed in the controller is 1, while integral and derivative actions are not imposed. Alike, the time domain performance parameters for each of the tested cases, are summarized in Table 4.1.



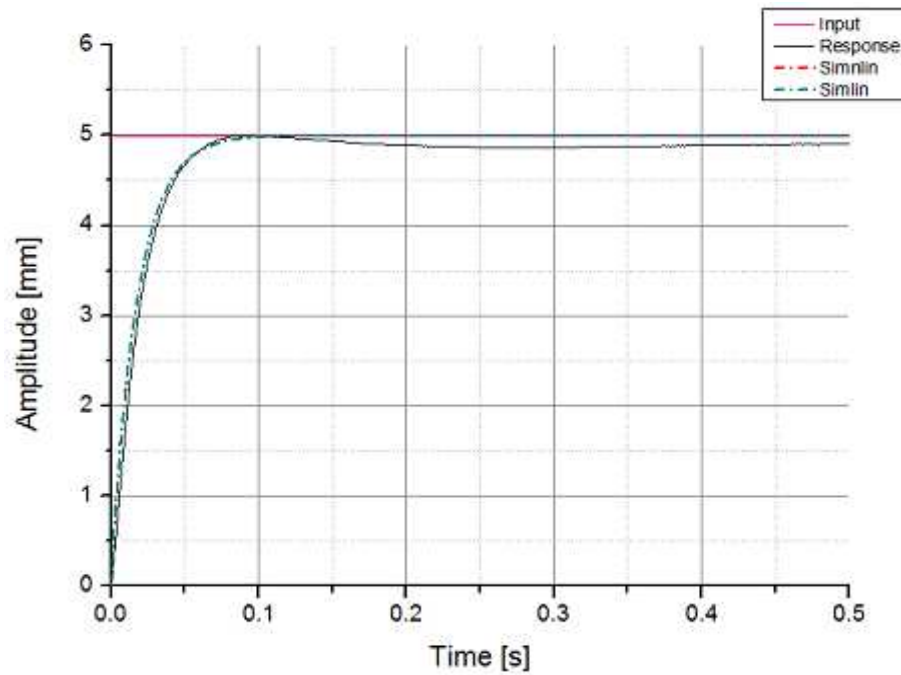


Figure 4.1 actual and simulated 5 mm step response for controlled servo-hydraulic system – non load case

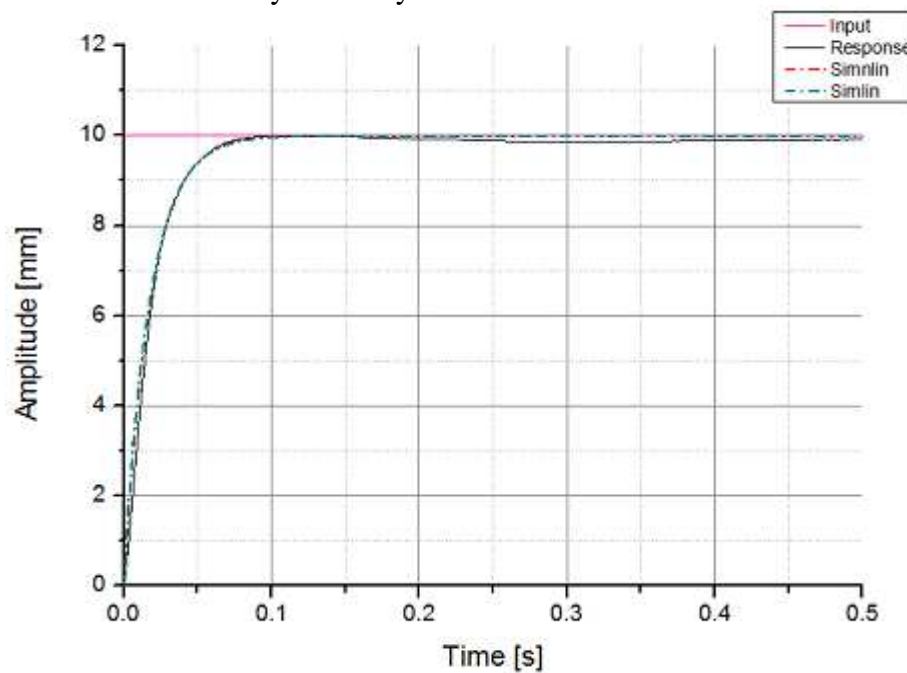


Figure 4.2 actual and simulated 10 mm step response for controlled servo-hydraulic system – non load case

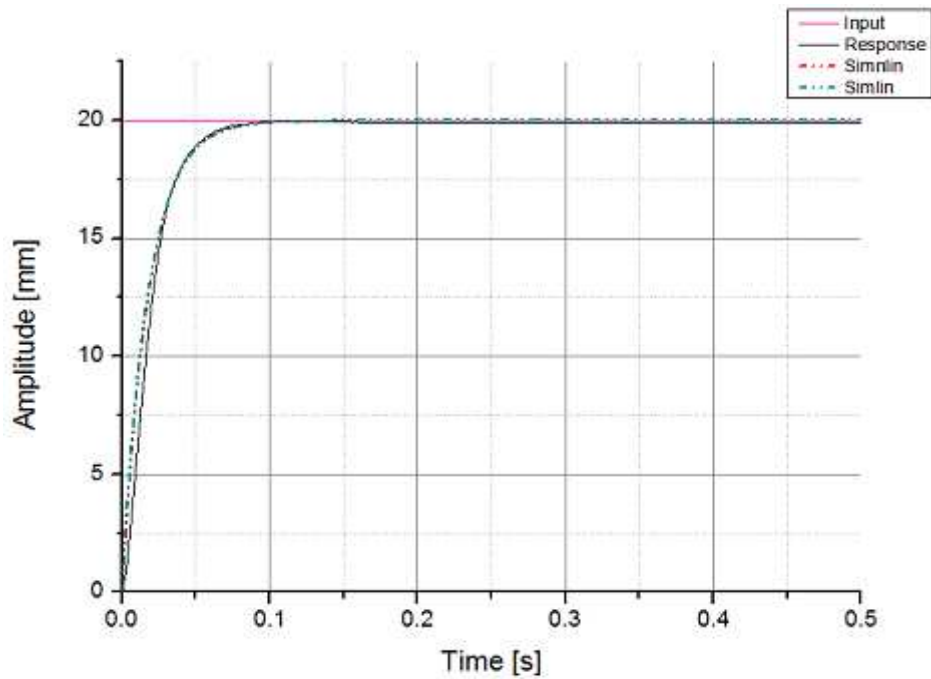


Figure 4.3 actual and simulated 20 mm step response for controlled servo-hydraulic system – non load case

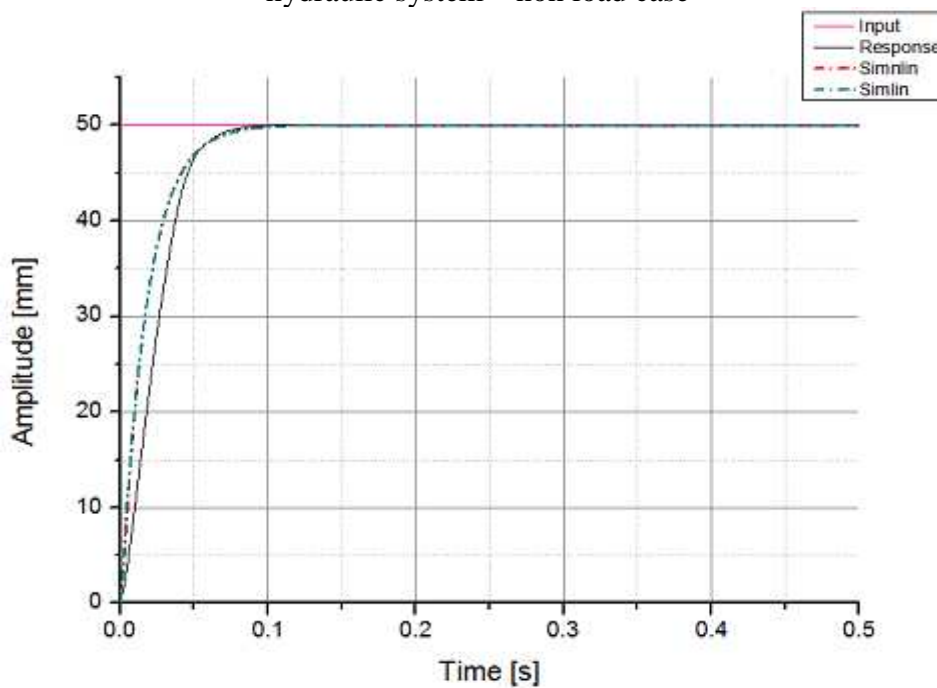


Figure 4.4 actual and simulated 50 mm step response for controlled servo-hydraulic system – non load case

Table 4.1 Time domain performance parameters for step input response at different amplitude values – non load case

| Amplitude [mm] | Case                   | Overshoot  [%] | Sr [mm/s] | Tr [s] | Mean steady state error |
|----------------|------------------------|----------------|-----------|--------|-------------------------|
| 5              | Simulation – linear    | 0.18%          | 102.170   | 0.039  | 0.000%                  |
| 5              | Simulation – non liner | 0.18%          | 102.360   | 0.039  | 0.000%                  |
| 5              | Test                   | 0.94%          | 108.352   | 0.038  | 1.793%                  |
| 10             | Simulation – linear    | 0.18%          | 204.340   | 0.039  | 0.000%                  |
| 10             | Simulation – non liner | 0.18%          | 205.140   | 0.039  | 0.000%                  |
| 10             | Test                   | 0.17%          | 221.616   | 0.037  | 0.794%                  |
| 20             | Simulation – linear    | 0.18%          | 408.630   | 0.039  | 0.000%                  |
| 20             | Simulation – non liner | 0.18%          | 412.140   | 0.039  | 0.000%                  |
| 20             | Test                   | 1.90%          | 464.623   | 0.034  | 0.519%                  |
| 50             | Simulation – linear    | 0.18%          | 1022.470  | 0.039  | 0.000%                  |
| 50             | Simulation – non liner | 0.18%          | 1041.830  | 0.038  | 0.000%                  |
| 50             | Test                   | 0.79%          | 1011.050  | 0.040  | 0.097%                  |

An initial evaluation of the results shown in Table 4.1, shows a difference between the actual and the simulated responses. The steady-state response on the simulated cases shows a zero mean steady-state error due to the presence of the zero pole on the simulated servo-hydraulic system; while the measured case does not show the same characteristic with mean steady-state error oscillating between 1.793 to 0.097 % along the different amplitudes. This non zero mean steady-state error is characteristic of a system which does not have a zero pole in the origin, therefore the actual system has a different behaviour compared to the simulated system. Such conditions can be explained only in terms of conditions that were not included into the model and adds stiffness or damping to the servo-hydraulic system at low frequencies. The non included characteristics of the servovalve are not of interest because the servovalve dynamics is representative at frequencies at least 5 to 10 times higher than the expected bandwidth as explained in chapter 1. On the contrary, a different modelling of the hydraulic actuator can explain such differences. On the model of the servo-hydraulic system, the piston actuator mass was considered as a point mass. However the piston is not a rigid body and has its own structural stiffness and damping, dependent on the physical characteristics of the component, and the constructive characteristics of the cylinder, like radial and axial tolerances, and misalignment. Such values are representative in the non load case as no other stiffening or damping structural mechanisms are present in the test rig, and changes the behaviour of the system. The model of the servo-hydraulic system used to develop the simulations, is accurate enough to visualize the global behaviour of the actual system, and is particularly useful to determine proportional gain of the controller for a particular operation point. In other hand, integral and derivative

action can not be modelled properly if structural stiffness and damping values are not included in the model, because this values have great incidence in the behaviour of the system at low frequencies. Therefore, the model must be used to calculate the useful range of proportional gains at a particular operation point, and if the structural parameters are known, to obtain the ranges of integral and derivative times for the integral and proportional action of the controller.

The response time on each amplitude case is quite similar on all the amplitude cases, and between the simulations and the experimental tests. Such condition leads to have similar response speeds between simulation and tests for each amplitude, with a variation oscillating between the 2 to 10%.

The response time just depends of the proportional gain imposed in the controller and do not vary according to the amplitude impose to the input signal while the response speed speed varies because is a function of both, time response and amplitude, as defined in chapter 2. As expected in the simulation stage, the imposition of the proportional gain in the controller is a keystone in the adequate function of the controller, in order to determine a response speed that satisfies the set-point following characteristics and do not include undesired harmonics in the transient response.

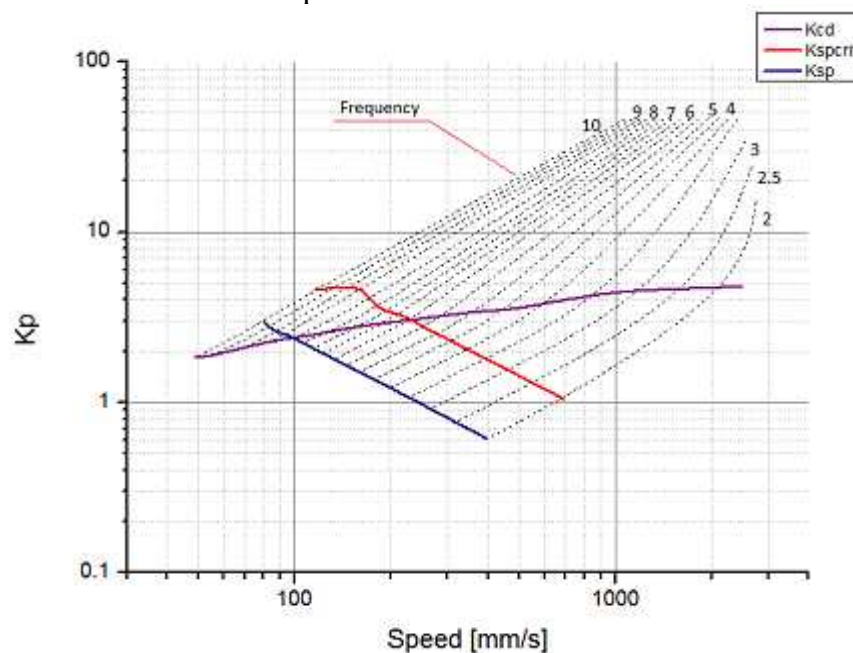


Figure 4.5 Proportional gain vs response speed for non load case

At a fixed step gain, the step responses at different amplitudes show different

behaviours, observed in the values of mean steady-state error which is reduced according the amplitude is increased. Such behaviour can be explained overlooking the Figure 4.5.

Higher response speed values represent better response behaviour, with the limitations determined by the expected characteristics of the response, explained in chapter 2.3.3. At a fixed proportional gain value, higher speeds represents higher input signal amplitudes, but at same gain condition as the speed is increased such gain becomes comparatively closer to the gain required to obtain the critical speed of the servo-hydraulic system. Therefore at higher input amplitudes, which represents higher response speeds, a lower proportional gain is enough to obtain the required response of the system with better performance parameters. However, it is important to remind that the gain necessary to obtain the critical speed is not necessary the optimal gain for the controlled system as undesired harmonics can be included in the response. The optimal gain is achievable by simulation and further evaluation on test conditions in order to obtain the expected response in step of sinusoidal input signals.

Further tests were developed in the controlled servo-hydraulic system in order to verify the integral and derivative action when the system is excited with sinusoidal input signals. Test were carried at different frequency and amplitude conditions as shown Table 4.2, with fixed PID controller gains.

Table 4.2 Frequency and amplitude conditions for sinusoidal tests non load case

| Amplitude<br>[mm] | Frequency [Hz] |   |   |   |    |    |
|-------------------|----------------|---|---|---|----|----|
|                   | 1              | 2 | 5 | 8 | 10 | 15 |
| 5                 | X              | X | X | X | X  | X  |
| 10                | X              | X | X | X | X  | X  |
| 20                | X              | X | X | X |    |    |
| 50                | X              | X | X |   |    |    |
| 90                | X              | X |   |   |    |    |

The gains imposed in the PID controller were maintained constant for every test condition in order to define a frequency response function for the controlled system, and verify the incidence of the operational points in the response of the system. The proportional gain is the maximum gain at 10 Hz and 20 mm conditions, that assures a stable response of the system. The integral time was found under same operational conditions, and was defined as the minimum time that keeps a stable behaviour of the system and therefore establish the limit of integral action; if lower values are imposed with same proportional gain value,

the system behaves unstable. A similar procedure was conducted in order to obtain the limit derivative time value. As the controller gains were obtained at a frequency condition equal to the upper limit of the expected bandwidth, such gains must assure an stable behaviour for operational conditions at lower frequencies. Proportional gain was established in 6, integral time in 0,01 seconds and derivative time in 0,003 seconds. Sinusoidal responses for each frequency value at the maximum test amplitudes are shown in Figures 4.6 to 4.11. For each frequency – amplitude combination, a series of 6 tests were developed in order to have a representative amount of data to be analysed. A sampling frequency of 5000 Hz was used to record the data of the four available signals on the controller electrical box, with a record length of 10 seconds.

With the critical gain values used in the controller, is possible to foresee that the controlled servo-hydraulic system satisfies the controller characteristics defined in chapter 2.3.3. As the gains used during the tests are the critical conditions to avoid instability, using a proportional gains lower that this value still assures a stable behaviour of the system. Integral and derivative gains depend on the corresponding integral and derivative times, and the proportional gain, therefore the integral and derivative times imposed during the tests, must be changed according to the required operational conditions; however the values used during this tests ( $K_p = 6$ ,  $T_i = 0.01$ ,  $T_d = 0.003$ ) can be used as reference for further cases.

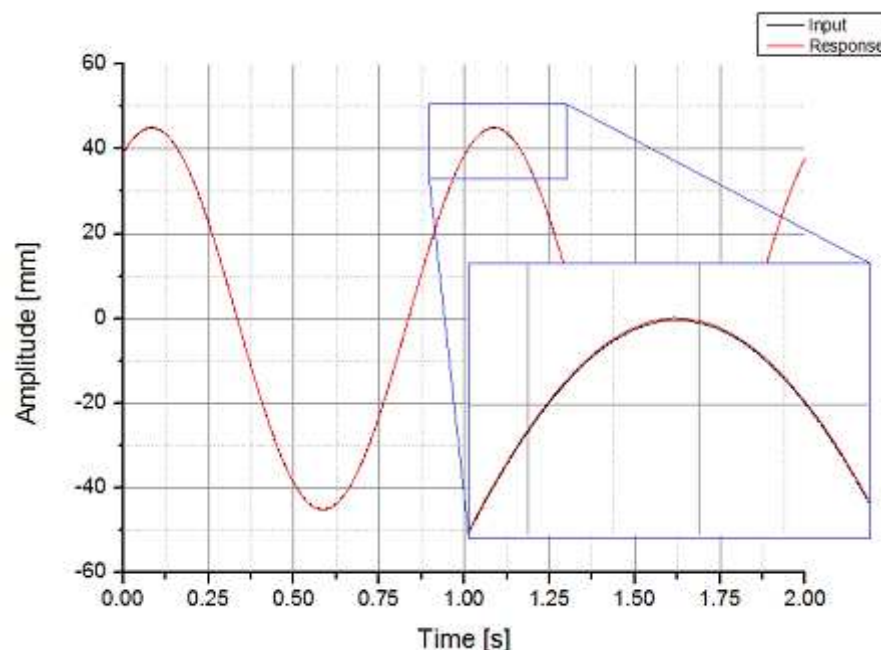


Figure 4.6 Sinusoidal response non load case, 1 Hz – 90 mm

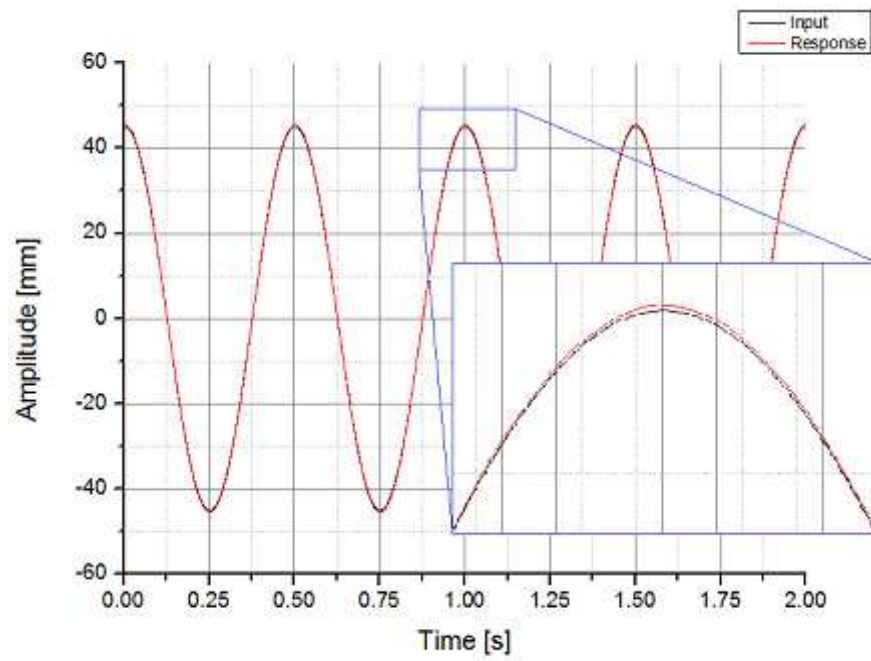


Figure 4.7 Sinusoidal response non load case, 2 Hz – 90 mm

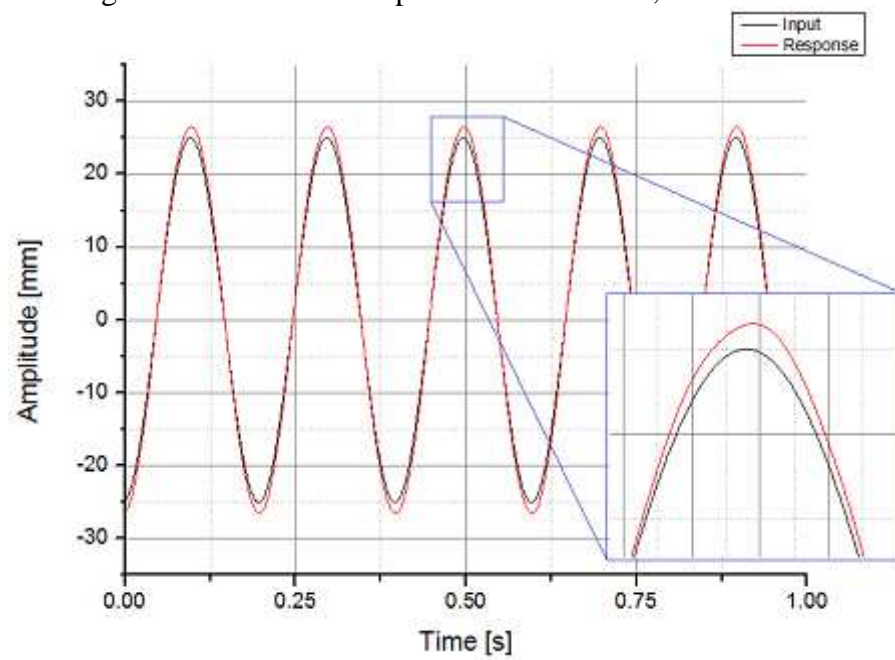


Figure 4.8 Sinusoidal response non load case, 5 Hz – 50 mm

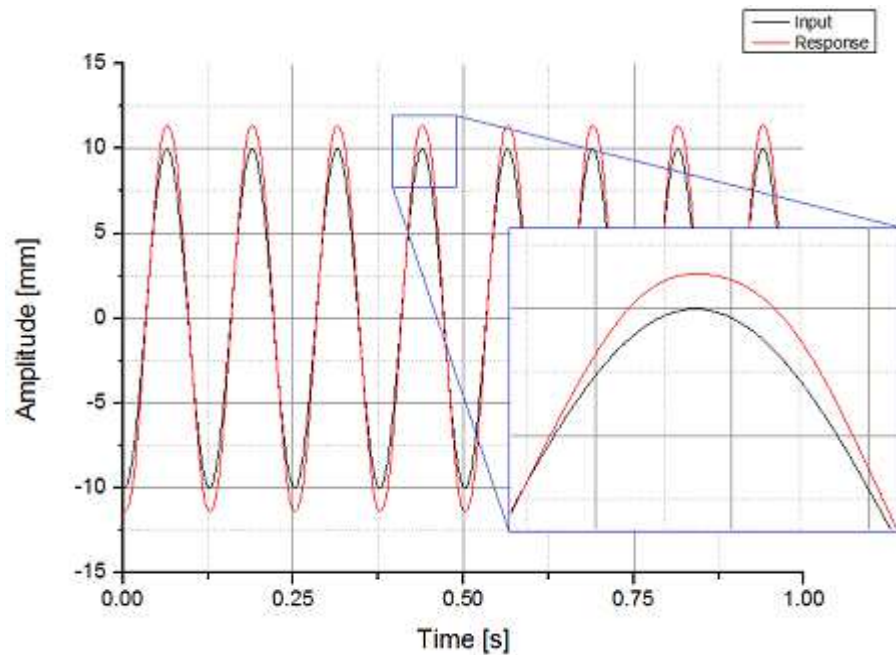


Figure 4.9 Sinusoidal response non load case, 8 Hz – 20 mm

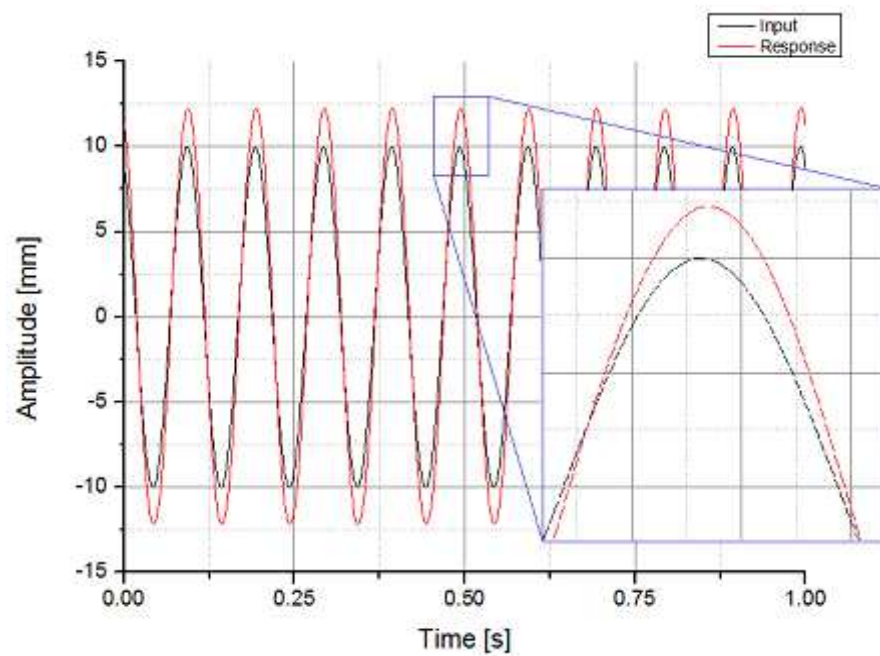


Figure 4.10 Sinusoidal response non load case, 10 Hz – 20 mm



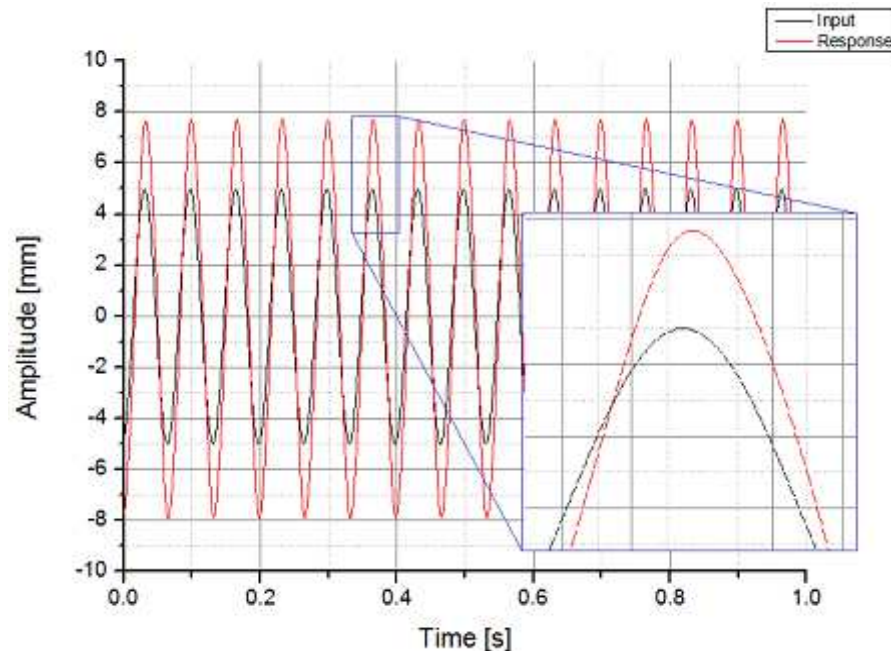


Figure 4.11 Sinusoidal response non load case, 15 Hz – 10 mm

In order to characterize the behaviour of the system, averaged frequency response function estimations are calculated. Figure 4.12 shows the frequency response function estimation at each frequency value, at the different amplitude operative conditions.

Through the frequency response function estimation for the controlled servo-hydraulic system, it is possible to observe that the system shows a stable behaviour for all the tested frequencies. The controlled servo-hydraulic system shows a characteristic frequency response function of an under-damped system, with a constant gain range at low frequencies (up to 2 Hz approximately). The poles of the controlled system are placed in the neighbourhood of 17 to 25 Hz, with under-damped characteristics. This explains why the magnitude of the frequency response function increases as the frequency increases, and why the negative phase delay between the input and response signals increases too.

The behaviour of the servo-hydraulic system is also calculated through the estimation of the frequency response function between the piston position signal and the voltage measured in the shunt resistance that gives a measure of the current which commands the servovalve, as shown in Figure 4.13.

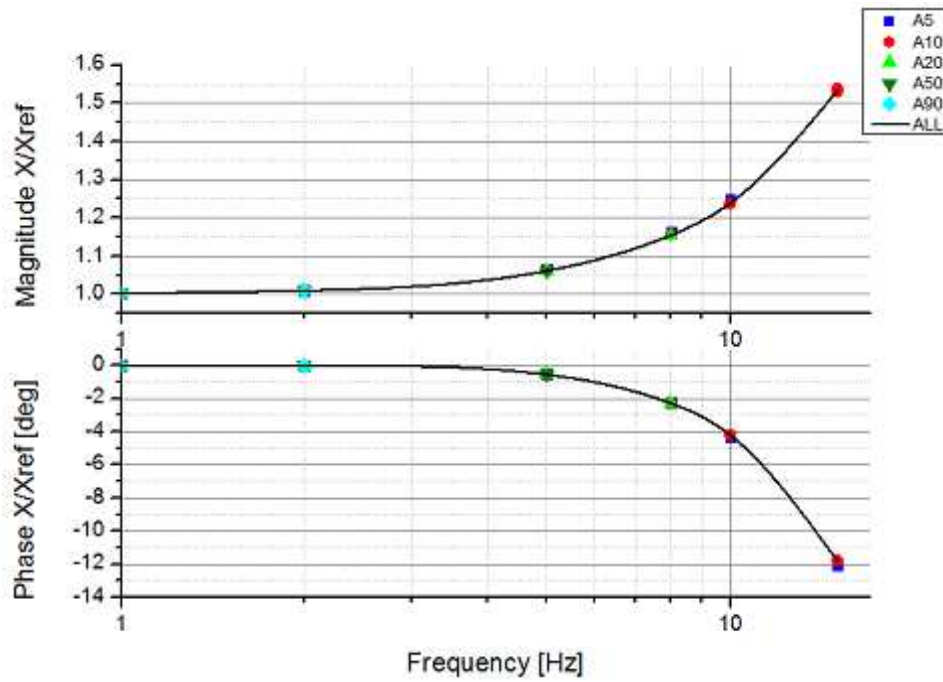


Figure 4.12 Controlled servo-hydraulic system frequency response function estimation

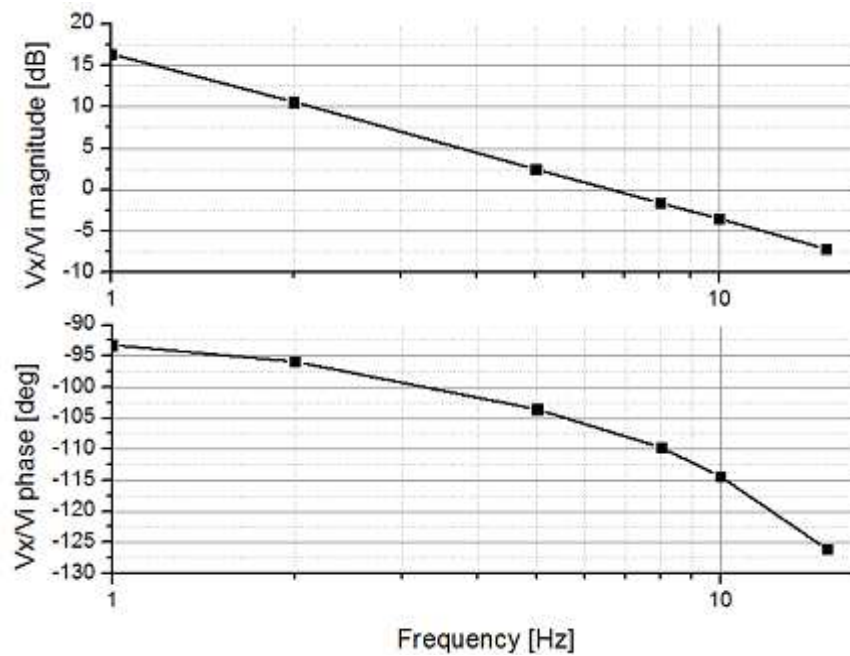


Figure 4.13 Servo-hydraulic system frequency response function estimation

Under non load conditions, the servo-hydraulic system presents the behaviour of a system with a zero pole in the origin, and the next pole is not placed inside the frequency range where the tests were developed. Such performance is the one obtained during the simulation stage, therefore the procedures and the considerations established for the controller tuning are applicable, and the values obtained through the simulations are a good start point when the controlled servo-hydraulic system will be used in real structures.

## Conclusions

Through the development of an automatic system for experimental modal analysis of large structures, the following conclusions in terms of model, controller design and controller implementation are obtained:

- The dynamic models used to simulate the servo-hydraulic system had been constructed under a series of assumptions, that give models accurate enough to foresee the general behaviour of the system, but not to obtain accurate parameters of the system in either time or frequency domain, due to the lack of accurate parameters such leakage coefficients, load stiffness and damping; the presence of phenomenon not considered during the model stage like structural stiffness and damping of the actuator piston; and the neglecting of non linear phenomenon like friction.
- The use of a PID algorithm to control a servo-hydraulic system composed by a linear hydraulic actuator and a double stage servovalve, is a good solution in order to satisfy the stability, sensitivity to noise measurement and set-point following characteristics required for this particular application. In addition, the flexibility of the PID controller to modify easily and intuitively the behaviour of the controlled system, allow to overcome the degree of uncertainty on the simulation stages, generated by the the lack of accurate knowledge about the load in terms of structural damping and stiffness, and the non modelled phenomenon of the system.
- The model used to simulate the servo-hydraulic system do not include structural damping and stiffness values therefore the system transfer function has the presence of a pole in the origin. In experimental conditions this behaviour is not true and must be conceived when the PID tuning is developed. On simulation conditions no integral action is expected to be imposed in the controller, however in experimental conditions had been observed that integral action can be included, in order to assure a zero steady-state error, up to the value that avoid unstable behaviour of the responses. Therefore, the objective of PID tuning through simulations is tp obtain the proportional gain that gives the best response characteristics at the different operational conditions. During the experimental tests, such gain must be used, and further modifications of the gains, particularly the integral and proportional, can be done if its required.
- As the experimental modal analysis requires the use of a sinusoidal wave signal excitation, accurate frequency response function estimation at the excited frequency can be obtained. This information can be used as input

---

on the amplitude compensator in order to satisfy the set-point following conditions for the controlled servo-hydraulic system. The implementation and use of an amplitude compensator do not neglect the PID tuning process, and must be implemented once adequate PID gains had been obtained. The main idea through the amplitude compensator is the reduction of the main harmonic error, in order to obtain a system response signal with a frequency and amplitude equal to the required for the modal analysis.

Further work around the development of an automatic system for experimental modal analysis of large structures can be developed, using the experiences obtained in the present work. It is suggested to deeply investigate the tuning process in order to implement a real time adaptative PID control algorithm where the control gains are modified according to the load and operational characteristics of the system. In addition, a control algorithms of the piston acceleration is suggested to be included, to control the maximum acceleration value that the structure is expected to experience.

## Appendix A-I Simulation parameters

$A_1$  : 0,00059  $m^2$  .  
 $A_2$  : 0,00059  $m^2$  .  
 $\beta$  : 1,8 e 9  $N/m^2$  .  
 $C_{el}$  : 2,11 e-11  $m^5/(Ns)$  .  
 $C_{il}$  : 2,11 e-11  $m^5/(Ns)$  .  
 $C_l$  : 0  $Nm/s$  .  
 $I_{sat}$  : 50 e-3  $A$  .  
 $K_l$  : 0  $Nm$  .  
 $M_c$  : 9  $kg$  .  
 $M_l$  : 0 and 450  $kg$  .  
 $P_r$  : 6,89 e 6  $Pa$  .  
 $P_{s0}$  : 20,7 e 6  $Pa$  .  
 $P_{return}$  : 0  $Pa$  .  
 $Q_r$  : 0,0009  $m^3/s$  .  
 $V_0$  : 0,000059  $m^3$  .

# Appendix A-II Simulation block diagrams

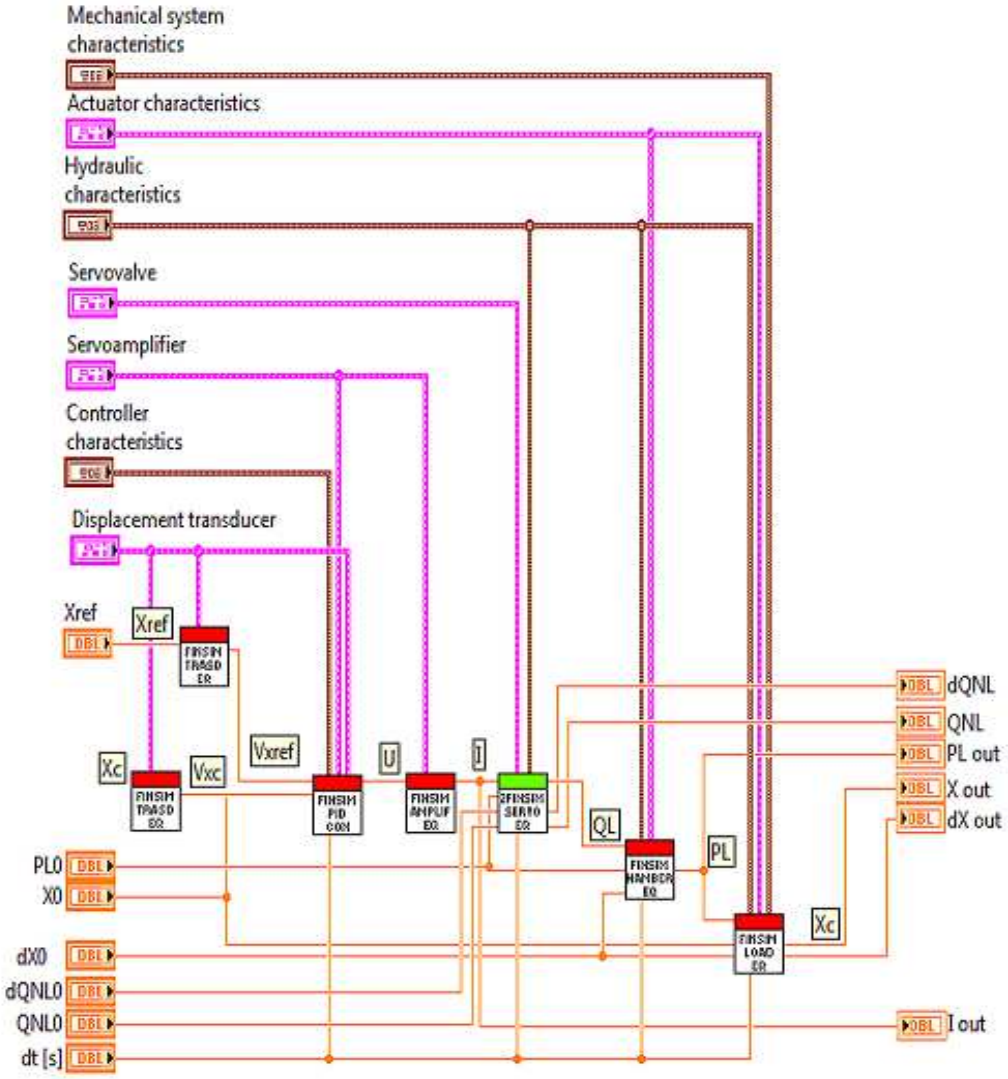


Figure A-II.1 General structure for controlled servo-hydraulic system block diagram

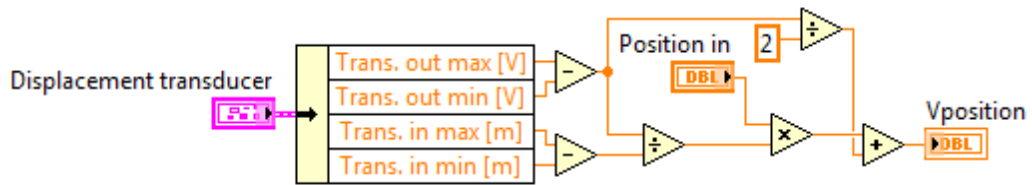


Figure A-I.2 Displacement transducer block diagram

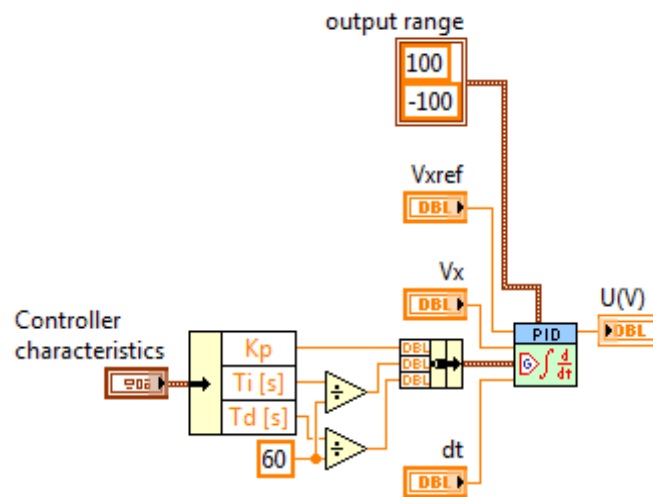


Figure A-I.3 Controller block diagram

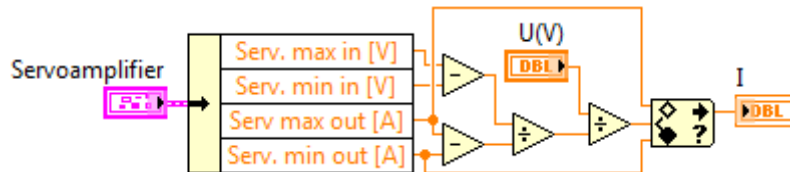


Figure A-II.4 Servo amplifier block diagram



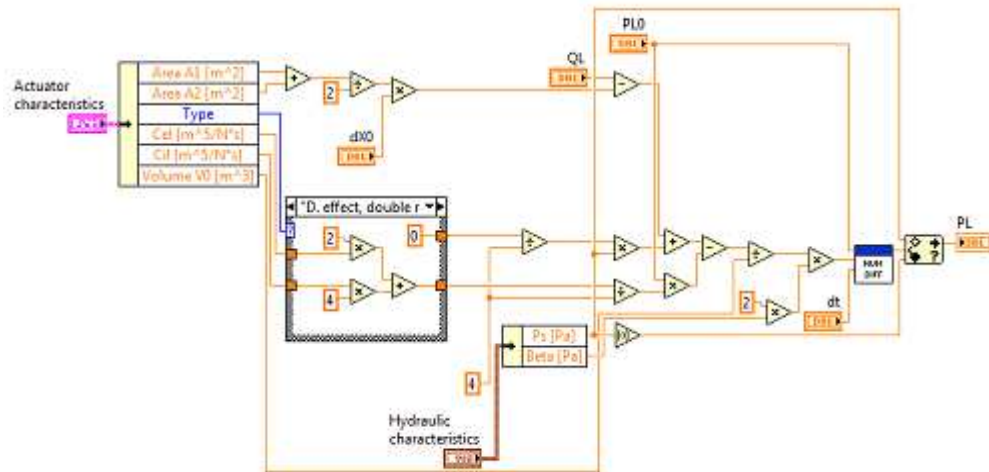


Figure A-II.5 Actuator chambers block diagram

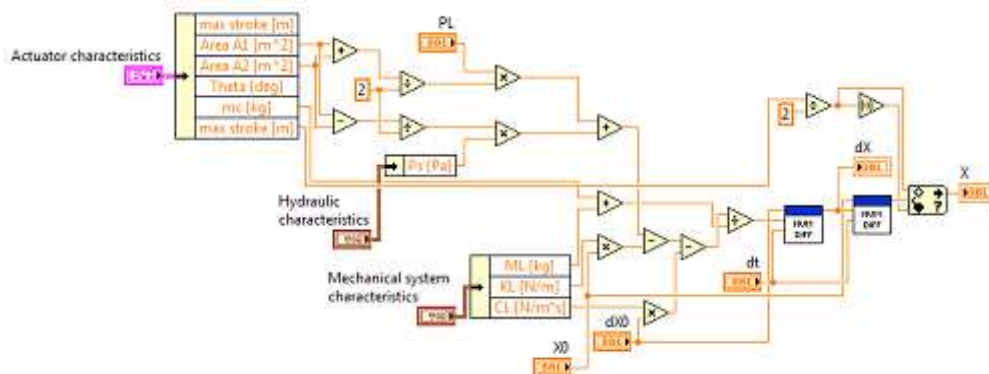


Figure A-II.6 Load block diagram

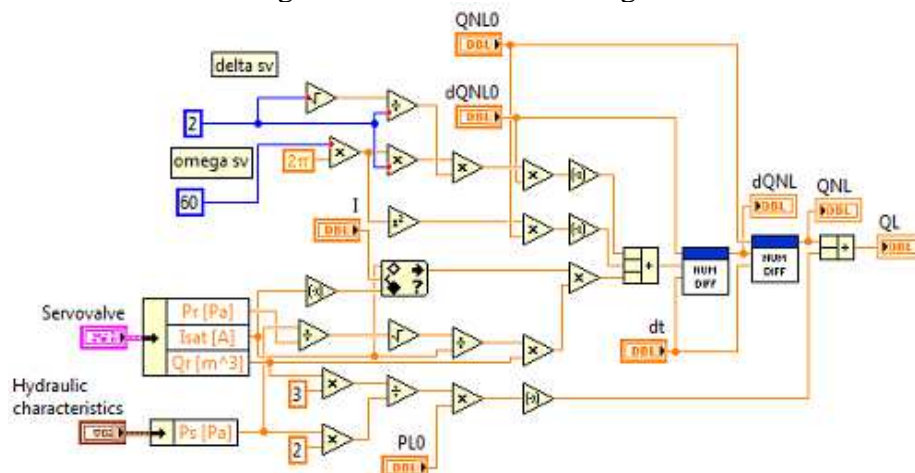


Figure A-II.7 Linear servovalve block diagram

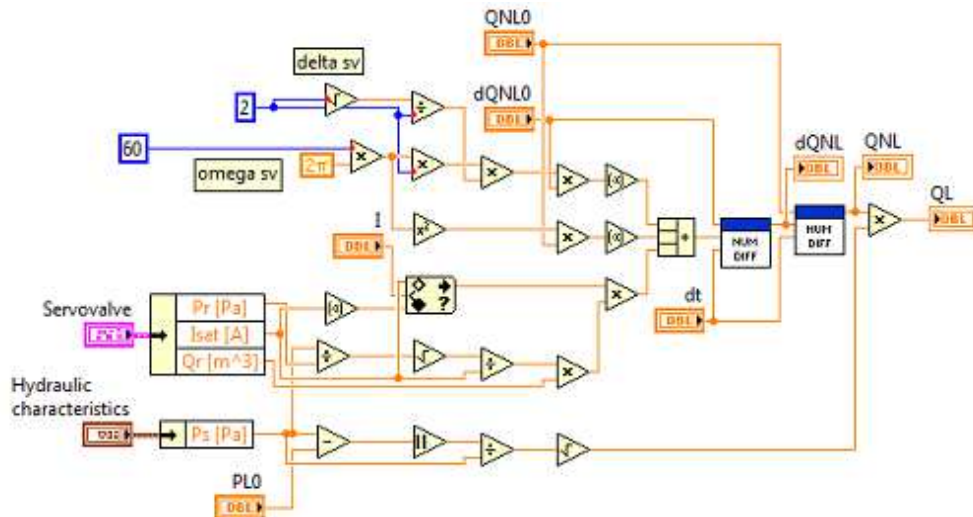


Figure A-II.8 Non linear servovalve block diagram

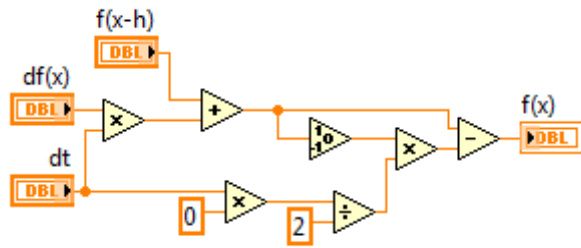
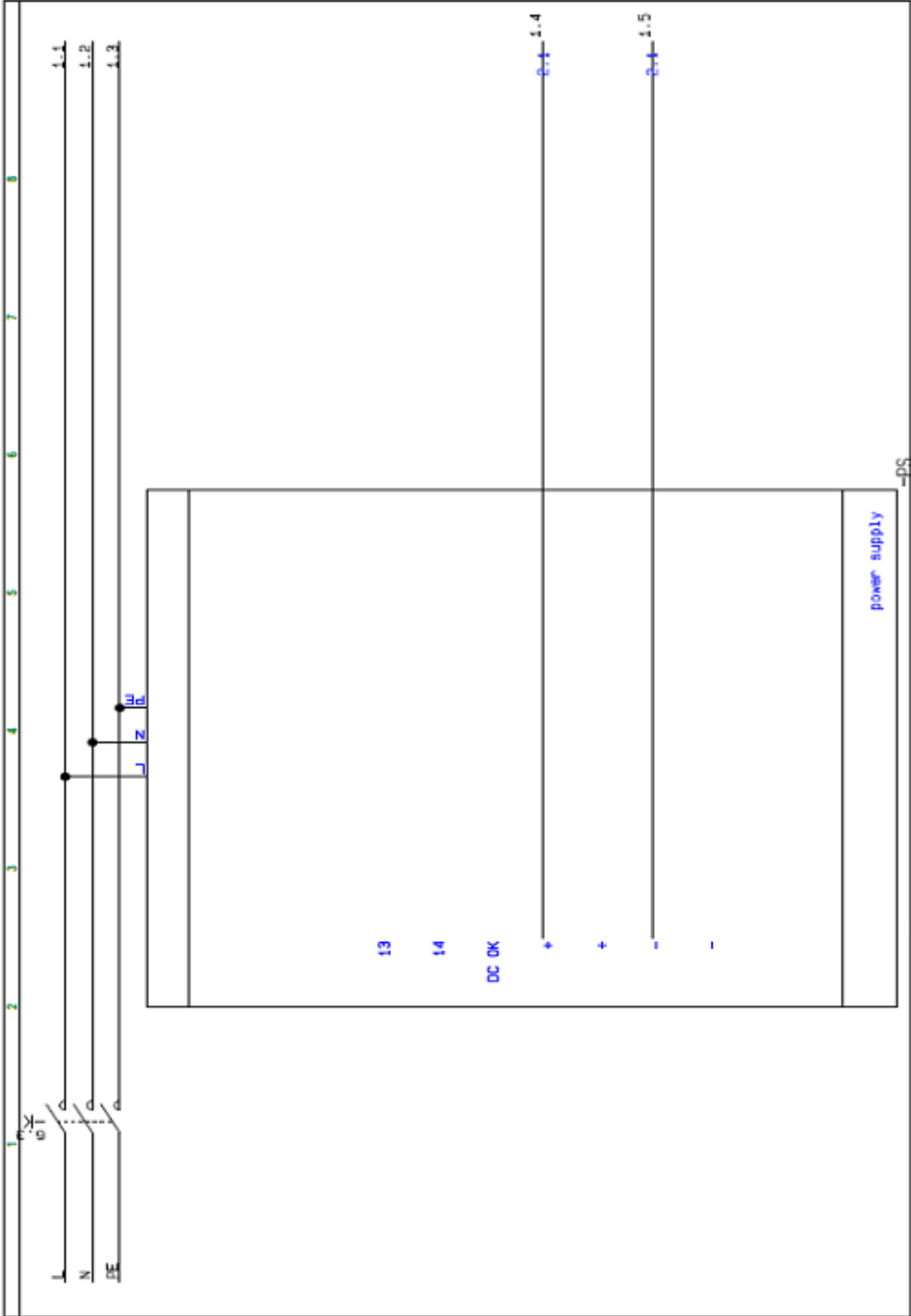
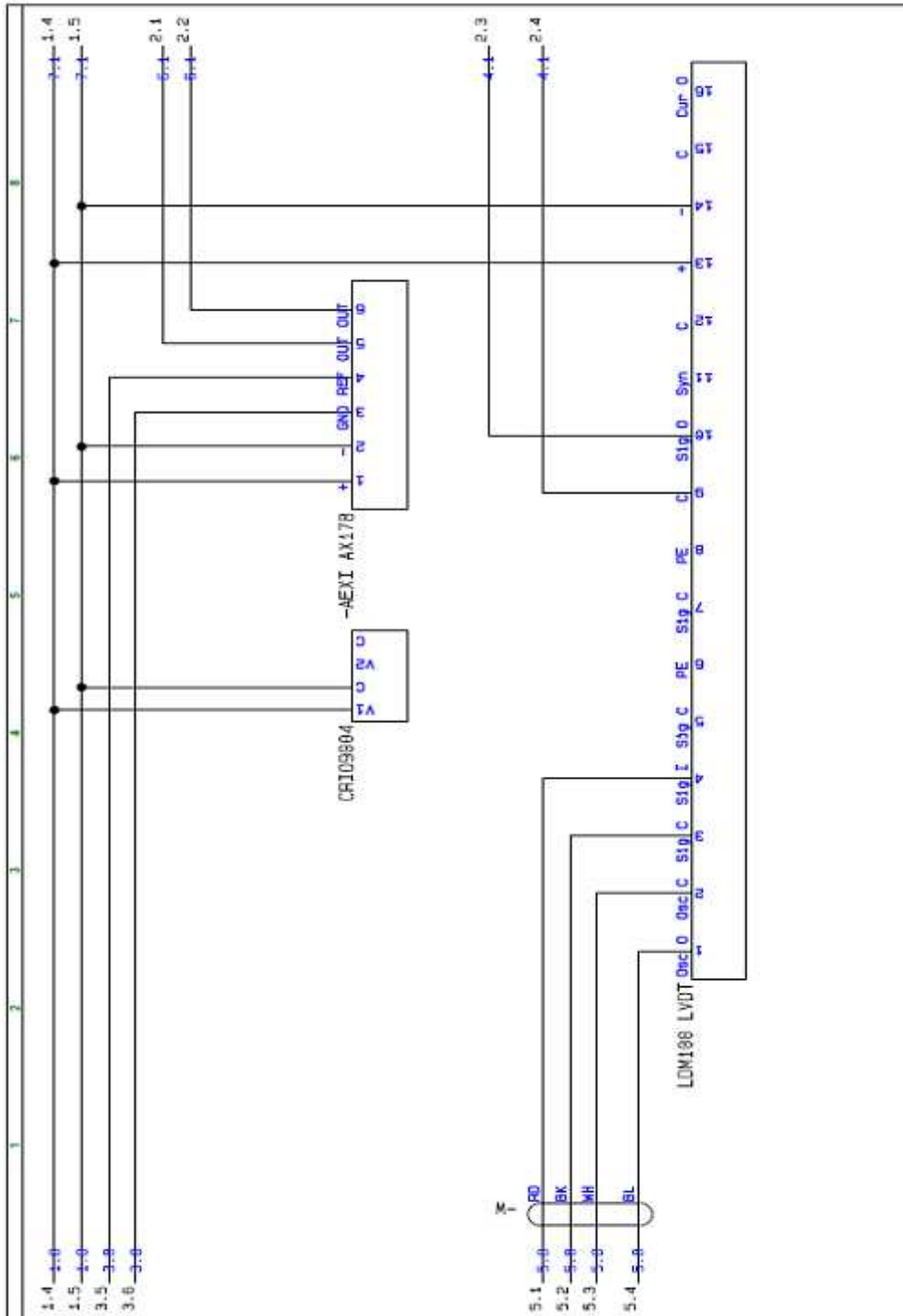
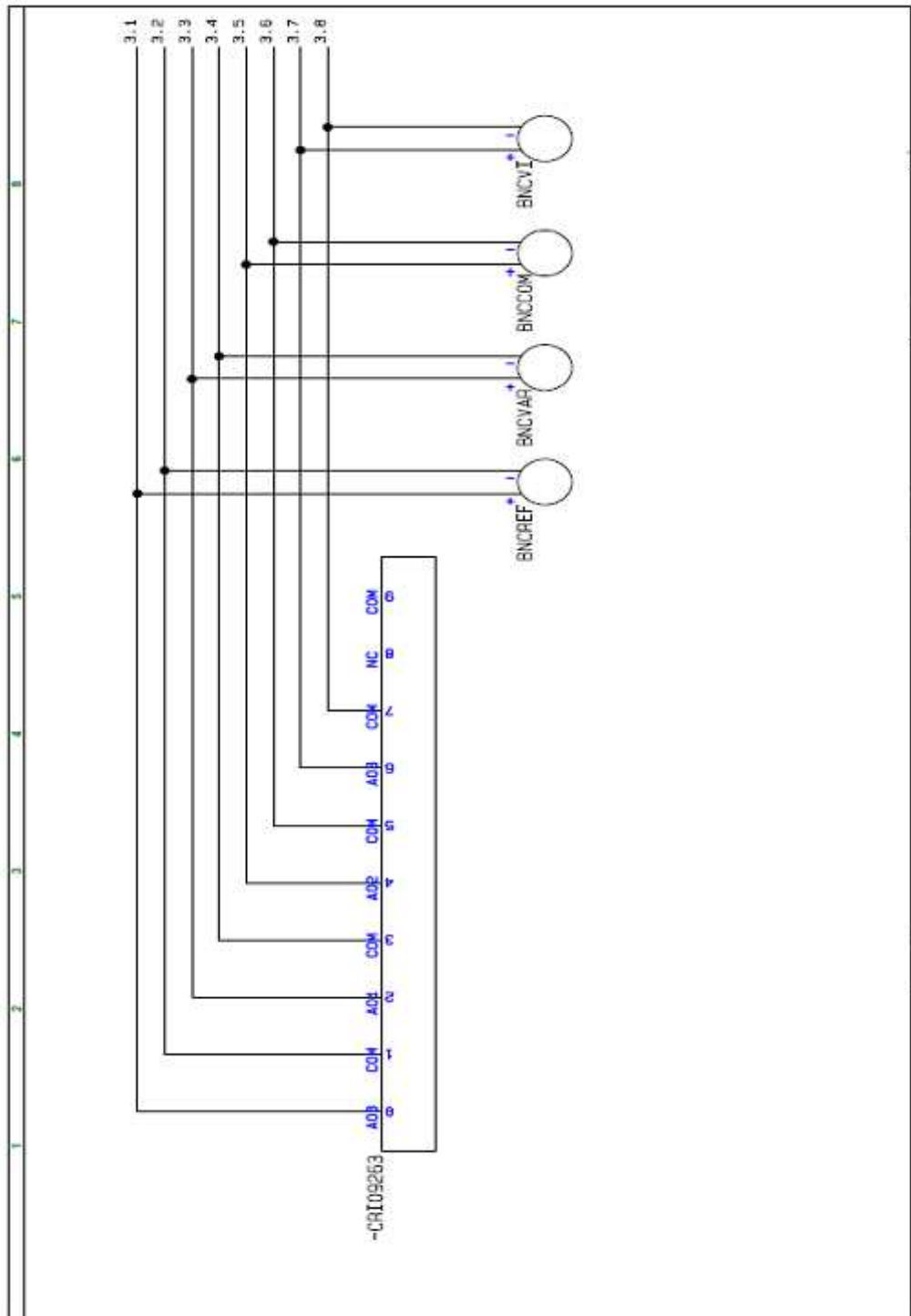


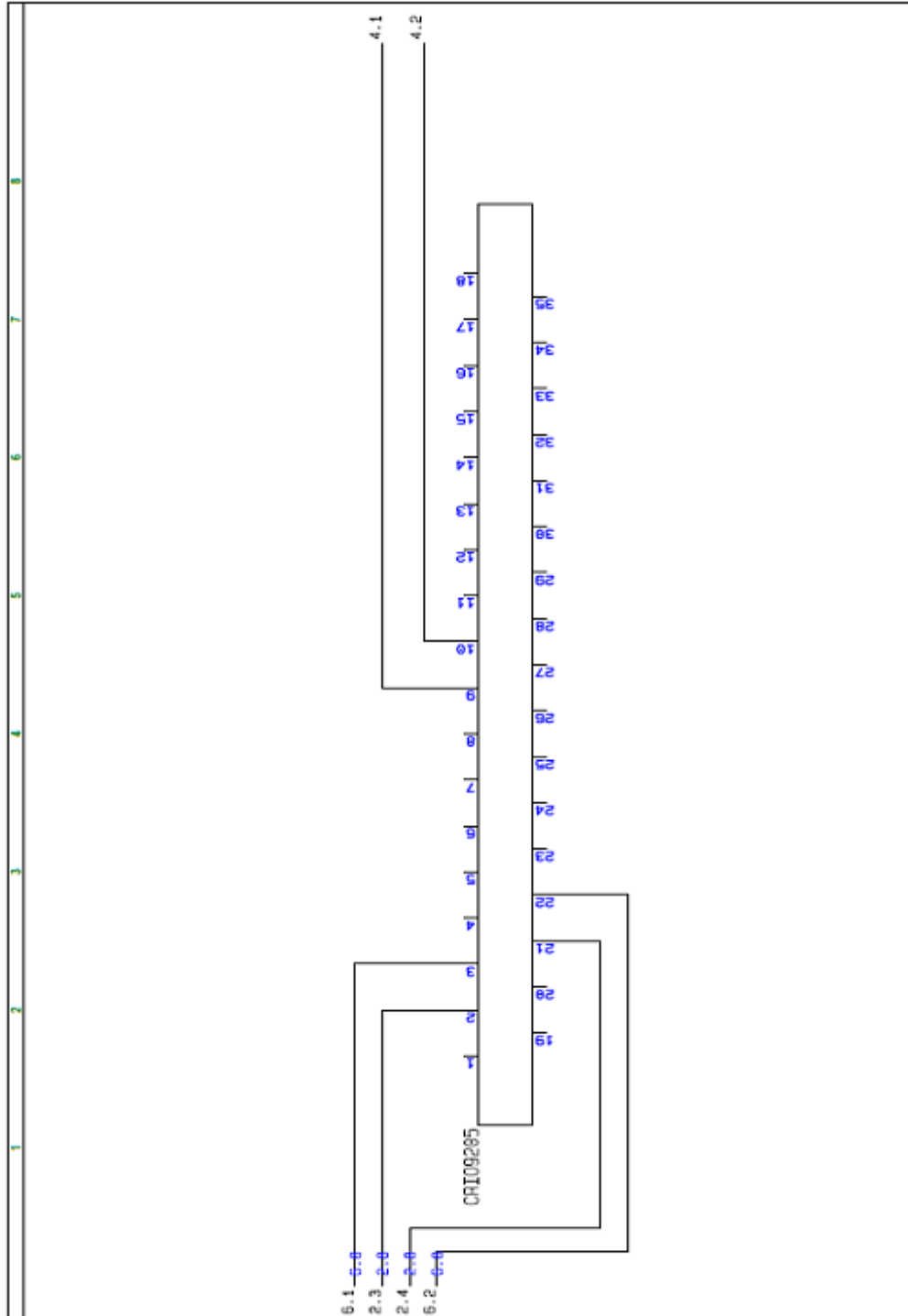
Figure A-II.9 Numerical differentiation block diagram

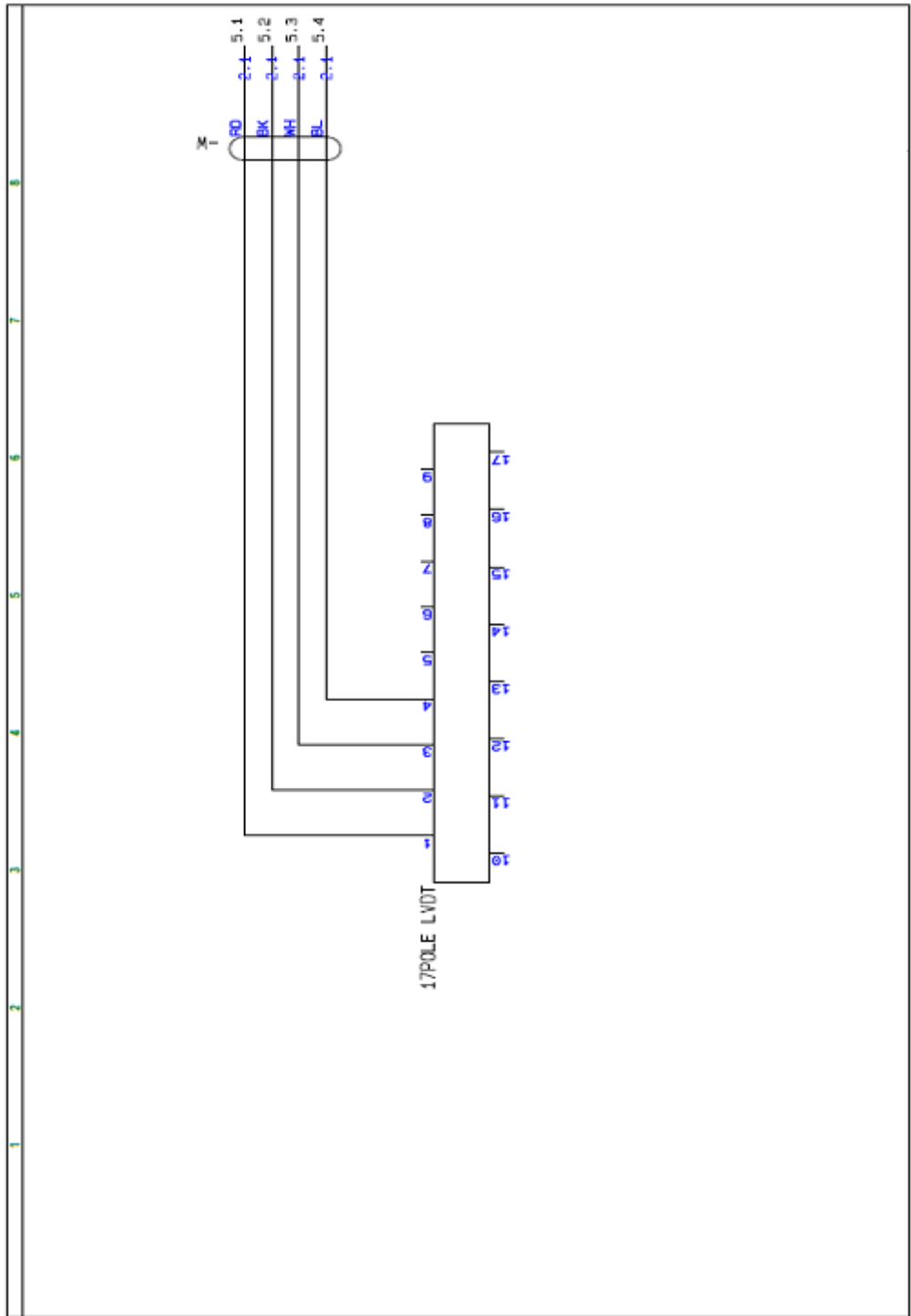
# Appendix A-III Electrical schemes

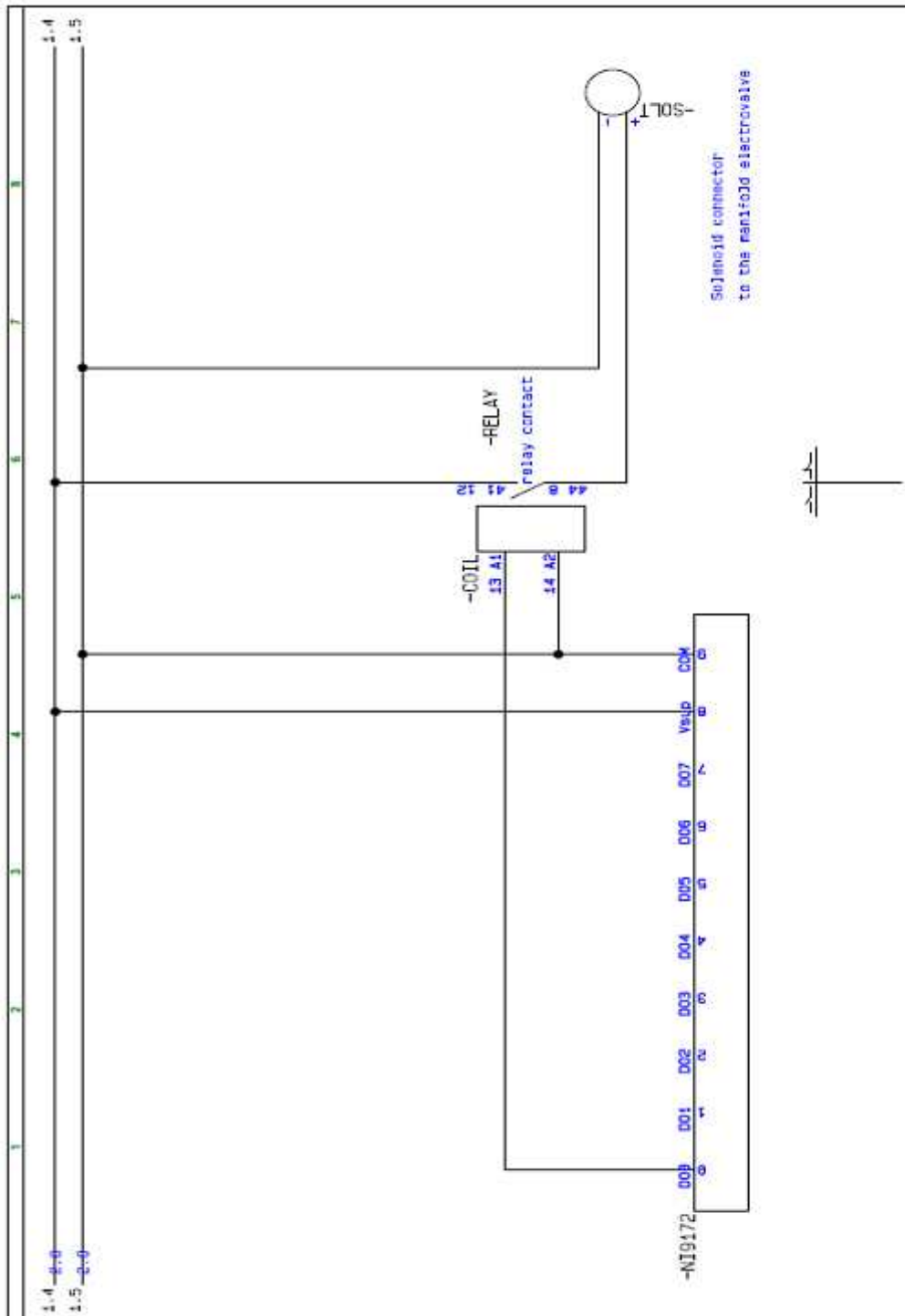














## Appendix A-VI Controller user interface

The controller user interface is composed by three groups, visualization charts, system controls and operational controls.

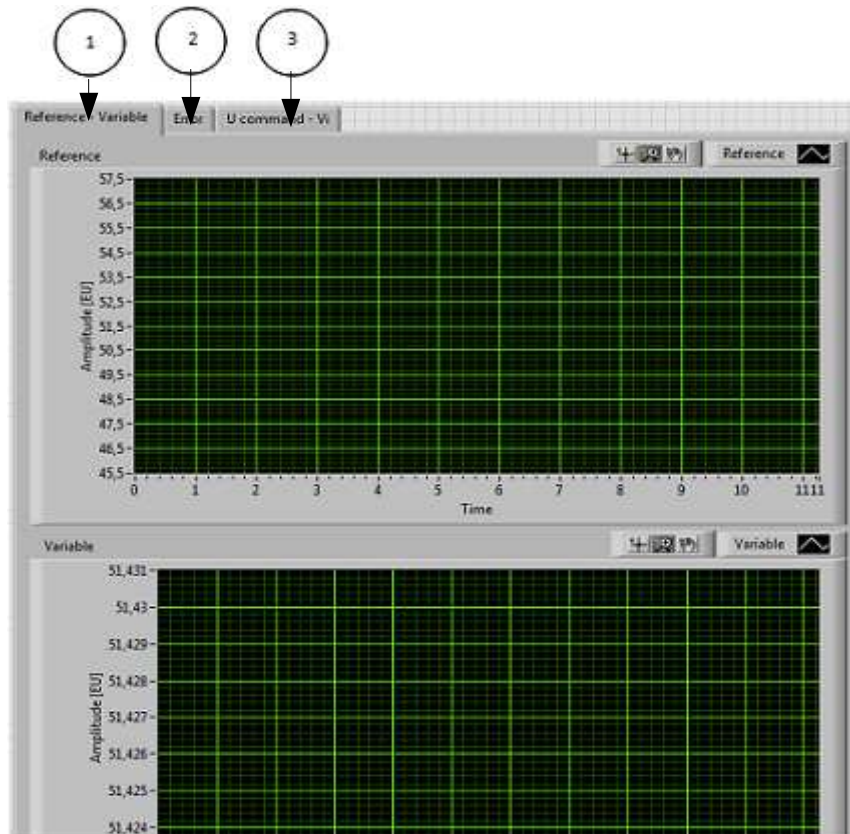


Figure A-VI.1 Visualization charts on controller user interface

The visualization charts allow the user to visualize in real time the measured variables involved in the control process. Figure A-VI.1 shows the user interface to this group, where are present the following indicators:

- Reference variable (1): refers to the the signal associated to the signal generator. Can be either be visualized in voltage or millimetres units according the configuration imposed in the general controls.
- Feedback variable (1): refers to the signal measured by the LVDT position transducer. Can be either be visualized in voltage or millimetres units according the configuration imposed in the general controls.
- Error (2): refers to the error signal which enters to the controller in order to execute the PID control action. Is calculated through the reference and feedback variable signal. Can be either be visualized in voltage or

millimetres units according the configuration imposed in the general controls.

- U command signal (3): refers to the signal coming out the PID controller and goes to the servovalve signalling group in order to command the servovalve. The visualization is in voltage.
- Vi signal (3): refers to the current signal that commands the servovalve. As no current analog modules are predisposed in the hardware, the signal is measured through the voltage on a shunt resistance placed in the servovalve circuit.

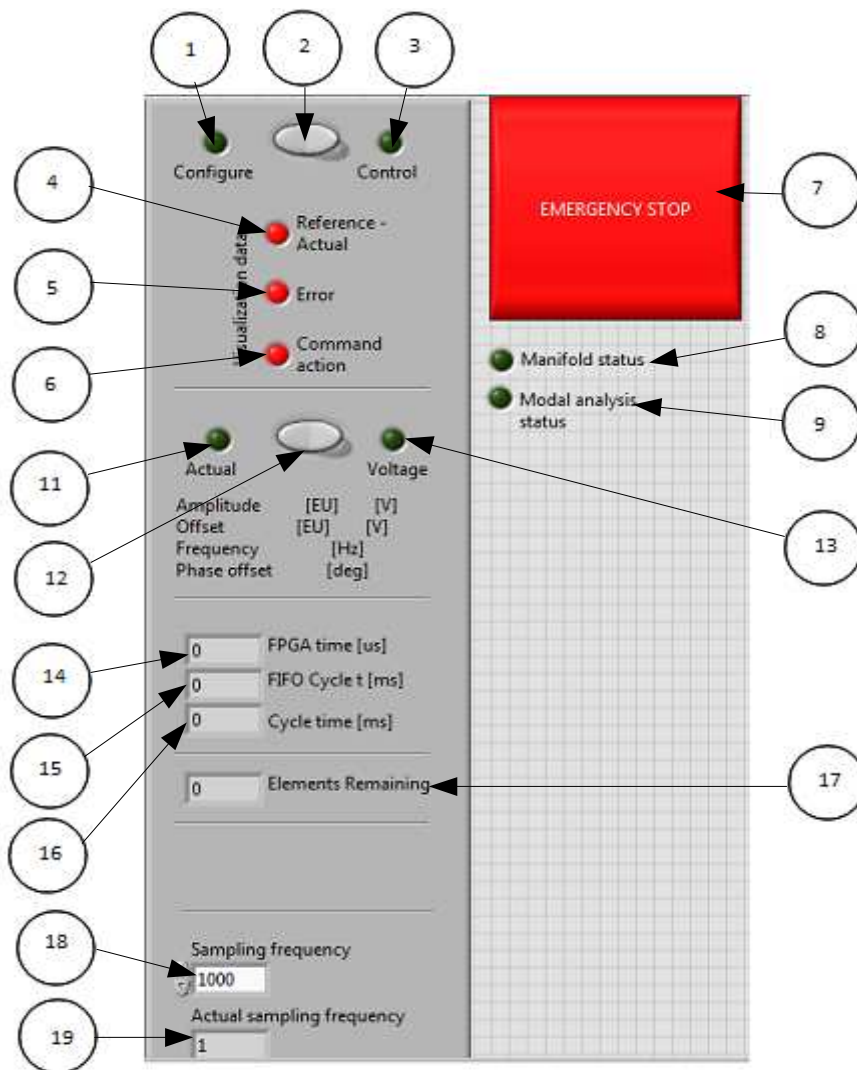


Figure A-VI.2 System controls on controller user interface

---

The system controls allow the visualization of system performance parameters and the configuration of the visualization charts group. Figure A-VI.2 Shows the user interface of this group, where are present the following controls and indicators:

- Configure status led (1): indicates the if the controller is in configuration status. If the Configure – Control selector is in position towards Configure, the led turns on.
- Configure – Control selector (2): allows the user to select between configuration or controlling status on the operational controls in the user interface.
- Control status led (3): indicates the if the controller is in control status. If the Configure – Control selector is in position towards Control, the led turns on.
- Visualization data – Reference – Actual control (4): allows visualization of reference and feedback signal on the visualization charts interface. If the visualization is allowed the control turns blue, while a red lighted control refers to a non visualization condition.
- Visualization data – Error (5): allows visualization of error signal on the visualization charts interface. If the visualization is allowed the control turns blue, while a red lighted control refers to a no visualization condition.
- Visualization data – Command action (6): allows visualization of servovalve command signal on the visualization charts interface. If the visualization is allowed the control turns blue, while a red lighted control refers to a no visualization condition.
- Emergency stop control (7): turning on this control, stops the control action, turns the controller to configuration status and turns off the manifold electrovalve.
- Manifold status led (8): shows the status of the signal going to the manifold electrovalve. If the led turns on the electrovalve is working, while turn off the electrovalve is off and does not allow oil flow to the servovalve.
- Modal analysis status led (9): if the controller is running in modal analysis condition, the led turns on. Otherwise, the signal amplitude and frequency must be imposed manually.
- Actual unit measure led (11): indicates the if the visualization charts and the signal generator are running in millimetres. If the Actual – Voltage selector is in position towards Actual, the led turns on.
- Actual – Voltage selector (12): allows the user to select between position

(actual) or voltage units on the visualization charts and the signal generator.

- Voltage unit measure led (13): indicates the if the visualization charts and the signal generator are running in voltage. If the Actual – Voltage selector is in position towards Voltage, the led turns on.
- FPGA time indicator (14): indicates the time the FPGA takes to do a processing cycle. The time is measured in microseconds.
- FIFO cycle time indicator (15): indicates the time the FPGA sends data to the user interface device through FIFO methodology. The time is measured in milliseconds.
- Cycle time indicator (16): indicates the time the user interface device sends data to the FPGA. This time is measured in milliseconds.
- FIFO remaining elements indicator (17): indicates the amount of remaining data inside the FIFO which transfers from the FPGA to the user interface device. If the FIFO goes to 10000 value, the transferring data rate has overcome overflow. In such case deselect visualization of some variables using the controller (4), (5) or (6).
- Sampling frequency control (18): allows the user to impose a sampling frequency for the FIFO transferring rate. The maximum sampling frequency is 1000 Hz.
- Sampling frequency indicator (19): Indicates the real FIFO transferring rate. The maximum frequency is 1000 Hz.

The operational controls allow the imposition of the operational parameters for the controller operation. Is divided in two tabs, according the state of the controller, configure and control. Figure A-VI.3 shows the user interface on configuration state, where the following controls and indicators are present:

- Signal wave type selector (1): allows the selection of the type of signal generator for the particular application. Sinusoidal wave and step generator are available.
- AO CRIO 9263- maximum voltage control (2): sets the C-RIO 9263 module range maximum voltage value.
- AO CRIO 9263- minimum voltage control (3): sets the C-RIO 9263 module range minimum voltage value.
- AO CRIO 9205- maximum voltage control (4): sets the C-RIO 9205 module range maximum voltage value.
- AO CRIO 9205- minimum voltage control (5): sets the C-RIO 9205 module range minimum voltage value.

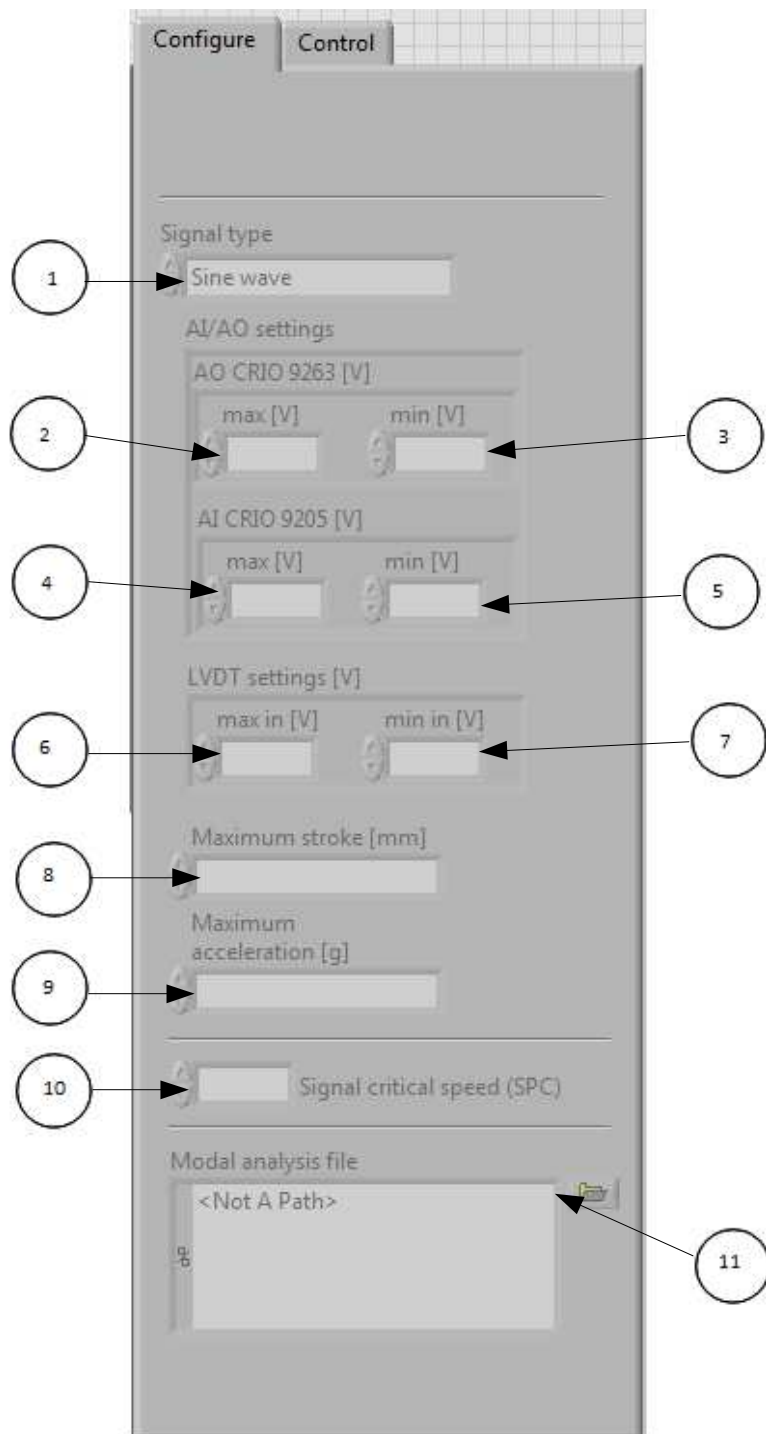


Figure A-VI.3 Operational controls – configuration state user interface

- LVDT settings - maximum voltage control (6): determines the LVDT conditioner range maximum voltage value.
- LVDT setting - minimum voltage control (7): determines the LVDT conditioner range minimum voltage value.
- Maximum stroke control (8): allows the imposition of the hydraulic linear actuator maximum stroke. The value is imposed in millimetres.
- Maximum acceleration control (9): allows the imposition of the maximum acceleration value on the modal analysis tests. The value is imposed in Gs.
- Signal critical speed (SPC) indicator (10): indicates the value of the critical speed for a sinusoidal wave form signal as function of the signal frequency and amplitude. The value is shown in millimetres per second.
- Modal analysis file control (11): in order to carry out automatic modal analysis, a file \*.txt containing a two columns array with the required test frequencies and amplitudes must be loaded into the controller. The Modal analysis file control, allows the file loading, and enables the modal analysis test mode.

Alike configuration state user interface allows the configuration of the common parameters that are used on every test and must not be modified unless hardware, cylinder or overall test conditions are changed, control state user interface allow the user to modify the actual service parameters while the controller is executing a command action in the servovalve. Figure A-VI.4 shows the user interface on control state, where the following controls and indicators are present:

- Servovalve ON – OFF selector (1): when is selected towards ON position, the FPGA sends the command signal to the servovalve. In OFF position the command action has a constant value of 0 volts.
- Manifold ON – OFF selector (2): when is selected towards ON position, the FPGA sends the command signal to the manifold electrovalve allowing the oil flow from the hydraulic circuit to the servovalve.
- Amplitude compensator ON – OFF selector (3): when is selected towards ON position, the amplitude compensator executes the amplitude correction action. In OFF position, the input signal is not compensated.

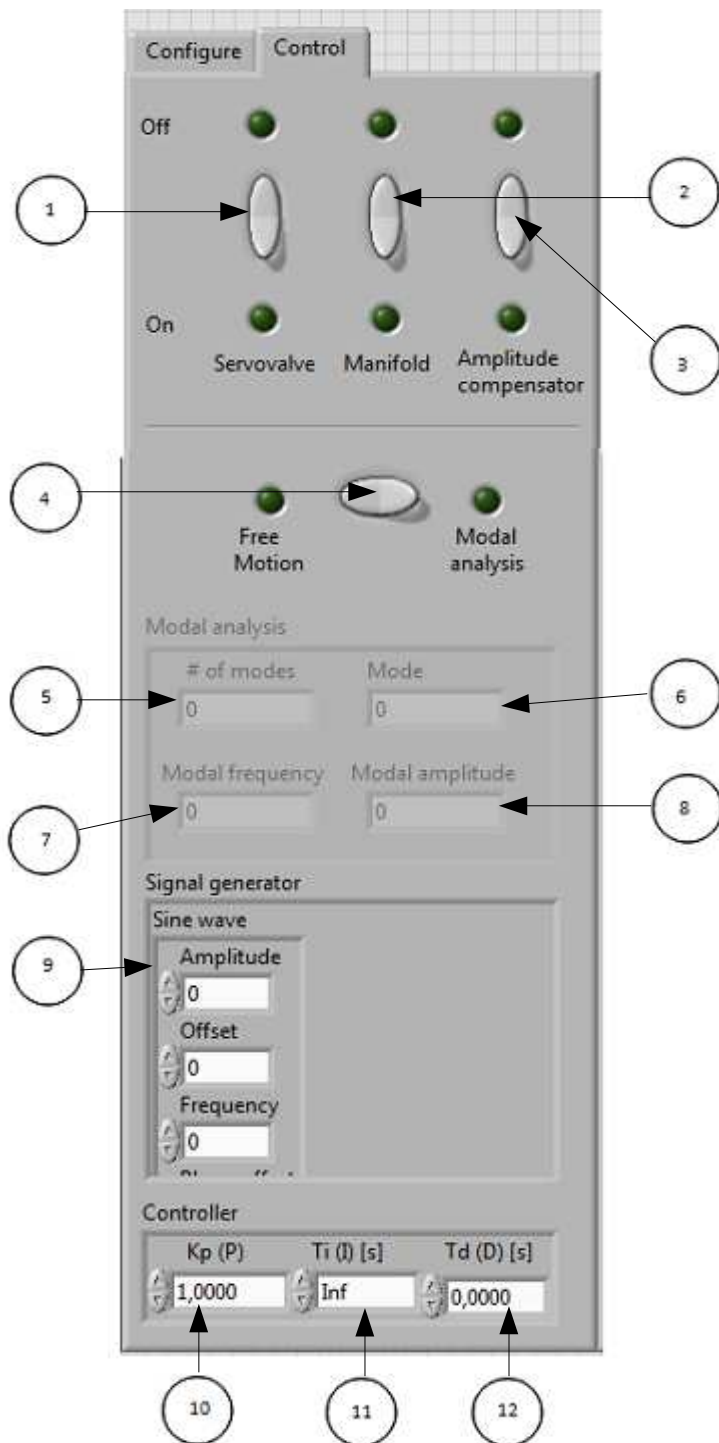


Figure A-VI.4 Operational controls – control state user interface

- Free analysis – Modal analysis selector (4): when is selected towards Free analysis position, enables the signal generator control, disables the modal analysis controls, and allows the manual imposition of signal parameters according to the signal wave type selected on the configuration user interface. In other case, enables the modal analysis controls, disables the signal generator and executes an automatic imposition of amplitude and frequency parameters for a sine wave signal according to the existing data on the \*.txt file loaded in configuration user interface.
- Manifold ON – OFF selector (2): when is selected towards ON position, the FPGA sends the command signal to the manifold electrovalve allowing the oil flow from the hydraulic circuit to the servovalve. In OFF position, the electrovalve is closed.
- Amplitude compensator ON – OFF selector (3): when is selected towards ON position, the amplitude compensator executes the amplitude correction action. In OFF position, the input signal is not compensated.
- Free analysis – Modal analysis selector (4): when is selected towards Free analysis position, enables the signal generator control, disables the modal analysis controls, and allows the manual imposition of signal parameters (amplitude, offset and frequency), according to the signal wave type selected on the configuration user interface. If is selected on Modal analysis position, enables the modal analysis controls, disables the signal generator and executes an automatic imposition of amplitude and frequency parameters for a sine wave signal according to the existing data on the \*.txt file loaded in configuration user interface.
- Modal analysis controls - # of modes indicator (5): indicates the number of modes to be excited in the current test according to the existing data on the \*.txt file loaded in configuration user interface.
- Modal analysis controls - mode indicator (6): indicates the actual mode being tested. The number goes from zero to # number of modes.
- Modal analysis controls – modal frequency indicator (7): indicates the signal frequency for the actual mode being tested. The value is shown in Hz.
- Modal analysis controls – modal amplitude indicator (8): indicates the signal amplitude for the actual mode being tested. The value is shown in millimetres.
- Signal generator controls (9): controls the signal parameters on free analysis mode. In a sinusoidal wave signal amplitude, offset and frequency are the parameters that can be modified, in millimetres and Hz, respectively. On step signal, is possible to modify amplitude and



---

offset.

- Controller – Kp (10): allows the imposition of the proportional gain used on the PID controller.
- Controller – Ti (11): allows the imposition of the integral time used on the PID controller. The value is taken in seconds.
- Controller – Td (12): allows the imposition of the derivative time used on the PID controller. The value is taken in seconds.

# Appendix A-V FPGA block diagrams

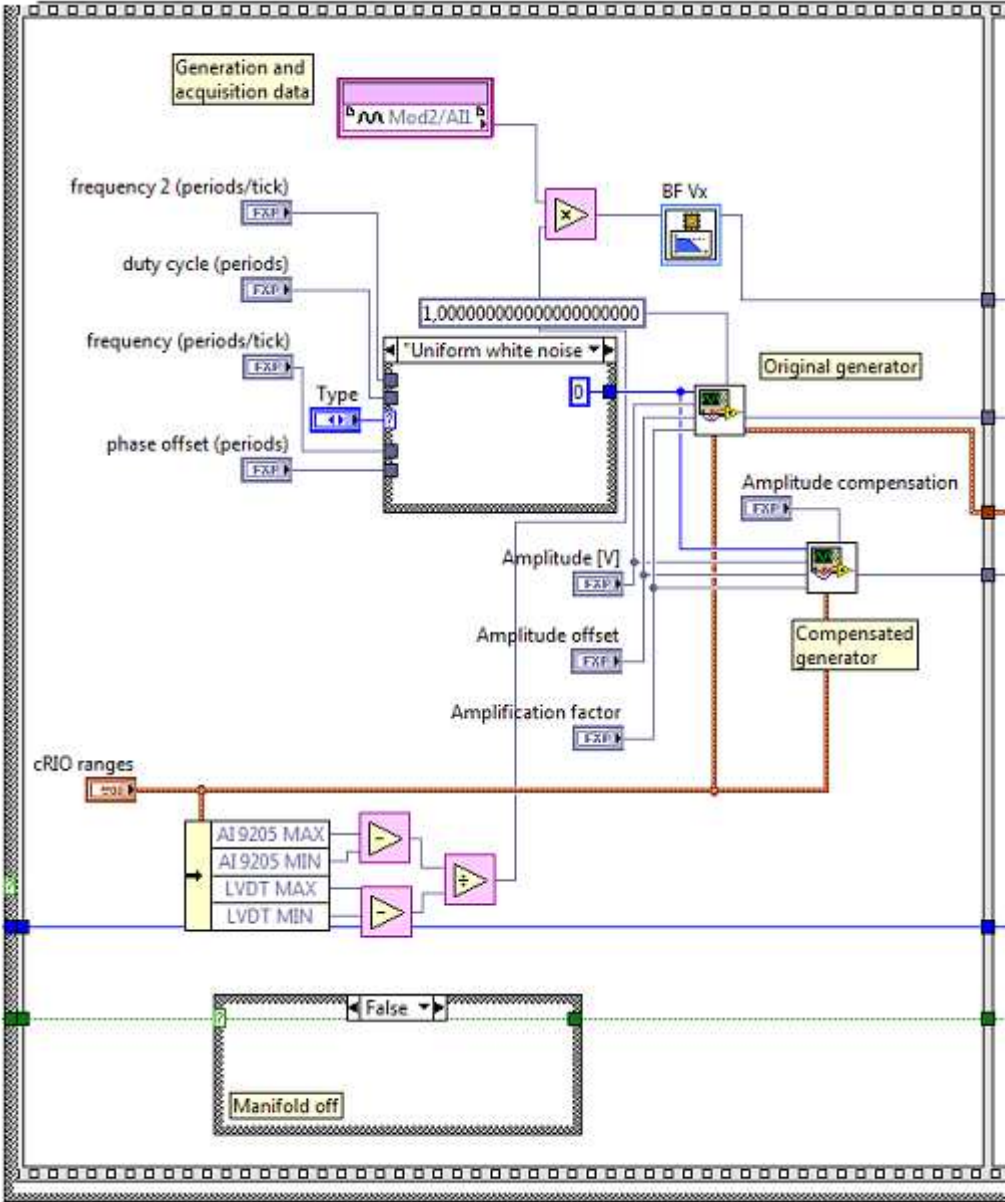


Figure A-V.1 FPGA block diagram – signal generation stage

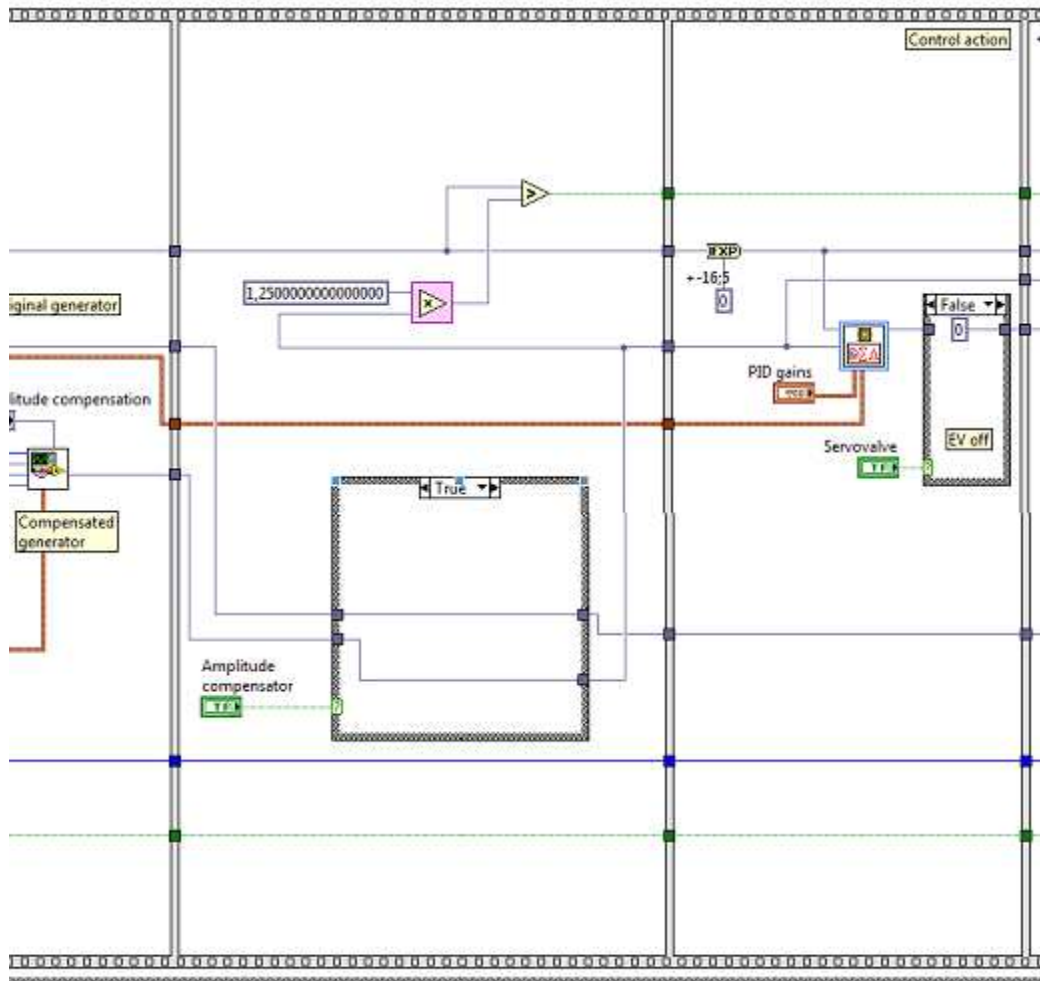


Figure A-V.2 FPGA block diagram - amplitude compensation and control stage

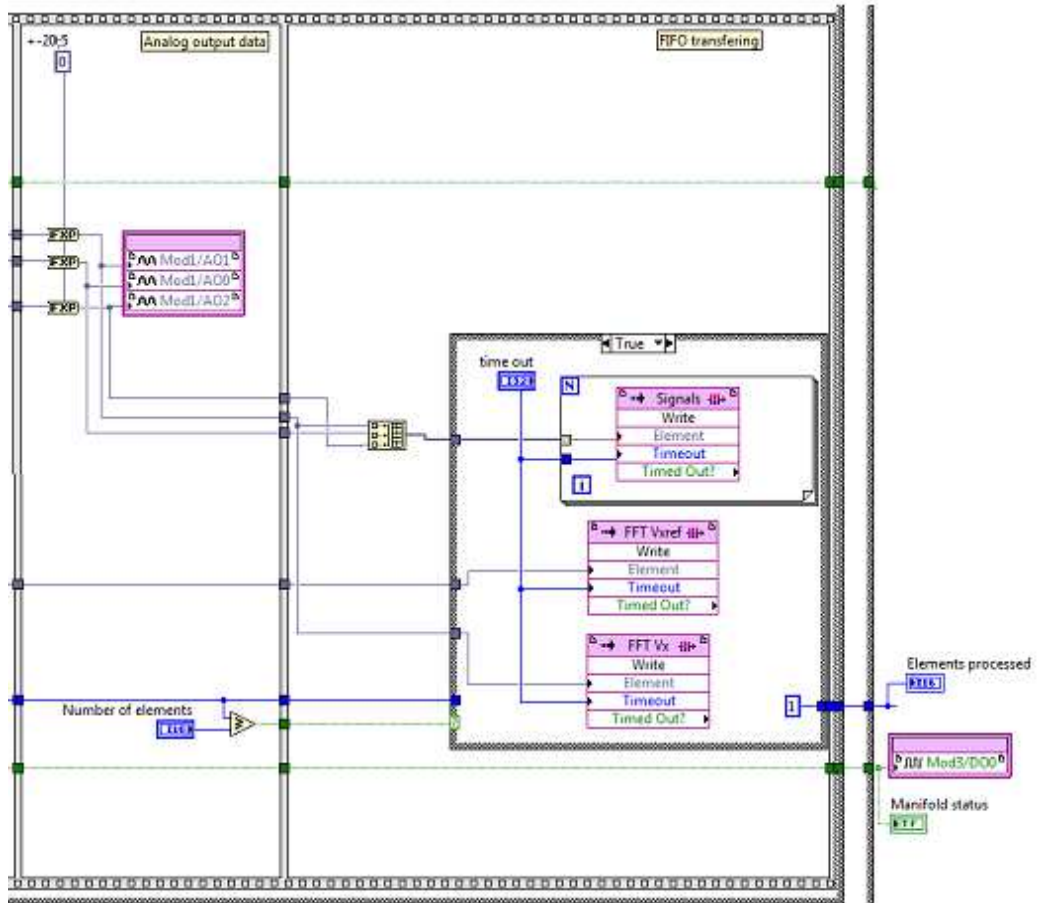


Figure A-V.3 FPGA block diagram – output signalling and output user interface communication stages

## Bibliography

- [1] Á. Cunha, E. Caetano, and P. Feup, “Experimental Modal Analysis of Civil Engineering Structures,” *Span*, no. June, pp. 12–20, 2006.
- [2] M. Bocciolone and E. Zappa, “Measuring techniques and sensors for automation course - Frequency response function.” Politecnico di Milano, Milan, 2010.
- [3] “<http://www.indiamart.com/sachinhydraulics/products.html>.” .
- [4] “<http://www.mts.com/en/products/producttype/test-components/actuators-hydraulic-components/index.htm>.” .
- [5] J. K. Tar, I. J. Rudas, and J. F. Bitó, “Adaptive Control of a Differential Hydraulic Cylinder with Dynamic Friction Model,” pp. 361–374, 2006.
- [6] S. Sobczyk and A. Eduardo, “A continuous approximation of the lugre friction model,” *Mechatronics*, vol. 4, pp. 218–228, 2010.
- [7] H. E. Merritt, *Hydraulic control systems*. John Wiley and Sons, 1967, p. 358.
- [8] M. systems Corp., “Product specification Series 252 servovalve.” p. 8, 1994.
- [9] M. Inc., “Electrohydraulic Valves... A Technical Look - Datasheet,” *Direct*. MOOG inc, p. 24, 2002.
- [10] R. Poley, “DSP Control of Electro-Hydraulic Servo Actuators,” *Texas Instruments - Application report*, no. January, pp. 1–26, 2005.
- [11] C.-T. Chen, *Linear system theory and design*, Third. The Oxford University Press, 1999, p. 334.
- [12] F. Golnaraghi and C. K. Benjamin, *Automatic control systems*, 9th ed. John Wiley and Sons Inc., 2010, p. 944.
- [13] D. Xue, Y. Chen, and D. Atherton, *Linear Feedback Control, Analysis and design with MATLAB - Advances in Design and Control*, 1st ed. Philadelphia: , 2007, p. 354.
- [14] G. Cusimano, “Lecture 35 LINEAR QUADRATIC OPTIMAL

- CONTROL :,” *Master in Mechanical Engineering - Motion and Vibration Control of Mechanical Systems*, p. 39, 2011.
- [15] K. Åstrom and T. Hägglund, *PID Controllers : Theory , Design and Tuning*. Instrument Society of America, 1995, p. 354.
- [16] R. Tymerski and F. Rytönen, “Control System Design,” p. 122.
- [17] R. J. Mantz, “Introducción al control óptimo,” *Cátedra de control Moderno - Universidad Nacional de La Plata*, p. 19, 2003.
- [18] R. Burden and J. Douglas Faires, *Numerical analysis 9th edition*. 2011.
- [19] N. Instruments, “Introduction to FPGA technology: Top 5 benefits,” 2012. [Online]. Available: <http://www.ni.com/white-paper/6984/en>.
- [20] WiseGEEK, “What is an ethernet cable?,” 2012. [Online]. Available: <http://www.wisegeek.com/what-is-ethernet-crossover-cable.htm>.
- [21] M. systems Corp., “Series 242 Hydraulic Actuator.” p. 8, 2007.
- [22] J. Fraden, *Handbook of Modern Sensors. Physics, designs, and applications*, 3rd ed. New York: Springer-Verlag, 2004, p. 608.
- [23] “Instrumentation and controllers.” [Online]. Available: <http://instrumentationandcontrollers.blogspot.it/2010/05/linear-variable-displacement-transducer.html>.
- [24] Hydraulics Bosch Rexroth AG, “2/2, 3/2 and 4/2 directional poppet valve with solenoid actuation - TYpe M-,SED.” p. 16.